**UNIVERSITY OF SOUTHAMPTON**

**FACULTY OF MEDICINE**

# TOWARDS A TARGETED NON-INVASIVE DIAGNOSIS AND TREATMENT OF ENDOMETRIAL PATHOLOGIES

**Aikaterini Zisimopoulou**

Thesis for the degree of Master of Philosophy

**Southampton, January 2015**

**UNIVERSITY OF SOUTHAMPTON**
**FACULTY OF MEDICINE**

Master of Philosophy

# TOWARDS A TARGETED NON-INVASIVE DIAGNOSIS AND TREATMENT OF ENDOMETRIAL PATHOLOGIES

**by Aikaterini Zisimopoulou**

ABSTRACT

Polymersome nanoparticles (NPs) are comprised of biodegradable amphiphilic block copolymers (PEG-b-PCL) and can be efficiently engineered for cell-specific targeting, drug encapsulation and delivery. The versatility of nanoparticles as delivery and reporter systems is now being exploited in clinical medicine, nanomedicine and to enhance medical healthcare. The human endometrium is associated with a number of life-altering pathophysiologies, including endometriosis. Endometriosis is a common gynaecological pathology affecting 20-30 % of women in reproductive age. Accurate non-invasive and diagnosis and treatment in the early stages of endometrial pathologies, and in particular endometriosis, is limited by the lack of sensitivity and specificity of the current detection techniques.

The present study investigated the interaction

between endometrial cells and polymersome NPs, which were used for the delivery of hydrophilic drugs directly and targeted into endometrial cells using a minimally invasive, non-surgical, procedure. Using PEG-b-PCL polymersomes that targeted all cell types ubiquitously and loaded with a novel hydrophilic model cargo and quenched fluorescein isothiocyanate (FITC), we have demonstrated the uptake of polymersomes by the human endometrium epithelial and stromal cells, and their release of fluorescent FITC. This is the first time that NPs have been shown to be taken up by *ex vivo* human endometrial cells. Using this paradigm, polymersomes could be loaded with drugs or imaging agents and used to target endometrial cells. These results highlight the potential of targeted NP therapy for future diagnosis and treatment of endometrial pathologies.

## *Declaration of Authorship*

I, Aikaterini Zisimopoulou, declare that the thesis entitled ***"Towards a targeted non-invasive diagnosis and treatment of of endometrial pathologies"*** and the work presented in the thesis are both my own, and have been generated by me as the result of my own original research. I confirm that:

- this work was done wholly or mainly while in candidature for a research degree at this University;
- where any part of this thesis has previously been submitted for a degree or any other qualification at this University or any other institution, this has been clearly stated;
- where I have consulted the published work of others, this is always clearly attributed;
- where I have quoted from the work of others, the source is always given. With the exception of such quotations, this thesis is entirely my own work;
- I have acknowledged all main sources of help;
- where the thesis is based on work done by myself jointly with others, I have made clear exactly what was done by others and what I have contributed myself;
- parts of this work have been published in peer-reviewed conferences and journals (please see list of publications in the following page).

**Signed:** ……Aikaterini Zisimopoulou……

**Date:** ……26/01/2015…….....……

## *Conferences where the work was presented*

- ESHRE 2012, 28th Annual Meeting of the European Society of the Human Reproduction and Embryology, Istanbul, Turkey, 1-4 July 2012.

  "Targeted nanoparticles for the early diagnosis of endometriosis." Bailey JL, Newman TA, Johnston A, Zisimopoulou K, White M, Sadek K, Shreeve N, Cheong Y.

- 11th Word Congress of Endometriosis, Montpellier, France, 4-7 September, 2011.

  "Targeted nanoparticles for the early diagnosis of Endometriosis". Bailey JL, Newman TA, Johnston A, Zisimopoulou K, White M, Sadek K, Shreeve N, Cheong Y.

## *Acknowledgements*

The work described herein was conducted over the course of two years within the Nanoneuroscience group of the Faculty of Life Sciences of the University of Southampton under the supervision of Dr Tracey Newman and Dr Ying Cheong. I would like to gratefully acknowledge all the people who have in one way or another contributed to the realisation of the experimental work described herein. First and foremost my supervisors Dr Tracey Newman and Dr Ying Cheong for their extensive guidance, support, advice and understanding. I would also like to thank Dr Alex Johnston for sharing his thorough knowledge of nanoparticle preparation and fabrication. I also have to specially thank Dr Joanne Bailey for her comprehensive support in all aspects of lab work in these last two years. Dr Charlotte Weimar of the University of Utrecht for introducing and familiarising me with the protocols of primary cell culture. Linden Stocker for our fruitful collaboration on the collection of tissue and blood samples in Princess Anne hospital. Additionally I have to thank my colleagues and friends Agathi Christofidou, Christine Reitmeyer, Nash Matinyarare and Patrick Stumpf for their earnest friendship. I have also to acknowledge my parents and my sister for their ongoing support during my time in Southampton and last but don't least I would like to thank my husband, Alexis for his understanding, support and help.

# Table of Contents

*Declaration of Authorship* ..... **5**

*Conferences where the work was presented* ..... **7**

*Acknowledgements* ..... **8**

*List of Figures* ..... **12**

*List of Tables* ..... **19**

*List of Abbreviations and Acronyms* ..... **21**

**Chapter 1 Introduction** ..... **19**

**1.2 Polymersomes** ..... **25**

1.2.1 Polymersomes in Cancer treatment ..... 26

1.2.2 Polymersomes in Cancer diagnosis ..... 28

1.2.3 Surface modification of polymersomes for enhanced delivery and targeted therapy ..... 29

1.2.4 TAT peptide ..... 30

**1.3 Investigations of nanoparticles in the endometrium** ..... **31**

1.3.1 Testing nanoparticles in primary cell cultures ..... 31

1.3.2 Nanoparticle's intracellular fate ..... 32

**Chapter 2 The reproductive system** ..... **35**

**2.2 *The uterus*: Anatomy and physiology** ..... **38**

**2.3 The menstrual cycle** ..... **40**

**Chapter 3 Pathophysiology of endometrium & of related disorders of the reproductive tract** ..... **43**

3.1.1 Pathogenesis of endometriosis ..... 46

3.1.2 Do women with endometriosis carry a unique molecular signature for targeting? ..... 46
3.1.3 Current diagnosis and treatment of endometriosis ..... 50
**3.2 Endometrial Cancer ..... 52**
3.2.1 Pathogenesis of endometrial cancer ..... 53
3.2.2 Molecular basis of endometrial cancer ..... 53
3.2.3 Current diagnostic and treatment methods for endometrial cancer ..... 54

**Chapter 4 Aim of Project ..... 57**

**Chapter 5 Material and Methods ..... 61**
**5.1 Polymersome preparation and characterisation ..... 63**
5.1.1 Polymersome preparation ..... 63
5.1.2 Dialysis tubing preparation ..... 65
5.1.3 Preparation of size separation columns ..... 65
5.1.4 Polymersome NPs characterisation: Dynamic light scattering ..... 66
**5.2 Collection of Endometrium ..... 66**
**5.3 Incubation of *ex-vivo* endometrial tissue with polymersomes ..... 71**
**5.4 Hematoxylin staining of endometrial tissue ..... 72**
**5.5 Immunohistochemistry ..... 72**
**5.6 Primary endometrial stromal cells culture ..... 74**
5.6.1 Making of the media SKUT ..... 74
5.6.2 Preparation of endometrial stromal cells from fresh tissue ..... 74
5.6.3 Changing media for cultured endometrial stromal cells ..... 75
5.6.4 Splitting cultured endometrial stromal cells ..... 76
5.6.5 Freezing endometrial stromal cells ..... 76
5.6.6 Thawing endometrial stromal cells ..... 77
5.6.7 Incubation of endometrial stromal cells with PEG-b-PCL polymersomes loaded with FITC ..... 77
5.6.8 Immunohistochemistry of biotinylated FITC ..... 78

**Chapter 6 Results ..... 81**

**6.2 Hematoxylin staining to check tissue integrity ..... 84**

**6.3 Synthesis of polymersomes: assessment of size distribution ..... 88**

**6.4 Uptake of polymersomes by *ex vivo* human endometrium and release of fluorescent FITC load into the tissue ..... 92**

**6.5 Uptake of polymersomes by primary endometrial cells ..... 108**

**Chapter 7 Discussion ..... 111**

7.1.1 Hematoxylin staining of endometrial tissue ..... 115

7.1.2 Dynamic light scattering ..... 115

7.1.3 Immunohistochemistry ..... 116

**7.2 Investigating polymersomes uptake by primary endometrial cell ..... 117**

**7.3 Future studies ..... 118**

**Chapter 8 References ..... 121**

## *List of Figures*

**Figure 1.1. Different types of nanoparticles.** There is a wide variety of nanoparticles comprised of a range of materials and different architecture, size and molecular mass. ..... 23

**Figure 2.1. Anatomy of the female reproductive tract.** The internal reproductive organs in the female include the fallopian tubes, the ovaries, the uterus and the vagina. These organs are working together for the reproduction. ..... 37

**Figure 2.2. Anatomy of the female reproductive tract.** Illustration of the anatomy of the uterus showing the anatomical position of the different uterus layers, the endometrium and myometrium as well as the position of the fallopian tubes, cervix and vagina. ..... 39

**Figure 2.3. Histology of endometrial tissue.** (a) Endometrial tissue section stained with haematoxylin. Epithelial cells are observed forming the endometrial luminal border of the uterus and circular structures forming glands. Glands are surrounded by connective tissue stromal cells. (b) Close-up of a region of (a) showing the border of the tissue. (c) Illustration of luminal endometrial boarder, glandular cells and stromal cells. ..... 39

**Figure 2.4. Cellular morphological differences between the different menstrual phases under the influence of hormones.** (a)The morphology of the endometrium changes due to different levels of pituitary gonadotropins (FSH, LH) and the ovarian hormones (estrogen, progesterone) during the menstrual cycle. (b), (c) Haematoxylin staining of endometrial tissue in proliferative and secretory phase shows straight, narrow glands and long, tortuous glands respectively. ..... 41

**Figure 2.5. Hormonal and endometrial changes during the menstrual cycle.** In a sexually-mature human female there is a highly synchronised and interdependent series of cycles that take place. These cycles include the release of pituitary gonadotropins (LH and FSH) into the bloodstream, the ovarian steroid response cycle (estrogen synthesis and also later progesterone synthesis) and the uterine endometrium cycle of proliferation and destruction (menses). ..... 42

**Figure 3.1. Appearance of endometriotic lesions.** The size, the colour the morphology and the site of the endometriotic lesions are variable. ..... 45

**Figure 5.1. Polymersome preparation.** PEG-b-PCL block copolymer chains self-assemble in an aqueous environment to form polymersome structures. A hydrophobic membrane is formed by the PCL units of the polymer while the PEG units form a hydrophilic corona and line the interior cavity of the polymersome. The surface can be functionalised with targeting moieties (TAT). Polymersomes can also be loaded with hydrophilic compounds, sodium fluorescein..... 64

**Figure 5.2. Results from the Nanosizer.** The graph demonstrates the average size of the particles and the width of the peak. The diameter of the particles in the above example is 45.58 nm and the width 7.402 nm thus the size of the particles is 45.58 ±7.402. ..... 66

**Figure 5.3. A flow chart of the method for treating tissue with the NPs, fixation and processing.** The tissue is collected by a pipelle biopsy then is incubated with NPs, fixed and cut using a cryostat in 7 and 12μm thick sections..... 71

**Figure 6.1. Hematoxylin staining of endometrial tissue.** Functional layer of endometrial tissue stained with Hematoxylin. (a, c) Endometrial sections from patients numbers 315 and 321 show good tissue integrity. Epithelial cells form intact glandular structures and the cellular layer close to the endometrial

lumen. Stromal cells can be observed forming the connective tissue surrounding intact glands. (b, d) Close-up of a region from images (a) and (c). ..... 85

**Figure 6.2. Hematoxylin staining of endometrial tissue.** Functional layer of endometrial tissue stained with Hematoxylin. (a) Endometrial sections from patient number 316 show good tissue integrity. Epithelial cells form intact glandular structures and the cellular layer close to the endometrial lumen. Stromal cells can be observed forming the connective tissue surrounding intact glands. (b) Close-up of a region from images (a). ..... 86

**Figure 6.3. Hematoxylin staining of endometrial tissue.** Hematoxylin staining of functional layer of endometrial tissue from patient numbers 280, 297and 294 showed poor tissue integrity. Endometrial glands are not intact and holes appeared at the connective tissue which surrounds the gland..... 75

**Figure 6.4. Characterisation with DLS of TAT and No TAT polymersomes made on 16.07.12 used for tissue from patient number 311. (**a) Polymersomes functionalised with TAT peptide on their surface, Z-Average (diameter): 69.48 nm and width 17.10 nm (size: 69.48 ± 17.10 nm). (b) Polymersomes without TAT peptide on their surface, Z-Average: 83.03 nm and width 20.75 nm (size: 83.03 ± 20.75 nm). ..... 89

**Figure 6.5. Characterisation with DLS of TAT and No TAT polymersomes made on 01.10.12 used for tissue from patient number 321.** Polymersomes functionalised with TAT peptide on their surface, Z-Average (diameter): 73.26 nm and width 16.78 nm (size 73.26 ± 16.78 nm). ..... 90

**Figure 6.6. Characterisation with DLS of TAT and No TAT polymersomes made on 15.10.12 used for tissue from patient numbers 326 and 327.** Polymersomes functionalised with TAT peptide on their surface, Z-Average (diameter): 46.34 nm and width 7.46 nm (size 46.34 ± 7.46 nm). ..... 91

**Figure 6.7. Characterisation with DLS of TAT and No TAT polymersomes made on 22.10.12 used for tissue from patient numbers 325, 324 and 330.** (a) Polymersomes without TAT peptide on their surface, Z-Average (diameter): 45.58 nm and width 7.40 nm (size: 45.58 ± 7.40 nm). (b) Polymersomes functionalised with TAT peptide on their surface, Z-Average (diameter): 62.12 nm and width 11.76 nm (size: 62.12 ± 11.76 nm). ..... 91

**Figure 6.8. Anti FITC labelling in tissue treated with PBS (No NPs) for 10 min at room temperature.** Tissue sections were incubated with PBS and not polymersomes are processed for IHC. (a) No signal at the wavelength of FITC (518nm) was observed. (b) Stain of cell nucleus with DAPI (blue). (c) Overlay image of images (a) and (b). ..... 93

**Figure 6.9. MUC-1 positive control. Functional layer of endometrial sections stained with MUC-1.** MUC-1 can be observed marking the inside of glands demonstrating intact glandular structures (yellow stars) and the luminal surface of the epithelial cells that form the borders of the endometrial tissue (green stars). ..... 94

**Figure 6.10. Functional layer of endometrial tissue from patients numbers 321 and 311 was incubated with polymersomes with TAT peptide on their surface at the concentration of 3ug/ml, sectioned in 7μm thick sections and labelled for NPs.** Endometrial tissue from patient number 321 was incubated with polymersomes. (a) 40x magnification image showing that polymersomes are taken up by endometrial stromal cells and release their cargo FITC into them (green). (b) Overlay image of DAPI (blue) which stains the cell nucleus and FITC (green). (c, d) close-up (100x magnification) of a region (a, b) presenting FITC signal in endometrial cells. Endometrial tissue from patient number 311 was incubated with polymersomes. (a) 40x magnification image showing that

polymersomes are taken up by endometrial epithelial cells, which form the borders of the endometrial tissue, and release their cargo FITC into them (green). (b) Overlay image of DAPI (blue) which stains the cell nucleus and FITC (green).....95

**Figure 6.11. Functional layer of endometrial tissue from patient number 325 was incubated with polymersomes with TAT peptide on their surface at the concentration of 3ug/ml, sectioned in 7μm thick sections and labelled for NPs.** Endometrial tissue from patient number 325 was incubated with polymersomes. (a) 40x magnification image showing that polymersomes are taken up by endometrial stromal and epithelial cells and release their cargo FITC into them (green). (b) Overlay image of DAPI (blue) which stains the cell nucleus and FITC (green). (c, d) close-up (100x magnification) of a region (a, b) presenting FITC signal in endometrial stromal cells. (e, f) close-up (100x magnification) of a region (a, b) presenting FITC signal in endometrial epithelial cells. .....97

**Figure 6.12. Functional layer of endometrial tissue from patients numbers 315 and 316 was incubated with polymersomes with TAT peptide on their surface at the concentration of 3ug/ml, sectioned in 7μm thick sections and labelled for NPs.** Endometrial tissue from patient number 315 was incubated with polymersomes. (a) 40x magnification image showing that polymersomes are taken up by endometrial stromal cells and release their cargo FITC into them (green). (b) Overlay image of DAPI (blue) which stains the cell nucleus and FITC (green). (c, d) close-up (100x magnification) of a region (a, b) presenting FITC signal in endometrial stromal cells. Endometrial tissue from patient number 316 was incubated with polymersomes. (a) 40x magnification image showing that polymersomes are taken up by endometrial stromal cells and

release their cargo FITC into them (green). (b) Overlay image of DAPI (blue) which stains the cell nucleus and FITC (green). ..... 98

**Figure 6.13. Functional layer of endometrial tissue from patient number 327 was incubated with polymersomes with TAT peptide on their surface at the concentration of 3ug/ml, sectioned in 7μm thick sections and labelled for NPs.** Endometrial tissue from patient number 327 was incubated with polymersomes. (a) 40x magnification image showing that polymersomes are taken up by endometrial stromal and release their cargo FITC into them (green). (b) Overlay image of DAPI (blue) which stains the cell nucleus and FITC (green). (c) 40x magnification image showing that polymersomes are taken up by endometrial stromal and epithelial cells and release their cargo FITC into them (green). (d) Overlay image of DAPI (blue) which stains the cell nucleus and FITC (green). ..... 99

**Figure 6.14. Endometrial tissue from women in different phase of the menstrual cycle.** Endometrial tissue from 2 patients in different phase of the menstrual cycle, first patient number 321 in secretory phase (a, b) and second patient number 327 in secretory phase (c, d) was labelled for polymersomes. Polymersomes are taken up by endometrial cells from both patients. ..... 101

**Figure 6.15. No TAT polymersomes are taken up by endometrial cells.** Polymersomes without TAT peptide on their surface are taken up by both endometrial stromal (a, b) and epithelial cells (c, d). ..... 102

**Figure 6.16. TAT polymersomes are taken up by endometrial cells.** Polymersomes functionalised with TAT peptide on their surface are taken up by both endometrial stromal (a, b) and epithelial cells (c, d). ..... 103

**Figure 6.17. Endometrial tissue incubated with polymersomes functionalised with TAT peptide in 0.06ug/ml concentration.** Endometrial tissue was

incubated with NPs functionalised with TAT in the concentration of 0.06ug/ml. (a) NPs are taken up by endometrial stromal cells even in this low concentration. (b) Overlay image of DAPI (blue) which stains the cell nucleus and FITC (green). ..... 104

**Figure 6.18. Endometrial tissue is stained for Cytokeratin.** (a, b) Successful labelling of epithelial cells with Cytokeratin in endometrial tissue. (c,d) Close-up of a region from figure (a) clearly shows that Cytokeratin (red signal) reacts only with epithelial cells and not with stromal cells in endometrial tissue. ..... 105

**Figure 6.19. Endometrial tissue is stained for Vimentin.** (a, b) Vimentin is an effective marker for endometrial stromal cells. (c,d) Close-up of a region from figure (a) demonstrate that Vimentin stains effectively only stromal cells in endometrial tissue. ..... 106

**Figure 6.20. Functional layer of endometrial tissue was stained for Vimentin and FITC (antibodies incubation 90min).** (a, c) Vimentin (red) which is a marker for stromal cells stained also endometrial epithelial cells which form the borders of the endometrial tissue and glands. (b, d) Tissue sections were labelled for Vimentin (red), FITC (green) and DAPI (blue). ..... 107

**Figure 6.21. Functional layer of endometrial tissue was stained for Vimentin and FITC (antibodies incudation 60min).** (a, c) Vimentin (red) which is a marker for stromal cells stained also endometrial epithelial cells which form the borders of the endometrial tissue and glads. (b, d) Tissue sections were labelled for Vimentin (red), FITC (green) and DAPI (blue). ..... 108

# *List of Tables*

**Table 1.1. Nanoparticles are tested in order to be used for cancer therapy.** Nanoparticles have been examined for ovarian, cervical, breast, endometrial and brain cancer. ..... 22

**Table 3.1. Selection of proteins which display significant different expression levels in uterine fluid from women with endometriosis compared to uterine fluid from healthy women.** Changes were observed in proteins implicated in cell signalling and movement, cytoskeleton structure and immune reaction [74]. ..... 49

**Table 3.2. Incidence and treatment options for management of endometriosis.** Endometriosis is a prevalent disease, which is treated with surgical and systemic drug therapy (Royal College of Obstetricians and Gynaecologists 2005) [81]. ..... 50

**Table 3.3. Tumour classification.** Tumour is classified as grade 1, 2 and 3 by the degree of abnormality in the glandular architecture [88] ..... 52

**Table 3.4. Incidence, prognosis and treatment options for endometrial cancer management.** Endometrial cancer is a disease with high incidence mostly in women older than 50 years and is currently treated with systemic administration of hormonal drugs, radiation therapy and chemotherapy ..... 55

**Table 5.1. Summary of the biopsies that have been collected.** Endometrial biopsies from 19 patients have been collected. The integrity of the tissue has been checked for 12 of them. 9 showed bad tissue integrity and 3 good, the rest of the tissue hasn't been checked yet. Tissue from 6 patients has been processed

for immunohistochemistry. Is unknown whether or not the patient had endometriosis when laparoscopy has not taken place; (Y= YES, N=NO). .....62

**Table 5.2. Primary antibodies dilutions.** The table summarize the primary antibodies and the dilutions that have been used for these experiments. ……..65

**Table 6.1. Nanoparticle size distribution.** Nanoparticles with and without TAT peptide on their surface were checked after their preparation and tissue incubation for their monodispersity using dynamic light scattering. .....78

**Table 6.2. Summary table present women's cycle phase, polymersomes' concentration during incubation with endometrial tissue and polymersomes' uptake by endometrial cells.** When endometrial tissue was incubated with polymersomes in the high concentration of 3ug/ml NPs were taken up by cells independent of women's cycle phase. .....88

**Table 7.1. Cell penetrating peptides.** Penetratin, Transportan and pVEC are cell penetrating peptides that have been used to deliver in cells a broad variety of cargos. .....104

**Table 7.2. Samples of uterine fluid (n=20) and blood (n=12) from 23 women with endometrial pathologies**…….....105

## *List of Abbreviations and Acronyms*

| | |
|---|---|
| AFS | American Fertility Society |
| BMI | body mass index |
| CDC | centre for disease control and prevention |
| DLS | dynamic light scattering |
| DMF | dimethylformamide |
| DOX | Doxorubicin |
| DPX | Di-N-Butyle Phthalate |
| EPR | enhanced permeability and retention effect |
| FITC | fluorescein |
| FR | folate receptor |
| FITC | sodium fluorescein |
| Her-2/neu | human epidermal growth factor receptor 2 |
| IHC | immunohistochemistry |
| NP | nanoparticles |
| OCT | optimal cutting temperature |
| PBS | phosphate buffer saline |
| PCL | poly(ε-caprolactone) |
| PEG | polyethylene glycol |
| PEG-b-PCL | poly(ε-caprolactone)-block-poly(ethylene glycol) |

| | |
|---|---|
| PFA | paraformaldehyde |
| TAX | taxol |

# Chapter 1

## Introduction

## 1.1 Nanomedicine

Nanomedicine is a rapidly advancing field, which uses particles at the nanoscale (1-100 nm) in the discipline of medicine [1]. The first generation of nanoparticles (NPs) involved polymers and liposomes. Various types of NPs have been developed including micelles, metallic, magnetic, quantum dots, nanocapsules, polymersomes, liposomes and mesoporous silica nanoparticles that are composed of a range of organic materials including lipids, polymers and inorganic materials (Figure 1.1). NPs have been successfully used as drug-, DNA- and siRNA-delivery vehicles. Their popularity was based on several advantages that they provided for their delivering payload, such as prolonged circulation time in the body and protection of the loaded therapeutic from degradation. Furthermore, when cells were incubated with NPs loaded with a drug, an increase in the cellular uptake of the drug was observed compared to the free drug [2]. Different types of NPs have been used to improve treatment, diagnosis and imaging of cancers (Table 1.1) as well as infectious and age-related diseases [3, 4]. Furthermore, in order to reduce the side effects of treatments, specific targeting of NPs was introduced at the diseased area. The surface of the NPs is functionalised with antibodies and proteins, and afterwards in order to decrease their size, which is crucial for their uptake as well as for their extended circulation time, short peptides such as ligands and reporter molecules are used for different targeting purposes [5, 6]. In addition, cell-penetrating peptides, such as the TAT peptide, are introduced to enhance cellular penetration and internalisation of NPs [7].

Nanomedicine has been used broadly in the field of cancer for the development of new and more effective treatments. Cancer therapy using nanoparticles is rapidly progressing and employed to solve several limitations of the conventional drug delivery systems, such as nonspecific biodistribution and targeting, lack of water solubility and poor oral bioavailability [8]. Table 1.1 summarizes the different types of

NPs currently under investigation as possible treatments for the different types of cancer.

| Nanoparticle type | Disease | Reference |
|---|---|---|
| • Folate targeted-PLGA (poly(d,l-lactide-co-glycolide))-PEG (Polyethylene glycol)<br>• Epidermal growth factor receptor targeted-PLGA-PEG | Ovarian carcinoma | [6]<br>[9] |
| • Folate targeted-liposomes<br>• Supermagnetic Dextran Iron Oxide NPs<br>• Gold NPs | Cervical cancer | [10]<br>[11]<br>[12, 13] |
| • HER-1-magnetic nanocrystals<br>• Chitosan NPs | Breast cancer | [14]<br>[15] |
| • Folate targeted-PLGA-PEG | Endometrial cancer | [16] |
| • Cetyl alcohol/polysorbate NPs | Brain tumour | [17] |

**Table 1.1. Nanoparticles are tested in order to be used for cancer therapy.** Nanoparticles have been examined for ovarian, cervical, breast, endometrial and brain cancer.

In Figure 1.1 different types of NPs are presented from a variety of materials. NPs' structure and size is related to the materials they are made of. Furthermore, different types of NPs are synthesised in order to suit particular applications of interest.

Organic NPs offer advantages over inorganic NPs as they are made of biodegradable materials (such as polymers and lipids); hence they are more likely to be biocompatible and non-toxic. Information about the interaction of organic NPs

with biological tissue is important considering that organic NPs have been extensively used as drug delivery vehicles and many have already been approved by the Food and Drug Administration of the USA for clinical use [8].

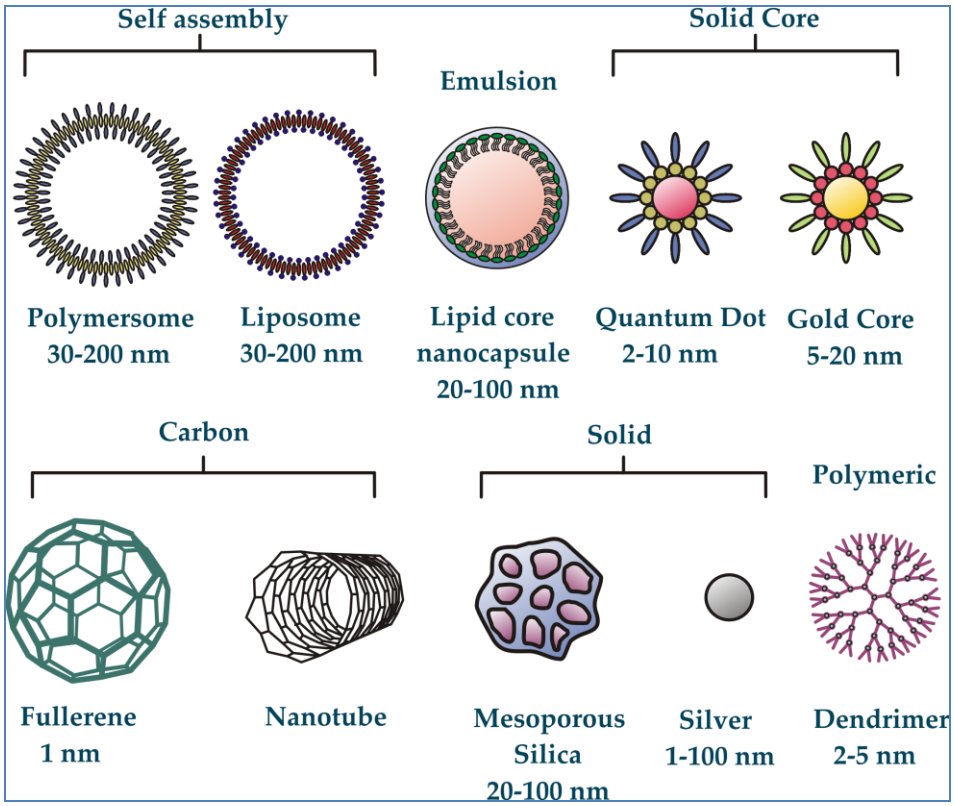


**Figure 1.1. Different types of nanoparticles.** There is a wide variety of nanoparticles comprised of a range of materials and different architecture, size and molecular mass. (Adapted from A. Johnston) [18].

Drugs encapsulated in liposomes and polymer-drug conjugates such as PEGylated drugs are widely used in clinical trials. Liposomes are self-assembled structures that are formed by phospholipids. An outer lipid bilayer surrounds the liposomes' aqueous core. Water soluble drugs can be entrapped in the liposome's core and hydrophobic drugs can be encapsulated in its lipid bilayer. Although liposomes are a successful tool for some clinical applications, their fast clearance from the blood by phagocytic cells of the reticulo-endothelial system, their poor

storage stability and rapid drug release profiles in vivo make their usage as drug carriers limited, the loading of liposomes is typically non-covalent and therefore cargo leakage can be an issue [19].

Dendrimers have also emerged as another type of organic nanocarriers that can carry several drugs on their surface or alternatively be loaded with drugs using the cavities in their cores. Dendrimers are three-dimensional nanoparticles which grow outwards from a multifunctional core molecule. The core molecule reacts with monomer molecules giving the first generation dendrimer. Then the new periphery of the molecule is activated for reactions with more monomers. The process is repeated for several generations until the dendrimer is eventually constructed layer by layer. Dendrimers have already been used in many *in vivo* studies showing that these NPs accumulate not only at the diseased tissue (e.g. tumour site), but also in healthy tissue and especially in kidneys, spleen and liver. [20] Because of their non-specificity, their clinical use has been delayed.

Polymer based drug carriers have been developed as a solution to overcome liposomes' limitations. Polymers can self-assemble into a variety of different structures, with two of the most common structures being micelles and polymersomes. Micelles are spheres of 20-100nm in size with a hydrophobic core and a hydrophilic exterior surface. Unlike polymer micelles polymersomes have a similar architecture to liposomes with a hydrophobic membrane, hydrophilic surface and aqueous core [21]. A range of therapeutics and active components have been successfully loaded in micelles and polymersomes [22]. Micelles as they only contain a hydrophobic interior are more limited for loading, making them suited for loading hydrophobic compounds. On the other hand, polymersomes having a similar structure to liposomes are able to be loaded with both hydrophobic and hydrophilic drugs. In parallel they show a number of advantages over liposomes

including higher drug loading capability, increased stability in vivo thus prolonged circulation time and finally maintenance of loaded materials for longer time [23]. Furthermore their surface can be modified with a variety of molecules allowing them to interact with environment and thus provide either controlled or triggered release of the drug [24].

In contrast, inorganic NPs such as gold NPs are also interesting tools for imaging, diagnostics and therapy. Gold NPs for instance are already in the first stage of clinical trials as part of treatment of patients who suffer from cancer. Gold NPs have been emerged as delivery vehicles for anti-tumour drugs as well as for siRNA showing reduced side effects, when NPs were targeted specifically to tumours and resulting in stabilizing or even reducing tumour's development in some patients [25]. One important drawback, of using inorganic NPs that was observed in many trials is that they were found not only within the tumour tissues but also in healthy tissue, such as liver and spleen thus they are toxic by themselves [25].

## 1.2 Polymersomes

Amphiphilic block copolymers have attracted attention in terms of their ability to form various types of nanoparticles (micelles, polymersomes, nanospheres, nanocapsules, polyplexes). Polymersomes comprised of biodegradable amphiphilic block copolymers; they are stable for up to several months at 4°C and release their loaded drugs for up to five weeks at 37°C [26, 27]. In polymersomes hydrophobic compounds can be entrapped into the polymersomes' bilayer and hydrophilic molecules can be encapsulated in the polymersomes' core. The polymer carrier extends the stability of the encapsulated drug, increases the life time of the drug in the blood, and is an ideal candidate for a controlled drug release [28]. Moreover, polymersomes can change a drug's biodistribution by altering its accumulation at the

diseased area, either passively (enhanced permeability and retention effect, EPR) at tumour site, or actively when they are functionalised with ligands which can identify overexpressed molecules in the diseased area [29]. Further, polymersomes can not only be used as drug-delivery agents, but also as imaging agents in order to direct and non-invasively diagnose a disease [30].

One of several blocks of copolymers which is used to construct polymersomes is poly(ε-caprolactone)-block-poly(ethylene glycol) (PEG-b-PCL). Their hydrophilic membrane is formed by the poly(ε-caprolactone) (PCL) units of the polymer, while the polyethylene glycol (PEG) forms a hydrophilic corona and line the interior cavity of the polymersome. Both PEG and PCL are biodegradable polymers used in medical applications. Furthermore, PEG polymer is biocompatible and exhibits high resistance to both protein absorption and cell adhesion having as a result prolonged circulation times. Finally, toxicity studies of methoxy PEG-b-PCL polymersomes loaded with paclitaxel and indomethacin, an anticancer and anti-inflammation agent respectively, have not shown any histological changes in heart, liver or kidney, even after seven days of intraperitoneal application of the median lethal dose of the drug (much higher dose compared to the practical effective dose) loaded polymersomes [31].

### 1.2.1 *Polymersomes in Cancer treatment*

Nanomedicine has been used in the treatment of various types of cancer (Table 3.2, Chapter 3.1.). Currently, compounds with toxic side effects or low bioavailability are promising as therapeutic agents (for example chemotherapeutic drugs such as Doxorubicin and Paclitaxel). These disadvantages decrease the possibilities of a therapeutic agent to reach the diseased area, hence diminishing its therapeutic value. Consequently, synthesis of polymeric fully biocompatible delivery vehicles, entrapping therapeutic agents and releasing them in appropriate concentrations, only on the area of interest, may increase drug's efficacy as well as decreasing any

unwanted side effects. It has already been shown for instance that polymersomes are able to target human cells in the inner ear and deliver the drug Disulfiram, which is clinically used as an anti-alcoholism drug and recently have been also shown its anti-cancer effect [32].

Paclitaxel or Taxol (TAX) is an anticancer agent with significant activity against various types of cancer, though it is reduced due to its poor aqueous solubility. Currently, in order to overcome this limitation TAX is administrated in combination with Cremophor EL to produce a soluble formulation. Systemic administration of this drug is associated with lots of side effects in patients (such as hypotension and dyspnoea). Additionally, the solubilising Cremophor EL is associated with severe hypersensitivity responses [33, 34]. As a result several aqueous formulations of TAX, such as Micelles (Genexol-PM, composed of PEG-poly (D,L-lactic acid) (PEG-PLA) block copolymer) as well as PEO-b-PBD polymer vesicles have been examined in order to reduce the side effects, and at the same time to increase its water solubility by maintaining the cytotoxic properties of the drug against cancer cells only [35-37].

Polymersomes have also been examined as carriers of combination drugs, TAX and Doxorubicin (DOX). The delivery of two different drugs such as TAX, in the hydrophobic bilayer and DOX, in the hydrophilic core, at normally prescribed concentrations, from the same polymeric vesicle on the diseased area, has been shown to have a synergistic effect and maximize their cytotoxicity. PEG-b-PLA and PEG-b-PBD polymersomes were used for DOX and TAX delivery at tumour site *in vivo* [38]. The results demonstrated increased and faster shrinkage of the tumour following the injection of (TAX+DOX)-polymersomes, compared to the tumours treated with the free drug cocktail [38].

### 1.2.2 *Polymersomes in Cancer diagnosis*

The fact that polymersome NPs can be non-invasively imaged *in vivo* gives the advantage of using them not only as therapeutic, but also as diagnostic compounds. Polymersomes can encapsulate fluorescent agents for optical imaging to monitor their biodistribution. This can be used for non-invasive detection of the diseased area, leading to an easier more precise way of diagnosis. The final location of the NPs after they have released their encapsulated drug can also be monitored. To track NP uptake and targeting fluorescent tags and fluorophore-conjugated molecular probes have been used to show nanoparticles biodistribution. Previous studies have shown that polymersomes loaded with near infrared (NIR) fluorophores can be injected at tumour sites to allow deep-tissue optical imaging. Additionally, NIR has shown that nanoparticles are able to penetrate through 1cm of solid tumour [39]. In addition, NIR emissive polymersomes injected into the tail of mice have been employed to track their biodistribution *in vivo* via non-invasive NIR fluorescence-based optical imaging [40]. Furthermore, recent research in our group showed that poly (ethylene-glycol) and poly (capro-lactone) (PEG-b-PCL) polymersome nanoparticles with fluorescent tags conjugated on their surfaces have been used to track nanoparticle distribution *in vivo* and *in vitro* [41]. Thus it is clear that polymersome nanoparticles with encapsulated imaging agents can be used a) to track nanoparticles in order to screen them when they release a drug, b) for accumulation on the diseased area either passively (EPR effect) or actively (ligands on their surfaces) in order to fluorescently label the diseased area and thus achieve surgical identification by fluorescence imaging.

### 1.2.3 *Surface modification of polymersomes for enhanced delivery and targeted therapy*

Functionalisation of polymersomes surface with molecules-ligands is used for specific cell targeting or for enhancing cellular internalisation. Conjugation of biological ligands on polymer surfaces permits targeting of upregulated receptors (e.g. Folate receptor in endometrial cancer and molecules on affected cells *in vitro* and *in vivo* and thus decreases the potential side effects of the systemic drug delivery [6]. In polymersomes targeting moieties can be conjugated to the end group of their hydrophilic polymer groups e.g. PEG and thus can be guided to specific sites (diseased area) *in vivo*. Roy et al. have shown the ability of PEG-b-PCL nanoparticles to specifically targeted to certain cells, especially Schwann cells and nerve fibres, by conjugating a short peptide sequence on their surface which binds to the tyrosine Kinase B (TrkB) receptor [42]. In addition *in vivo* studies with PEG-b-PCL polymersomes have shown that they can be targeted to and able to deliver drugs to neuronal cells as well as the outer ear hair cells after functionalisation of their surfaces with the appropriate targeting peptides [43, 44]. Furthermore, in vitro activation of TrkB receptors have been achieved by conjugation of a short peptide mimetic of human nerve growth factor β (NGFβ) on the surface of PEG-b-PCL polymersome nanoparticles [45]. Polymersomes functionalised with an antibody against the intracellular adhesion molecule-1 (ICAM-1) has been used to target endothelial cells in early inflammation [5]. In addition, polymersomes have successfully been used as vehicles for targeted delivery of siRNA to treat different types of cancer [46, 47]. Nanoparticles made of a cyclodextrin-based polymer functionalised with a ligand (transferrin protein) to interact with the transferrin protein receptors on the surface of cancer cells and loaded with the appropriate siRNA have been used in a clinical trial to decrease the expression of the M2 subunit of ribonucleotide reductase (RRM2) specifically in cancer cells of patients with melanoma [46].

Ligands attached to the surface of nanoparticles' can also be used to assist nanoparticle uptake into cells. TAT peptide, derived from the HIV virus, contains a protein transduction domain which can be internalised by cells, the exact mechanisms by which it works remains uncertain [7]. NIR-emissive polymersome nanoparticles, once functionalised with the TAT peptide, showed enhanced cellular uptake without affecting cells' viability [30].

### 1.2.4 *TAT peptide*

TAT peptide is a highly cationic peptide composed of 6 arginine and 2 lysine residues (sequence RKKRRQRRR) and belongs to the cell-penetrating peptide (CPP) family [48]. It was shown that these cationic residues are responsible for the translocation activity. When Arginine or Lysine was replaced with neutral residues (Alanine), cellular uptake was decreased showing that these cationic residues might be necessary for electrostatic interactions with the cell membrane such as interactions with lipid head groups or proteoglycans [48]. Membrane association of TAT peptide occurs at temperatures down to $4^0$C, at this temperature is known that all cellular energy-dependent pathways are inhibited. However, TAT peptide crosses the extracellular membrane in an energy dependent way and thus requires temperatures higher than $4^0$C and ATP. Once TAT is associated with the cell membrane is rapidly translocated at the cytosolic side probably within vesicle-like structures [49]. This is supported by findings of experiments with fluorescently labelled TAT peptide which showing that TAT in live cells is often observed as being punctuate or vesicular [50] and rarely diffused in cytosol [51]. TAT signal was detected close to the membrane at early points and at longer times was observed to form larger aggregations close to the nucleus and finally observed moving into the nucleus [49, 52].

In the present study, the TAT peptide was used to enhance the permeation of polymersomes into human endometrium, epithelial and stromal cells. The biochemical properties of this peptide are discussed below.

## 1.3 Investigations of nanoparticles in the endometrium

Nanoparticles have not yet been tested for the diagnosis or treatment of endometriosis, however, due to the accessibly of the pelvic cavity, where endometrial lesions are found, and the uterus where abnormal endometrial cells are exist (see Chapter 3.1.2.1) nanoparticles are a promising tool [53]. Nanoparticles could be delivered to the abnormal cells of the endometrium of women with endometriosis in order to prevent lesion formation. They could also be fluorescently labelled and targeted to the lesions in the pelvic area, which can be achieved due to the different properties of the cells that form the lesions compared with the cells that form the normal peritoneum (see Chapter 3.1.2.2), to specifically target them. This could help surgeons to identify and eradicate all stages and types of endometriotic lesions even the microscopic or clear lesions (see Chapter 3.1).

### 1.3.1 *Testing nanoparticles in primary cell cultures*

A lot of research has been done with established cell lines and NPs, usually loaded with a compound, such as a drug, in order to check their efficacy *in vitro* [2, 54]. The question that arises is whether established cell lines are adequate target cells with regard to clinical relevance of the results that derive from these studies. Primary cell lines isolated from target tissues are desirable for in vitro studies as these cells simulate the *in vivo* situation more closely than the established cell lines. On the other hand primary cell lines have some limitations, firstly they are not well characterized and secondly as they derive from different patients can behave differently in culture

conditions depending on the genetics and age of individuals from whom the tissue was obtained. However, primary cell lines are ideal tool in order to check a mechanism before *ex vivo* and *in vivo* experiments. Until today only few studies with primary cell lines and NPs have been done and the majority of them comprise only cytotoxicity tests [55]. Zhao et al. in delivery experiments have shown that chitosan NPs, loaded with EGFP DNA, are effective delivery vehicles by testing them in primary chondrocytes [56]. Although nanoparticles are very promising tools for drug or imaging agent encapsulation and their targeted delivery to the affected area (e.g. tumour site) there are still concerns related with their cytotoxicity which delay their usage in human therapy.

Polymersomes are biocompatible and fully biodegradable nanoparticles which mean they have minimum *in vivo* cytotoxicity. This study intends to exploit cellular differences in eutopic endometrium (Chapter 3.1.2.1) and the advantages of polymersomes (PEG-b-PCL) biocompatibility, targeting and delivery of potential therapeutic drugs to aid diagnosis and treatment of endometrial pathology without the need for invasive surgical procedures such as laparoscopy.

### 1.3.2 Nanoparticle's intracellular fate

As the therapeutic effect of the majority of the drugs is related with specific locations in the cell, their intracellular fate after internalisation is significant. Therefore it is pivotal to understand NPs' internalisation mechanisms as these mechanisms determine the drug's intracellular trafficking and the chemical environment that the therapeutic compound is exposed to. Whilst hydrophobic compounds with low molecular weights can passively pass through the cell membrane, other molecules such as hydrophilic molecules show limited uptake by

cells due to the lipids of cell membranes. In addition larger materials such as NPs enter cells via endocytosis [57]. In this mechanism, particles are surrounded by a lipid bilayer that completely isolates particles from the cytosol. Phagocytosis and pinocytosis are the two broad categories of endocytosis [58]. Phagocytosis generally happens in macrophages and dendritic cells. As this mechanism is one the first line of defence of the immune system, it is a continuing challenge to construct particles that could escape macrophage clearance and thus show prolonged circulation times. Pinocytosis occurs in almost all cell types and includes macropinocytosis, clathrin-mediated endocytosis, caveolae-mediated endocytosis, and clathrin/caveolae pathways [58]. When the route of NPs' uptake is clathrin-mediated endocytosis, particles uptake proceeds from early endosomes, to late endosomes, and onto lysosomes. Cargo that enters the cell via this route is subject of lysosomal degradation. If the caveolae-mediated route takes place, NPs are encapsulated within endosomes and then move to the Golgi apparatus or the endoplasmic reticulum. Finally, if macropinocytosis occurs, large endocytic vesicles up to 5μm in diameter are generated by actin driven invagination of plasma membrane [58, 59]. The endocytic vesicles in this case do not fuse with lysosomes. These vesicles are thought to be leaky compared to other types of endosomes. Thus cargo escape into the cytoplasm has been shown. For drug delivery, the most favourable pathways of internalisation are macropinocytosis and caveolae-mediated endocytosis as they are associated with less degradation of the cargo. NPs' size, surface charge, surface functionality, concentration and incubation time are some parameters that affect their internalisation rates.

Hence, it is important not only to show that NPs can enter the cell, but also understand their internalisation route and how they are able to release their cargo into the cell. To this end PEG-b-PCL polymersomes have been loaded with a model drug, FITC, to demonstrate NPs' internalisations and intracellular payload release.

# Chapter 2

## The reproductive system

## 2.1 *The reproductive system:* Anatomy and physiology

The reproductive system functions to allow oocyte fertilisation and embryo growth, fetal development and ultimately birth of a child. The female reproductive tract consists of the uterus, vagina, fallopian tubes and the ovaries (Figure 2.1). The vagina, also known as the birth canal, links the cervix with the outside of the body. The uterus is a pear-shaped organ which hosts the developing fetus. It is divided in two parts, the lower part of the uterus, the cervix that opens into the vagina and the corpus which is the main body of the uterus. The ovaries are small, oval-shaped glands which are found one in each side of the uterus. The function of the ovaries is to produce oocytes and hormones. Finally, the fallopian tubes are narrow tubes that are attached to the upper part of the uterus. The oocyte travels through the fallopian tubes from the ovaries to the uterus [60].

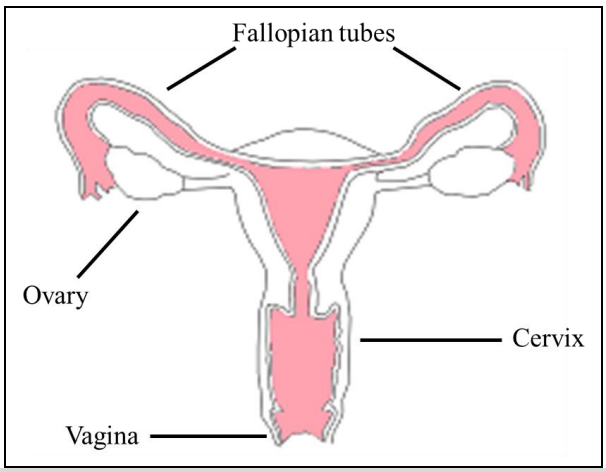


**Figure 2.1. Anatomy of the female reproductive tract.** The internal reproductive organs in the female include the fallopian tubes, the ovaries, the uterus and the vagina. These organs are working together for the reproduction.

The female reproductive system produces the female egg cells, the oocytes, which are necessary for the reproduction. The conception, the fertilisation of the

oocyte by a sperm, normally occurs in the fallopian tubes. The initial stages of pregnancy start once the fertilised egg implant into the walls of the uterus, a lining called the endometrium. If fertilisation and/or implantation do not take place, menstruation occurs (the monthly shedding of the uterine lining). The regulation of menstruation and uterus lining growth and renewal are controlled by the sex hormones, estrogen and progesterone. These hormones provide monthly, cyclic regulation of reproductive system [60].

## 2.2 *The uterus*: Anatomy and physiology

The human uterus is a vital organ of the female reproductive tract. Its reproductive function is to receive, hold and nourish the fertilised ovum. The size of the uterus changes significantly during pregnancy. Its size in an adult non-pregnant female is about 7cm long, 5 cm wide and 2.5cm in diameter [60]. It is located in the pelvis between the bladder and rectum [61]. The uterine corpus is composed of a mucosa lining which lines the uterine cavity, it is also known as the endometrium. The endometrium is the cellular layer which faces the lumen of the uterus. The endometrium is functionally divided in layers the functional and the basal layer and a fibro-muscular layer, called myometrium (Figure 2.2) [60].

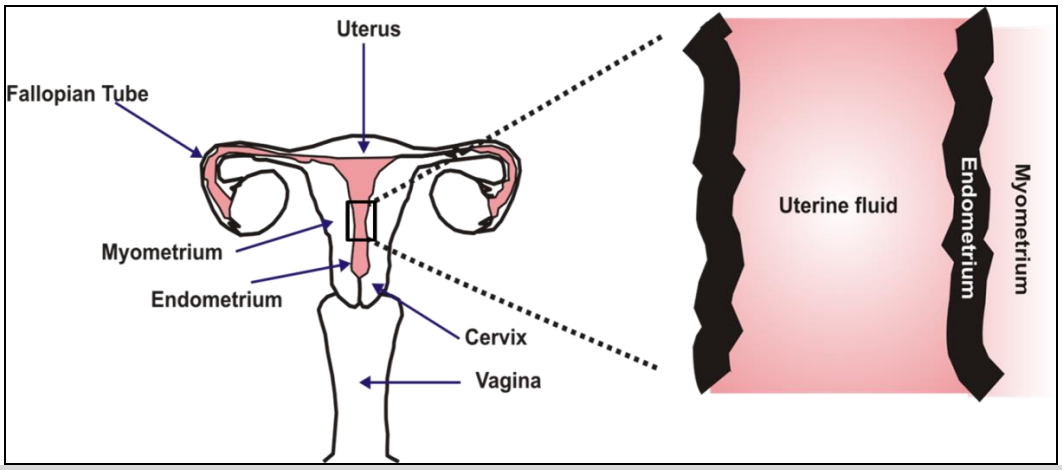


**Figure 2.2. Anatomy of the female reproductive tract.** Illustration of the anatomy of the uterus showing the anatomical position of the different uterus layers, the endometrium and myometrium as well as the position of the fallopian tubes, cervix and vagina.

The endometrium is made up of specialised cells which are able to accept the embryo and undergo cyclic changes in response to monthly fluctuations in pituitary gonadotropins (FSH, LH) and sex hormones (estrogen, progesterone) [60].

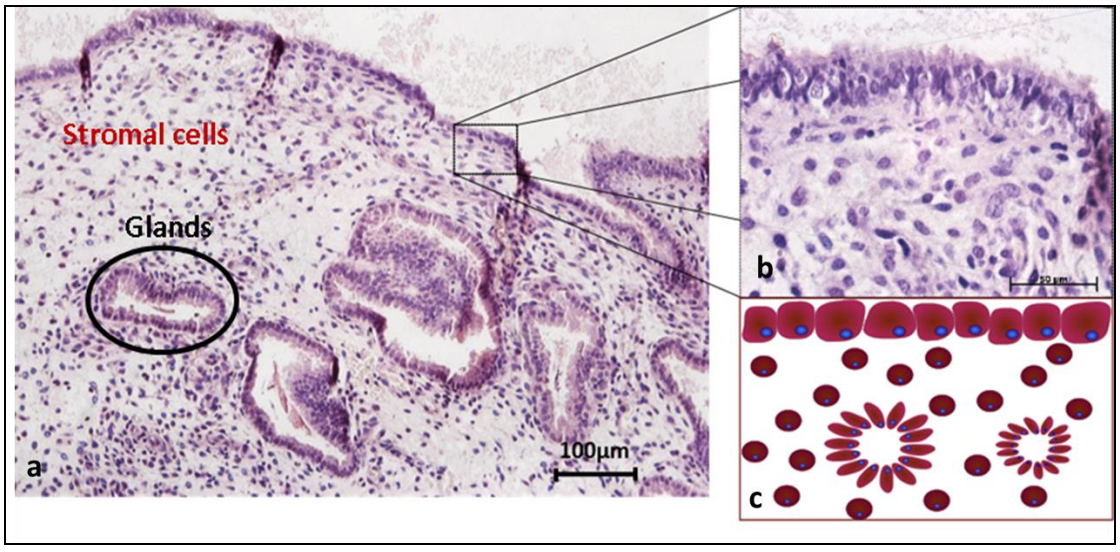


**Figure 2.3. Histology of endometrial tissue**. (a) Endometrial tissue section stained with haematoxylin. Epithelial cells are observed forming the endometrial luminal border of the uterus and circular structures forming glands. Glands are surrounded by connective tissue stromal cells. (b) Close-up of a region of (a) showing the border of the tissue. (c) Illustration

of luminal endometrial boarder, glandular cells and stromal cells.

The endometrium is broadly composed of two cell types, epithelial cells and stromal cells. Within this board classification there are subtypes of epithelial cells, columnar epithelium, which form the epithelial luminal border of the uterus and glandular epithelial cells which form endometrial glands. Stromal cells form the connective tissue which surrounds the glands (Figure 2.3) [62]. Endometrial stromal cells undergo major morphological changes which are related with the different phases of menstrual cycle. Stromal cells decidualize spontaneously under the influence of progesterone in order to prepare the endometrium for the implantation [62].

## 2.3 The menstrual cycle

The menstrual cycle is divided in three phases, the first phase of the menstrual cycle is the proliferative phase, which is followed by the secretory phase, and then by menstruation. During the menstrual cycle the morphological appearance of the endometrium changes [63]. During the proliferative phase the endometrium proliferates under the stimulation from estrogen and certain number of epithelial cells that from the columnar epithelium become equipped with cilia. In the secretory phase the endometrium attains its full maturity under the influence of progesterone and glandular structures become longer and tortuous [63] (Figure 2.4. b, c). At this stage full mature endometrium is ready to receive the embryo and this time period is termed the 'implantation window' [63].

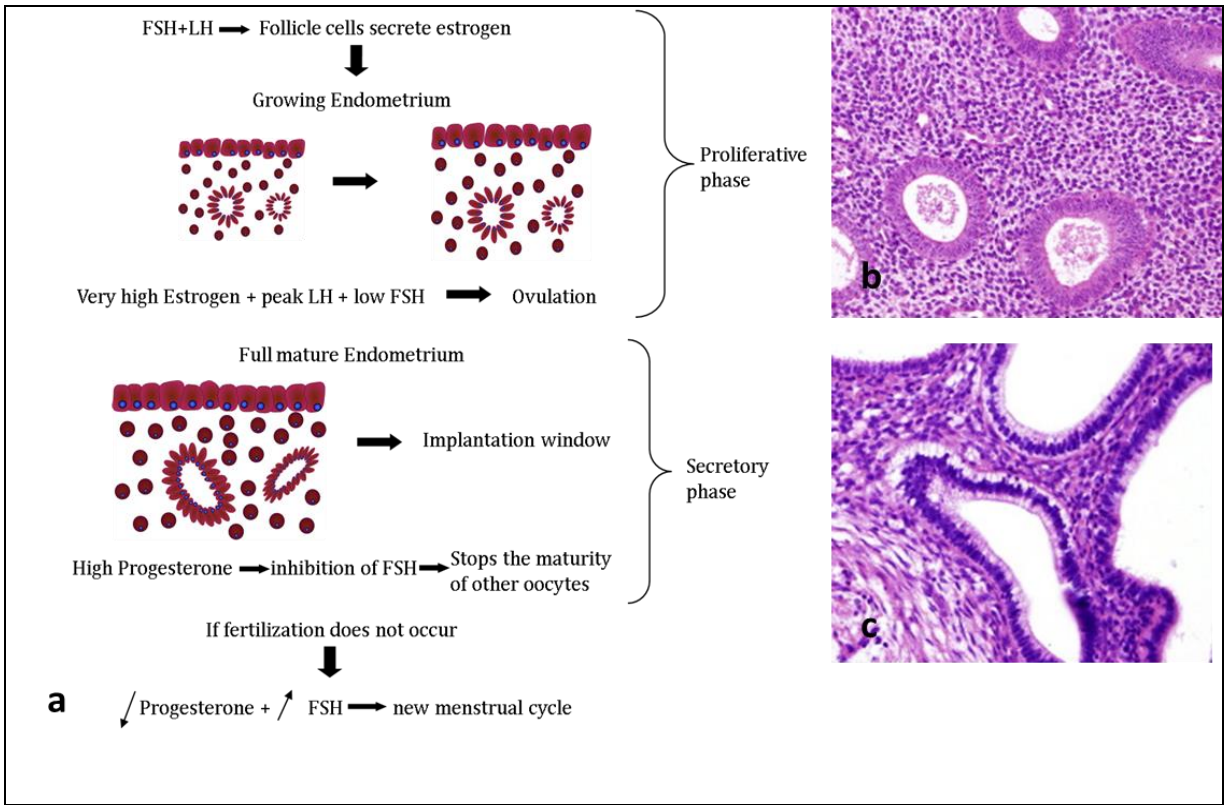


**Figure 2.4. Cellular morphological differences between the different menstrual phases under the influence of hormones.** (a)The morphology of the endometrium changes due to different levels of pituitary gonadotropins (FSH, LH) and the ovarian hormones (estrogen, progesterone) during the menstrual cycle. (b), (c) Haematoxylin staining of endometrial tissue in proliferative and secretory phase shows straight, narrow glands and long, tortuous glands respectively.

During the menstruation the cells which form the functional layer of the endometrium are shed; it is thought that the stem cells within the basal layer assist in the regeneration of a new functional layer after menstrual shedding [60]. The hormonal and endometrial changes which occur during the menstrual cycle are illustrated in Figure 2.5.

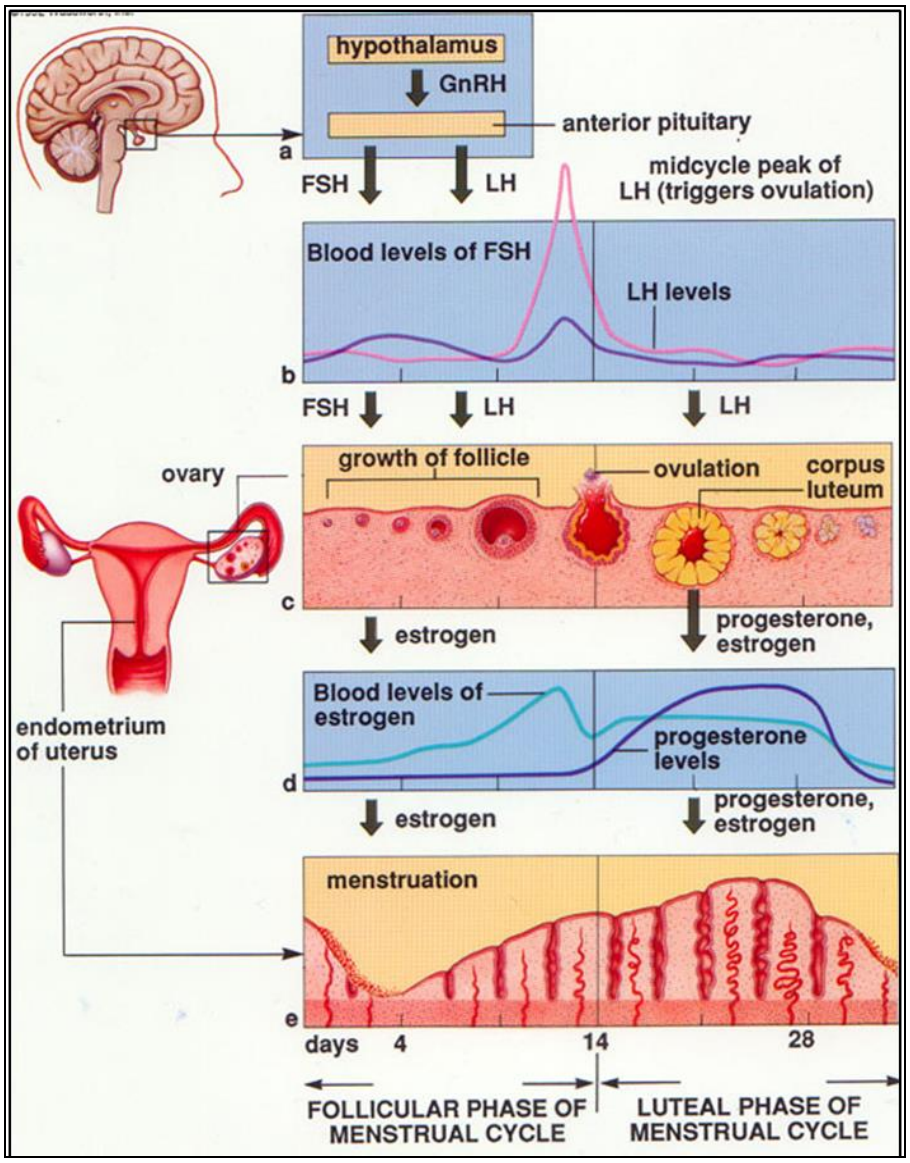


**Figure 2.5. Hormonal and endometrial changes during the menstrual cycle. In a sexually-mature human female there is a highly synchronised and interdependent series of cycles that take place.** These cycles include the release of pituitary gonadotropins (LH and FSH) into the bloodstream, the ovarian steroid response cycle (estrogen synthesis and also later progesterone synthesis) and the uterine endometrium cycle of proliferation and destruction (menses). (Adapted from ib.berkeley.edu)

# Chapter 3

## Pathophysiology of endometrium & of related disorders of the reproductive tract

## 3.1 Endometriosis

In order to translate the use of nanomedicine into clinical treatment of endometriosis, it is crucial to understand the salient clinical aspects of this entity. Endometriosis is a chronic disease characterised by the appearance of endometrial glands and stromal cells outside the uterine cavity. It is a very common gynaecological disorder affecting 1 in 10 women of fertile age, causing pelvic pain, progressive dysmenorrhea, dyspareunia and infertility [64]. Endometriotic lesions are frequently found on the pelvic peritoneum, on the bowel, bladder, ovaries and uterosacral ligaments [65]. There is considerable variation in the stage, size, site and appearance of endometriotic lesions between patients [66]. Lesions can be of different colours, red, black, white or they can even be invisible (clear) (Figure 3.1.). The most common form of endometriosis is the pelvic endometriosis [67].

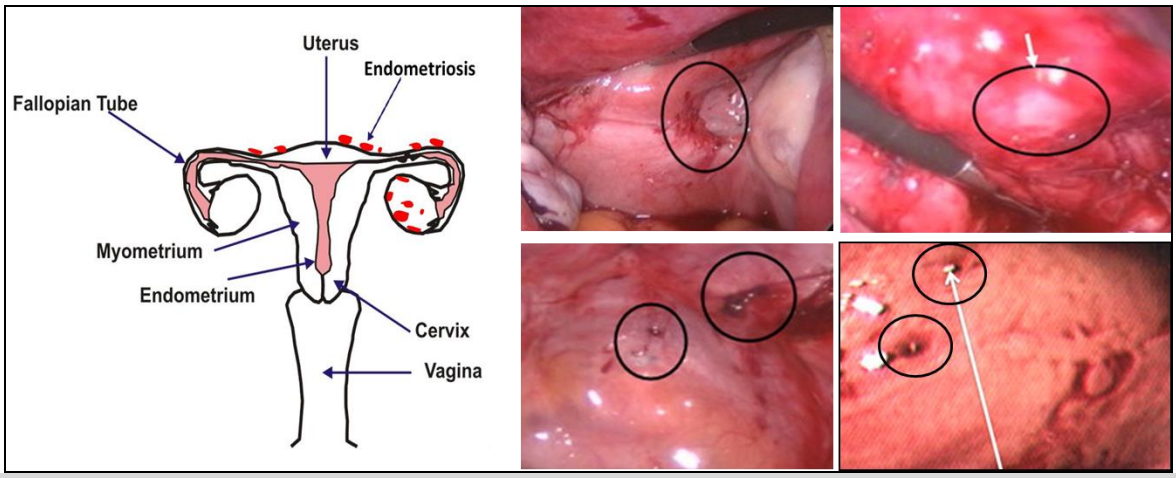


**Figure 3.1. Appearance of endometriotic lesions.** The size, the colour the morphology and the site of the endometriotic lesions are variable.

### 3.1.1 *Pathogenesis of endometriosis*

There are different theories on the pathogenesis of endometriosis. The first is the implantation theory which suggests the transplantation and then implantation of endometrial tissue outside the uterine cavity is a result of retrograde menstruation, where endometrial cells reflux back through the Fallopian tubes into the abdominal cavity where they implant [68]. Another theory is related to the common embryological origins of the endometrium and peritoneum, where either metaplasia or stem cell like activity within these embryological remnants results in the activation of the endometriosis. Many factors such as endogenous, biochemical or immunological factors can provoke the differentiation of undifferentiated cells into endometrial cells into endometriosis [68]. In vitro experiments indicated coelomic metaplasia of mesothelium when endometrial stromal cells and ovarian surface epithelium were co-cultured with 17β oestradiol [69]. Finally morphologic observations have shown that endometriosis may be a serial change in the ultrastructural and histological characteristics from the adjacent mesothelial cells.

### 3.1.2 *Do women with endometriosis carry a unique molecular signature for targeting?*

**The cellular and molecular changes of endometriosis within the eutopic and ectopic endometrium**

The search for the right ligand to target pathology within a biological system is always challenging for scientists in the nanomedicine field. In order to target a disease such as endometriosis, one needs to ensure that the treatment is not only sensitive but also specific so as to have significant clinical benefits with minimal adverse effects.

A significant number of studies in the literature already exist describing the molecular differences between the eutopic and ectopic endometrium of women with endometriosis and those without endometriosis. For example, it has been shown that endometrial cells from eutopic endometrium from women with endometriosis show decreased levels of apoptosis and in macrophage cytolysis with a parallel increase in the expression of anti-apoptotic genes such as Bcl-2 compared with endometrium from healthy women [70]. Thus accumulation and survival of endometrial cells in ectopic locations might be due to the ability of these cells to escape from apoptosis. Furthermore the eutopic endometrium from patients with endometriosis could have a predisposition to peritoneal implantation due to the higher expression of proteolytic enzymes such as matrix metalloproteinase (MMP). Endometrium from women with endometriosis when compared with endometrium from women without the disease expressed higher levels of MMP-2 and membranous type-1 MMP was observed. In parallel, these cells presented lower levels of the tissue inhibitor MMP-2 [71].

Excessive endometrial angiogenesis has also been proposed to play a principal role in the development and maintenance of endometriosis as blood transporting nutrients and oxygen helps endometrial cells to survive [72]. This hypothesis is supported by the fact that there is a higher micro-vessel density, expression of vascular endothelial growth factor A (VEGF-A) within the glandular epithelium and expression of the vascular endothelial growth factor receptor 2 (VEGFR-2) in endometrial blood vessels in the eutopic endometrium of women with endometriosis compared with healthy women [73]. Although endometriosis is a condition often associated with increased angiogenesis within the endometrium, ironically the levels of the Prokineticin-1 (PROK1), an angiogenic factor implicated in the vascular function of peri-implantation endometrium and early pregnancy, were found to be significantly lower or even undetectable in patients with endometriosis [74]. The

relatively lower level of PROK1 expression was also apparent in primary endometrial stromal cells cultures from eutopic endometrium from women with endometriosis [74]. PRKO1 is normally expressed in the endometrium of women in reproductive age and especially during the secretory phase of the menstrual cycle and have been proposed to play principal role in implantation and placentation [75]. It has therefore been hypothesized that the lower levels of PRKO1 in endometriosis patients could play a part in poor implantation and subfertility.

Furthermore, in eutopic secretory endometrium from women with endometriosis was observed that a number of progesterone-dependent genes were dysregulated, this is termed as 'progesterone resistance' [76]. Altered expression of progesterone receptor isoforms A and B or activation of inflammatory transcription factors could disrupt the interaction between the progesterone receptor and key transcriptional partners such as FOXO1 and HOX10 [77].

Finally, the findings of altered expression levels of adhesion proteins in endometrium of women with endometriosis compared with endometrium from control women (healthy/non-endometriosis women) could explain the ability of these cells to attach in ectopic locations initiating endometriosis [78]. Changes in the eutopic endometrium from women with endometriosis were also observed using proteomics. Uterine fluid has been examined for the presence of protein biomarkers for endometriosis. A summary of the proteins with altered expression levels in the uterine fluid of women with endometriosis compared to uterine fluid from healthy women is presented in Table 3.1.

| Protein Name | Functional groups |
|---|---|
| Moesin (MSN), | Cytoskeleton and motility proteins |

| | |
|---|---|
| Beta actin (ACTB) | |
| 14-3-3 protein sigma, Stratifin (SFN), 14-3-3 protein gamma(YWHAG) | Signal transduction and cell cycle regulation |
| Glycodelin precursor (PAEP) | Secreted protein (immunosuppressive, contraceptive activity) |

**Table 3.1. Selection of proteins which display significant different expression levels in uterine fluid from women with endometriosis compared to uterine fluid from healthy women.** Changes were observed in proteins implicated in cell signalling and movement, cytoskeleton structure and immune reaction [79].

Ectopic endometrium was associated with altered expression levels of metalloproteinase (MMP) compared with eutopic endometrium from healthy women [80]. MMP levels were significantly higher in ectopic endometrium and, in parallel, tissue inhibitor metalloproteinase-3 (TIMP-3) was significantly lower in normal and endometriosis patients [80]. Ectopic endometrium expressed higher levels of metalloproteinase-9 (MMP-9) and a higher ratio of MMP-9/TIMP-3, than eutopic endometrium [80]. Altered expression levels of adhesion proteins have been also observed in ectopic endometrium [78]. Finally, increased expression of the gene that encodes the vascular endothelial growth factor (VEGF) has been detected in ectopic endometrium of women with endometriosis [81, 82].

It is important to note that thus far, there have been differential expressions of cellular and molecular markers identified between health women and women with endometriosis. However, there has yet been no studies describing a molecular signature solely unique to women with endometriosis, and for targeting purposes in the context of nanoparticles, this could be challenging in terms of finding the right ligand.

### 3.1.3 *Current diagnosis and treatment of endometriosis*

Medical therapies for endometriosis involve the use of hormonal drugs in patients to supress the ovarian activity and encourage atrophy of ectopic lesions (Table 3.2). However, there are contraindicated in women trying to conceive and have unwanted adverse effects. Furthermore, recurrence of symptoms after discontinuance of treatment is very common [83].

| **Endometriosis** | **Current treatment** | | |
|---|---|---|---|
| **Incidence** | **Medical** | **Surgical** | **Assisted reproduction** |
| Affecting 1 in 10 women during the reproductive years | • Non-steroidal anti-inflammatory drugs (NSAIDs)<br>• Oral contraceptives<br>• Gonadotropin releasing hormone (GnRH) analogues<br>• Progestagens<br>• Androgenic agents | • Laparoscopy<br>• Hysterectomy, Bilateral oophorectomy | • In vitro fertilisation (IVF)<br>• Intrauterine insemination (IUI)<br>• Gonadotropin therapy |

**Table 3.2. Incidence and treatment options for management of endometriosis.** Endometriosis is a prevalent disease, which is treated with surgical and systemic drug therapy [86].

Visual inspection of the pelvis through laparoscopy is the most common surgical procedure used for the diagnosis of endometriosis. Diagnostic laparoscopy is the only test capable of diagnosing peritoneal endometriosis and adhesions [84]. The severity of the disease is classified according to the classification system formed by the American Society of Reproductive Medicine (ASRM) [85]. Laparoscopy is an

invasive procedure during which endometrial lesions are removed by resection and laser or diathermic ablation [86] (Table 3.2). Excision of endometriotic lesions reduces the pain associated with endometriosis [87].

Whilst surgical treatment can effectively deal with the macroscopically visible lesions, microscopic, atypical in appearance or deeply located lesions are not visible, thus cannot be effectively removed. Endometriotic disease can also be widespread and often the only way of removing all the disease is to completely remove the peritoneum, a rather radical and often impractical approach with significant risks of adhesion formation/reformation. The disease has a high recurrence rate following surgery and 20% of patients who had surgery see very little symptomatic improvement and a further 20% of women have disease recurrence within 4 years. The problem is further exacerbated by, a significant delay in diagnosis [87, 88].

Recently 5-aminolevulinic acid, which is a photosensitizer, was administrated intravenously 10-114 hours prior to surgery to women with suspected endometriosis. The authors reported detecting 100% of endometriotic lesions in non-pigmented areas compared to only 69% of sensitivity of endometriotic lesions visualisation under white illumination [89, 90]. 5-aminolevulinc acid is preferentially accumulated in endometriotic lesions, and thus significantly increased the sensitivity of detection of endometriotic lesions during laparoscopy. However this treatment is not currently used in routine diagnosis of clinical endometriosis. Clinically, a direct application method with immediate results will be preferable to a treatment, which required prolonged pre surgical workup and intravenous injections.

## 3.2 Endometrial Cancer

According to the Centre for Disease Control and Prevention (CDC) an estimated 35 thousand women in the United States are diagnosed with endometrial cancer annually. Hence endometrial cancer is the fourth most commonly diagnosed gynaecologic cancer. Furthermore, in Western Europe endometrial cancer is the seventh most common cause of death in women [91].

The majority of endometrial carcinomas are cancers of the cells that form glands in the endometrium and called adenocarcinomas. The most common type of endometrial cancer is the endometrioid adenocarcinoma. Endometrial carcinomas which include squamous and undifferentiated cells are less common types of endometrial cancer. More than 80% of endometrial cancers are typical adenocarcinomas, also known as endometrioid cancers [92]. Endometrial tumours are categorized into different grades classified by the degree of abnormality of the glandular architecture [93] (Table 3.3).

| Tumour Grade | Characteristics |
|---|---|
| **Grade 1** | • Lesion well-differentiated<br>• Glandular pattern similar to normal endometrial glands |
| **Grade 2** | • Moderately well-differentiated lesion<br>• Glandular structures admixed with solid areas of tumour |
| **Grade 3** | • Poorly differentiated lesion<br>• Solid glandular structures with lack of identifiable endometrial glands |

**Table 3.3. Tumour classification**. Tumour is classified as grade 1, 2 and 3 by the degree of abnormality in the glandular architecture [93]**.**

### 3.2.1 *Pathogenesis of endometrial cancer*

The exact cause of uterine cancer is not known [94, 95]. Estrogen stimulates the regeneration of the endometrium. Several studies have demonstrated that high estrogen levels cause excessive endometrial growth and cancer [94, 96]. Conditions such as diabetes and the use of Tamoxifen (a drug for breast cancer treatment and infertility) are some other factors which seem to increase the risk of endometrial cancer [97].

### 3.2.2 *Molecular basis of endometrial cancer*

Alteration of normal cells into tumour cells involves changes in the activity of a number of distinct genes and proteins in a cell, for example oncogenes, tumour suppressor genes, peptide growth factors and their receptors, G-proteins, nuclear transcription factors and finally DNA repair genes. The expression levels of the tumour suppressor gene, PTEN, which encodes a protein with tyrosine kinase function, have been described to be altered in more than 83 % of endometrioid carcinomas and 55 % of precancerous lesions. In addition, mutations in one copy of the p53 tumour suppression gene which leads to inactive protein product, have been reported in many types of cancer including endometrial cancer [98].

Overexpression of Her-2/neu (Human Epidermal Growth Factor Receptor 2) and amplification of the gene have been shown in several types of cancer including breast, ovarian cancer and in 10–15 % of endometrial cancers. Her-2/neu is an oncogene that encodes for a tyrosine kinase receptor involved in cell signalling. Furthermore, genetic alterations in endometrial cancers include up-regulation of ras proteins. Especially K-ras amplification and expression increases from primary to metastatic lesions and is related with the progression of the disease [99]. Ras proteins are a family of G proteins which play a crucial role in cellular proliferation. Mutations in the gene

that encode the K-ras protein have been shown to be occurred due to defects in the normal DNA repair during DNA replication in the number of the repeat elements in microsatellites [98,100]. Finally, the folate receptor (FR), also known as the high affinity membrane folate-binding protein, has been shown that is overexpressed in human tumours, including endometrial and ovarian cancer. FR is involved in folate transfer, a molecule which is implicated in numerous essential functions such as DNA replication, repair and methylation. While elevated expression of FR has frequently been observed in various types of human cancers, the receptor is generally absent in most normal tissues with the exceptions of choroid plexus, placenta, and low levels in lung, thyroid gland and kidney [101,102].

Also, similar to the case of endometriosis, there are differential expressions of molecular markers in endometrial cancer but none of these are unique to the disease alone. Direct application of treatment within the endometrial cavity may be a possible route with the least side effects if nanoparticles were to be used for treatment. Whilst the latter route may be useful in locally invasive disease, for example the earlier stages of endometrial cancer, this route of delivery does not address treatment of diseased tissue that has metastasized. However, local delivery of nanoparticles directly inside the uterine cavity may provide a new paradigm for treatment of women with early stage disease who wishes to preserve their fertility or their uteri; currently their only option of treatment is to have a hysterectomy.

### 3.2.3 *Current diagnostic and treatment methods for endometrial cancer*

Treatment and diagnosis of endometrial cancer involves hormonal therapy, radiation therapy, chemotherapy and surgery (Table 3.4).

| Endometrial Cancer | | |
|---|---|---|
| **Incidence** | **Prognosis** | **Current treatment** |
| Lifetime risk is 1 to 46 women in UK | 5-year survival rates of greater than 70 % of the patients | • Hormonal therapy<br>• Radiation therapy<br>• Chemotherapy<br>• Surgery |

**Table 3.4. Incidence, prognosis and treatment options for endometrial cancer management.** Endometrial cancer is a disease with high incidence mostly in women older than 50 years and is currently treated with systemic administration of hormonal drugs, radiation therapy and chemotherapy.

The surgical procedures involve total hysterectomy (removal of the uterine cervix and/or bilateral salpingo-oophorectomy) [103]. The majority of patients with endometrial cancer are diagnosed with disease confined to the uterus. Hysterectomy at this stage leads to a five year survival rate for approximately 70 % of the patients, with recurrences occurring -most commonly- within three years [91, 104]. Furthermore, current treatment methods for endometrial cancer are related to a range of unpleasant side effects.

# Chapter 4

## Aim of Project

## 4.1 Aim of the project

The lack of effective diagnostic and treatment techniques for the early detection and therapy of both endometriosis and endometrial cancer make imperative the development of new therapeutic and diagnostic methods.

In the last few and current years, nanomedicine has become a very fast moving field, which uses NPs in the discipline of medicine [1]. Various NPs have been developed (such as polymersomes, liposomes, micelles, metallic, magnetic and quantum dots) with a range of different characteristics and functionalities for application in imaging, diagnosis and treatment. Recently, targeted delivery of therapeutic or diagnostic agents using biocompatible and biodegradable NPs moved nanomedicine one step forward. Furthermore, proteomic methods can be used in order to identify novel biomarkers of endometrial pathology. These markers might then be synergistically employed in parallel with nanomedicine to enhance diagnosis and treatment of reproductive pathologies.

The paradigm of using organic nanoparticles (NPs) was for the first time introduced in this project. Taking advantage of a number of physical and chemical properties that the NPs exhibit, materials of a size between 1–100 nm were used as novel therapeutic tools to tackle this problem.

The purpose of the current study was:

1. to evaluate the uptake of PEG-b-PCL polymersomes by endometrial cells,
2. to assess the delivery of hydrophilic compounds via PEG-b-PCL polymersomes into endometrial cells with and without functionalisation with TAT, a cell penetrating peptide.

# Chapter 5

## Material and Methods

## Nanoparticles and Tissues used

The polymersomes PEG-b-PCL and TAT-PEG-b-PCL were prepared and endometrial tissue collected with pipelle biopsy from patients with fertility problems, infertility or chronic pelvic pain (Table 5.1). Then, the tissue was either incubated with polymersomes, fixed, cut in thin sections using a cryostat and the uptake of NPs by the *ex vivo* endometrial cells was checked using immunohistochemistry, or the tissue was digested, and following a particular procedure primary endometrial stromal cells, were isolated and cultured.

## 5.1 Polymersome preparation and characterisation

### 5.1.1 *Polymersome preparation*

Poly (ethylene glycol)-block-poly (ε-caprolactone), (PEG5K-b-PCL5K), block of copolymers were used for the polymersomes preparation supplied from Sigma Aldrich, UK. For the preparation of polymersomes loaded with sodium fluorescein, PEG-b-PCL blocks of copolymer (6.0 mg) were dissolved in 0.4 ml of anhydrous dimethylformamide (DMF) and the solution was placed in ultrasonic bath until it completely dissolves. Then the solution was added dropwise to 1.6 ml sodium fluorescein solution while being stirred rapidly. The solution was then transferred using 1 ml syringe into the dialysis tubing to separate against phosphate buffer saline (PBS) (300 ml). The PBS solution was changed three times within 24 hours. After these changes the sample was removed from the dialysis tubing and the nanoparticles were separated using size exclusion columns (Sephadex G-25, Sigma UK). Through this process any sodium fluorescein not encapsulated in the polymersomes is also removed. The NPs solution is filtered with 0.2 μm syringe filter into sterile eppendorf just before its usage.

The preparation procedure of the polymersomes which were functionalised with TAT peptide (CYGRKKRRQRRRA) on their surface and loaded with sodium fluorescein was the same as described above. The only difference is that 1.0 mg TAT-PEG-b-PCL and 5.0 mg of PEG-b-PCL were mixed and dissolved in 0.4 ml DMF (Figure 5.1).

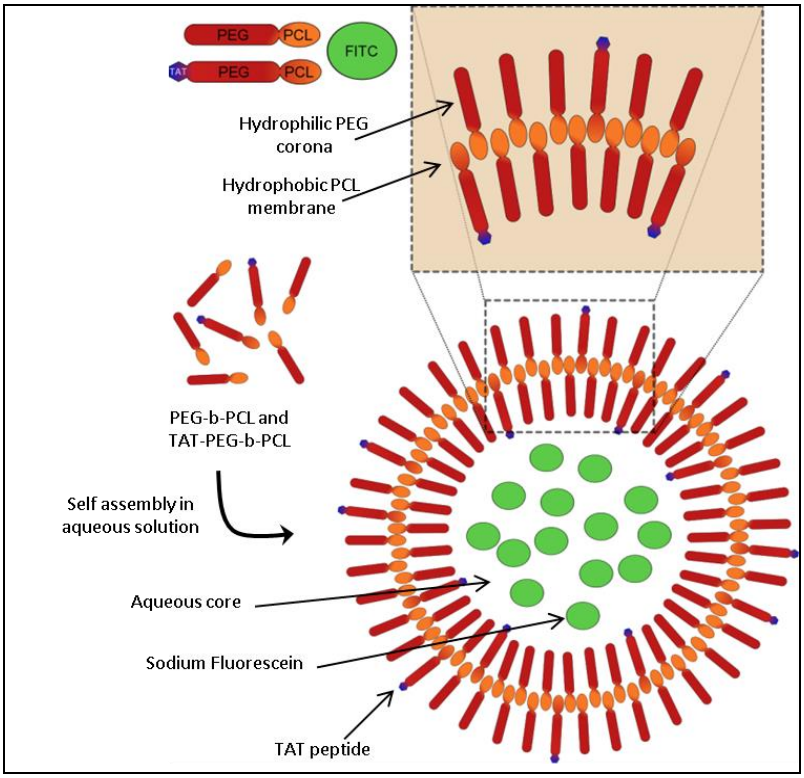


**Figure 5.1. Polymersome preparation.** PEG-b-PCL block copolymer chains self-assemble in an aqueous environment to form polymersome structures. A hydrophobic membrane is formed by the PCL units of the polymer while the PEG units form a hydrophilic corona and line the interior cavity of the polymersome. The surface can be functionalised with targeting moieties (TAT). Polymersomes can also be loaded with hydrophilic compounds, sodium fluorescein.

### 5.1.2 *Dialysis tubing preparation*

Glycerol, heavy metals and sulphur compounds must have been removed before the dialysis tubing was used. 300 mL distilled water warmed up to 80˚C, 6 g of sodium carbonate and 0.2 g of EDTA were added and left to stir for one hour. After one hour the heat was turned off and the dialysis tubing (Sigma UK) was added in the solution which was left stirring for another one hour. The dialysis tubing step is important because the polymer solution, which was dissolved in the DMF, was replaced with PBS. Thus, the sample was not cytotoxic. In addition, this step allows the removal of all the un-encapsulated fluorescein.

### 5.1.3 *Preparation of size separation columns*

Size exclusion columns contain a gel which was made of porous dextran beads. Small molecules are able to pass through the pores, while bigger molecules such as the nanoparticles could only travel around the beads and thus needed less time to pass through the column.

To prepare the column, a white frit was pushed to the bottom of an empty PD–10 column (Sigma, UK). 2.1 g of Sephadex G-25 was added to each column and Milli Q PBS was then poured in to hydrate the Sephadex. The hydrated Sephadex in the column was left to stand for at least 4 hours. Afterwards, excess PBS was removed from the top of the column and the tip on the other end of the column was cut off to elute the PBS. A second frit was then added on the top layer. Before adding the sample, a small amount of PBS was allowed to elute through the column. After the sample was added, the elute was collected serially in four sterile eppendorf tubes, with one eluate containing the nanoparticles.

### 5.1.4 *Polymersome NPs characterisation: Dynamic light scattering*

The size of the polymersomes was measured with a method called dynamic light scattering (DLS). DLS measures the hydrodynamic diameter by shining a laser at the sample and then measuring the diffracted light at a set angle (usually 90 degrees). 100 µl of the polymersome solution were taken using a 1 ml syringe without needle and diluted in 2 ml PBS. Before measuring, samples were filtered using a 0.2 µm syringe filter into a cuvette. The information that one gets from the Nanosizer is the average size of the particles and the width of the peak (Figure 5.2). The width indicates the distribution of the particle's size.

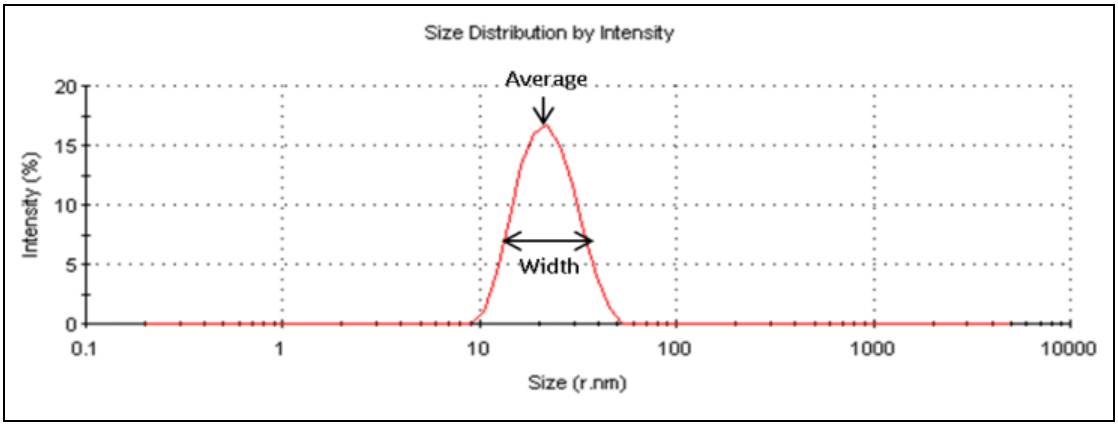


**Figure 5.2. Results from the Nanosizer.** The graph demonstrates the average size of the particles and the width of the peak. The diameter of the particles in the above example is 45.58 nm and the width 7.402 nm thus the size of the particles is 45.58 ± 7.402.

## 5.2 Collection of Endometrium

Twenty one women of pre-menopausal age with and without endometriosis (Table 5.1) undergoing laparoscopy or hysteroscopy at Princess Anne Hospital, Southampton, UK for benign gynaecological disorders gave informed consent for pipelle biopsy. Endometrium was collected by an endometrial pipelle biopsy

(Endocell, Wallach Surgical Devices Inc, USA). All the patients had no hormonal treatment for three months, were between 18-45 years and were not suffering from any type of cancer or infection. For each patient, information including their menstrual cycle stage, fertility problems, medical history, medication, BMI and smoking history was recorded. Finally, the different stages of endometriosis in patients who were diagnosed with the disease were defined according the American Fertility Society (AFS) score.

| Sample number/ recruitment number | Endometriosis /Control | Phase of cycle | Tissue integrity Good/Bad | Tissue sectioned Y/N? | Immunohistochemistry to assess NP uptake Y/N? |
|---|---|---|---|---|---|
| 1/280 | Control | Proliferative | Bad | Y | Y |
| 2/297 | Endometriosis | Unknown | Bad | Y | Y |
| 3/294 | Endometriosis | Secretory | Bad | Y | Y |
| 4/311 | Control | Secretory | Good | Y | Y |
| 5/291 | Endometriosis | Secretory | Bad | Y | N |
| 6/293 | Endometriosis | Secretory | Bad | Y | N |
| 7/305 | Control | Proliferative | Bad | Y | N |
| 8/292 | Control | Secretory | Bad | Y | N |
| 9/316 | Control | Secretory | Good | Y | Y |
| 10/295 | Control | Unknown | Bad | Y | Y |
| 11/315 | Control | Secretory | Good | Y | Y |
| 12/321 | Control | Secretory | Good | Y | Y |
| 13/326 | Endometriosis | Proliferative | Bad | Y | N |
| 14/327 | Control | Proliferative | Good | Y | Y |
| 15/325 | Endometriosis | Secretory | Good | Y | Y |
| 16/330 | Control | Proliferative | Medium | Y | N |
| 17/324 | Control | Proliferative | Tissue treated with TAT NPs–bad; Control tissue (PBS)–good integrity | Y | N |
| 18/352 | Unknown | Secretory | Not cut yet | N | N |
| 19/353 | Unknown | Secretory | Not cut yet | N | N |
| 20/281 | Control | Secretory | Bad | Y | N |
| 21/296 | Control | Proliferative | Bad | Y | N |

**Table 5.1. Summary of the biopsies that have been collected. Endometrial biopsies from 21 patients have been collected.** The integrity of the tissue has been checked for 19 of them. 12 showed bad tissue integrity and 7good, the rest of the tissue hasn't been checked yet. Tissue

from 6 patients has been processed for immunohistochemistry. Is unknown whether or not the patient had endometriosis when laparoscopy has not taken place; (Y= YES, N=NO).

## 5.3 Incubation of *ex-vivo* endometrial tissue with polymersomes

After the collection of the endometrium tissue, the tissue was immediately placed in a 0.9% saline solution (at room temperature). Once the tissue was transferred from the operating theatre to the laboratory, it was placed in fresh saline in order to wash off the blood, and then was cut in small pieces (about 1 cm each). Endometrial segments were then incubated with polymersomes which were either functionalised with the TAT peptide or not, for ten minutes at room temperature. Then the tissue segments were washed twice in PBS (five minutes per time) in order to remove any unbound polymersomes. The tissue was then fixed in 0.5% of PFA and kept overnight at 4°C. The following day the segments were cryoprotected in 30% sucrose, and again kept overnight at 4°C. Finally, the tissue was embedded in OCT and cut in 7 μm thick sections using a cryostat. The method is schematically presented in Figure 5.3.

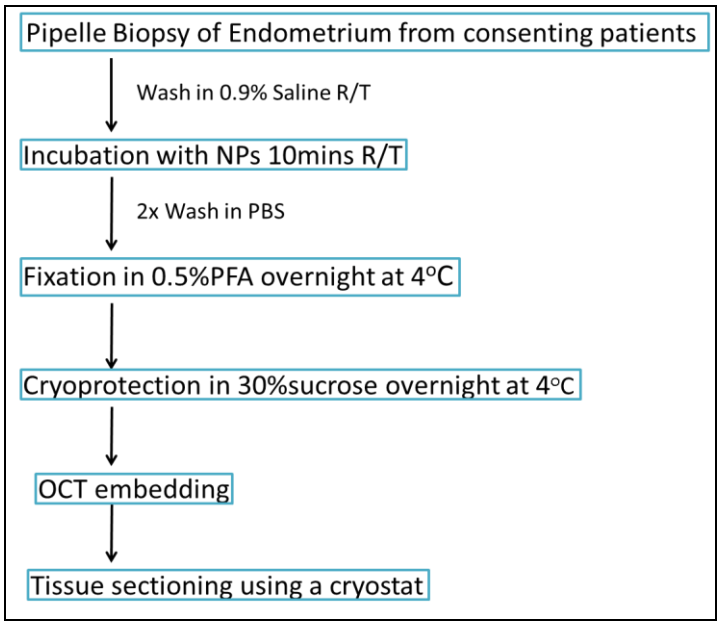


**Figure 5.3. A flow chart of the method for treating tissue with the NPs, fixation and processing.** The tissue is collected by a pipelle biopsy then is incubated with NPs, fixed and cut using a cryostat in 7 and 12μm thick sections.

## 5.4 Hematoxylin staining of endometrial tissue

The integrity of the tissue and the viability of the cells was tested using Hematoxylin staining which stains the nuclei purple–blue. Firstly, the tissue sections kept warmed at 37°C for 15 minutes. Then the sections were rinsed in distilled water for two minutes, and then stained with hematoxylin (Sigma, USA) for five minutes. Afterwards, the sections were rinsed in water, then decolorised by dipping twice in acid alcohol (1% acid-70% ethanol), rinsing in water in between. Hematoxylin stain was then differentiated by rinsing the sections with tap water for two minutes. Once the hematoxylin stain had turned the tissue blue, the tissue was rinsed and then dehydrated by placing it through a series of increasing alcohol concentration (70%, 80%, 90% and 100%) for five minutes at each concentration . Finally, sections were cleared twice for ten minutes by dipping in xylene before coverslipping with DPX (Leica UK).

## 5.5 Immunohistochemistry

Initially, tissue sections were kept warmed at 37°C, then rinsed in PBS and 'blocked' in serum for one hour. Sections were then incubated with the primary antibody. One section was incubated with PBS only, to serve as a secondary antibody only control. Another section was incubated with an anti-Mucin-1 antibody, to serve as a positive control to demonstrate the efficacy of the immunohistochemistry (IHC) protocol. The tissue sections were then rinsed twice in PBS Tween (0.05% concentration) for five minutes, before being treated with the secondary antibody. The secondary antibody was again rinsed off in PBS Tween (0.05% concentration) twice, for five minutes per wash. Removal of autofluorescence was achieved by incubating the section in 0.1 %

Sudan Black for 1 hour at room temperature, before treating with the secondary antibody.

In the IHC experiments when the primary interest was to detect the released of sodium fluorescein, in the form of fluorescein isothyocyanate (FITC), from polymersomes, tissue sections were incubated with the a-FITC biotinylated antibody overnight at 4°C (dilution 1:200). Streptavidin–546 (red signal) or Streptavidin–488 (green signal) used then used as secondary antibodies at 1:200 dilution.

When the a-MUC-1 antibody was used, the sections were incubated with the antibody overnight at 4°C in a dilution of 1:200. The goat- anti-mouse -546 antibody was utilized as secondary antibody (dilution 1:200).

Furthermore, when Vimentin and Cytokeratin antibodies were employed in the IHC experiments, they were both used at a dilution of 1:700 and the tissue sections were incubated for one hour at room temperature (RT). The goat-anti-mouse-546 (red signal) was then used as a secondary antibody for both antibodies. In addition, both antibodies were raised in mouse, hence it was not possible to stain the same tissue section with both antibodies. The primary antibodies and the dilutions that were used for these experiments are summarized in Table 5.2.

Moreover, when the a-FITC biotinylated antibody was used together with either Vimentin or Cytokeratin in a co-localisation assay, the antibodies were used at the same concentrations, as described above. However the tissue sections were incubated for 90 minutes in the case of a-FITC and Vimentin co-localisation, and 60 minutes for a-FITC and Cytokeratin. Streptavidin-488 was used as secondary antibody for a-FITC and the goat-anti-mouse-546 antibody was used as secondary for both Vimentin and Cytokeratin.

| Antigen | Source | Dilution |
|---|---|---|
| FITC | Vector | 1:200 |
| Vimentin | Millipore | 1:700 |
| Cytokeratin | Abcam | 1:700 |
| Mucin-1 | Abcam | 1:200 |

**Table 5.2. Primary antibodies dilutions.** The table summarize the primary antibodies and the dilutions that have been used for these experiments.

## 5.6 Primary endometrial stromal cells culture

### 5.6.1 *Making of the media SKUT*

For culturing and expanding Endometrial Stromal Cells (ESCs), DMEM/F12 (Dulbecco's Modified Eagle Media) without phenol red (pH indicator) mixed with 10% FCS (Fetal Bovine Serum), 1% penicilin/streptavidin, 1% amphotericine B and 1% L-Glutamine was used. DMEM medium with the aforementioned ingredients and normal FCS will be henceforth called SKUT. Phenol red was not included because it contains several growth factors, and since ESCs are prone to respond to these growth factors, it may infuence their migration and thus affect the experimental outcomes.

### 5.6.2 *Preparation of endometrial stromal cells from fresh tissue*

Endometrial tissues were collected with pipelle biopsy from patients with fertility problems. Tissues were immediately placed in Falcon tubes containing DMEM/F12. The tissue biopsy was then placed in a petri dish and washed with a small amount of

serum free-DMEM. All fluid around the tissue was removed and the tissue was cut using sterile scalpels in a sterile petri dish. In order to increase the surface area available for digestion, the tissues were cut into smaller pieces of no more than 2mm. The pieces of tissue were transferred into a falcon tube containing Digest medium (serum free-DMEM with collagenase). Tissue was digested in an incubator at 37˚C by stirring lightly for 60 minutes every 5 min. This process enables the stromal cells to come apart from the glands and float individually in solution. When tissue was fully digested, SKUT medium was added in order to stop the action of collagenase and cells were then spun. Supernatant medium, which contained the epithelial glandular cells, was aspirated and the remaining stromal cells were gently resuspended with a small amount of SKUT and finally topped up to 1ml SKUT. The aforementioned solution of cells and SKUT was added in two T75 flasks (0.5 ml in each flask), which were filled beforehand with 12ml SKUT media. The flasks were then placed in the incubator (37˚C) and media replaced with new medium 3 hours later.

### 5.6.3 *Changing media for cultured endometrial stromal cells*

SKUT medium was warmed in the incubator or in warm water bath at 37˚C. Culture flasks were removed from the incubator and the cells were checked under the microscope in order 1. to see whether the cells were alive and attached to the plastic bottom of the flask and 2. to assure that the cell culture was not contaminated. All media was then aspirated from the culture flasks and fresh cultured media was aliquoted in the flasks (4ml in T25, 12ml in T75). Finally the appearance of the cells was checked again under the microscope and the flasks were returned to the incubator.

It is worth noting that the primary protocol suggested that the media should be changed every second day. However as cells release several growth factors that are necessary for their growth and maintenance into the medium, it was decided that the media is changed every four days.

### 5.6.4 *Splitting cultured endometrial stromal cells*

Culture flasks were removed from the incubator and the appearance of the cells was checked under the microscope. All media were removed from the flasks and cells were washed with 1.5x culture volume with PBS by gently rinsing the total surface of the flasks (without causing any spillage) and aspirating PBS. Trypsin-EDTA was aliquoted (1ml/T25 and 3ml/T75) in each culture flask and the total surface was rinsed gently. Culture flasks were then returned to the incubator for 3-5 min. To stop trypsinization 2x culture volume of SKUT media was added, and cells were then harvested and transferred to falcon tubes. Cells were spun down for 3 min at 1200rpm, with the supernatant aspirated and cells resuspended with a small volume of SKUT medium. Finally cells were transferred equally into 3 flasks (1:3 split) and the appearance of the cells was again checked under the microscope before the flasks were returned to the incubator.

### 5.6.5 *Freezing endometrial stromal cells*

Freezing media (FCS / 10% DMSO) were prepared. The media and the Cryobuddy were placed on ice and the appearance of the cells were checked under the microscope if they are 80% confluent. All media were aspirated from culture flasks and cells were washed with 1.5x serum-free DMEM by gently rinsing the total surface of the flasks (without causing any spillage). The DMEM was then aspirated. Trypsin-

EDTA was aliquoted into each culture flask (1ml/T25 and 3ml/T75). The culture flasks were then placed in the incubator for 3-5 min. Cells were checked regularly for completed trypsinization. To stop trypsinization, 2x culture volume of SKUT media was added, cells were then harvested by transferring into falcon tubes. The cells were then spun for 3 min at 1200 rpm (670g). The supernatant was aspirated and cells were resuspended by adding freezing media (3ml FCS/10% DMSO for T75 and 1ml FCS/10% DMSO for T25). Cell suspension was aliquoted into the cryovials and placed directly on ice. Vials were transferred to the Cryobuddy and stored at -80˚C.

### 5.6.6 *Thawing endometrial stromal cells*

Vials were removed from the -80˚C freezer and cells were thawed in a 37°C water bath or in the incubator. Once the cells were partially thawed (forming an "ice cube"), they were taken out of the water bath or incubator. Cells were then mixed gently and added to T25 or T75 flasks. As each vial contains about 500,000 cells, 2 vials were used for the T25 flask. The appearance of the cells was checked under the microscope and the flasks were placed in the incubator. Five hours later, cells were checked again under the microscope and the medium was changed. This step is important in order to remove the DMSO. The media was then changed every 4 days.

### 5.6.7 *Incubation of endometrial stromal cells with PEG-b-PCL polymersomes loaded with FITC*

Split cells in 12 well plates

SKUT media was added to each well in a 12-well plate at 1.5ml/well and the plates were placed in the incubator for 15 min to equilibrate. Cells from one T75 flask were split into 12-well plates by adding 40,000 cells per well. Once the cells were 70%

confluent, they were transferred to a 0.5% Low Serum Media (containing only 0.5% FCS) 24 hours prior to NPs incubation.

NPs incubation

50% of the cultured media (in low serum), called conditioned media, was removed from the cells and added into sterile falcon tubes. Cells were placed back in the incubator. An equal volume of fresh low serum media was also added in the falcon tube. This was the solution in which the nanoparticles were then diluted in.

### 5.6.8 *Immunohistochemistry of biotinylated FITC*

In the IHC experiments, the primary interest was to determine whether PEG-b-PCL NPs can get into the endometrial cells *in vitro* and release their cargo of FITC. For this purpose, cells were first washed twice with pre-warmed PBS and then were fixed with 0.5% PFA in PBS for 15 minutes at RT. PFA was then washed x3 with PBS-Tween (0.001%). Cells were then blocked with 5% Normal Goat Serum (NGS) for 30mins at RT in order to avoid unspecific binding of the antibody. The blocking solution was then aspirated and the primary antibody (a-FITC biotinylated at 1:200 dilution) was added for overnight incubation at 4°C. The primary antibody was then washed off x3 with PBS-Tween and cells were then incubated with the secondary antibody (Streptavidin-488 at 1:200 dilution), for one hour at RT. The secondary antibody was then washed off x3 with PBS-Tween, then covered with DAPI (ProlongAntiFade) mounting medium and dried for almost 24 hours in the dark.

### 5.6.9 Polymersomes' uptake by primary endometrial cell

Pipelle biopsy was obtained from patients undergoing laparoscopy. Endometrial tissue from 6 patients with gynaecological problems has been collected. Tissue was first dissected and endometrial stromal cells were separated from epithelial cells. Endometrial stromal cells were then cultured, maintained and finally divided in 12 well plates for the NPs experiment. FITC signal from the NPs were detected with immunohistochemistry as mentioned above.

Endometrial stromal cells were incubated with PEG-b-PCL polymersomes loaded with FITC and labelled with TAT peptide for 10, 45 and 90 minutes. Immunohistochemistry was then performed, firstly to investigate whether NPs are taken up by endometrial cells; secondly, to determine if they release their model hydrophilic cargo (i.e. FITC) into the cells; and finally, to observe how signal from FITC changed over time. Endometrial stromal cells were counted for dead cells before and after incubation with polymersomes in order to be checked whether particles are toxic for cells or not. The hypothesis was that polymersomes were not toxic for the cells as they were made of the biocompatible polymers PEG. PEG is broadly used in nanomedicine as a coating polymer for nanoparticles in order to increase their circulation time by evading the cells' immune system. In addition DMF, the only toxic chemical that was used during polymersomes' preparation, was removed using dialysis tubing when the sample was dialyzed against PBS (Chapter 5.1.2). Previous experiments by co-workers with PEG-b-PCL polymersomes and fibroblasts have shown that these particles were not toxic to the cells.

# Chapter 6

## Results

## 6.1 Patients

Pipelle biopsy was obtained from patients undergoing gynaecological laparoscopic procedures. For the *ex vivo* experiments, endometrial tissue was obtained from patients with or without endometriosis at different stages of the menstrual cycle.

In total, tissue from 21 patients was collected; seven patients were in the proliferative phase when the biopsy was taken, twelve in the secretory phase and two patients whose phase in the cycle was unknown as the women did not provide this information (Table 5.1). Endometrial tissue was first sectioned and stained with hematoxylin stain to check the integrity of the tissue, and then NPs were labelled using immunohistochemistry techniques (Chapter 5.4 and 5.5).

## 6.2 Hematoxylin staining to check tissue integrity

The endometrial tissue was collected from the patients and then sectioned. However, before any immunohistochemistry experiments were conducted, sections were stained with hematoxylin in order to check for tissue integrity and cell morphology (see Chapter 5.4). This was a necessary first step in the series of experiments conducted in this project, as it was very important to ensure the reproducibility and reliability of these experiments.

In total, tissue blocks from 19 different patients was sectioned and stained with heamatoxylin and six of these showed good cellular integrity (sections from patient numbers 316, 321, 315, 327, 311 and 325; Table 5.1). Images from hematoxilyn staining from patients numbers 315, 321, 316, as well as tissue sections from patients numbers 280, 297, 294 and 311 that showed poor integrity are displayed in Figures 6.1, 6.2 and 6.3.

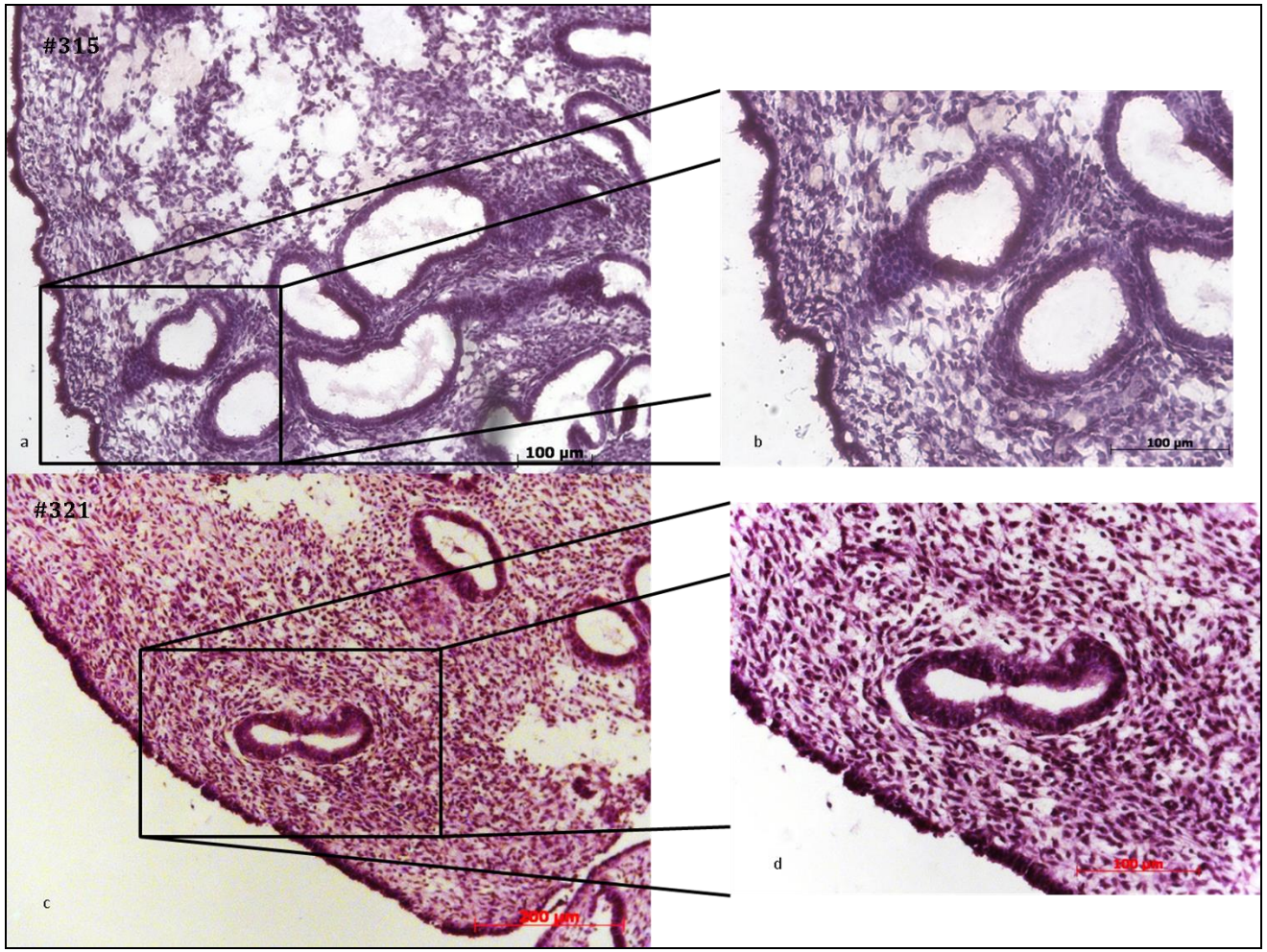


**Figure 6.1. Hematoxylin staining of endometrial tissue.** Functional layer of endometrial tissue stained with Hematoxylin. (a, c) Endometrial sections from patients numbers 315 and 321 show good tissue integrity. Epithelial cells form intact glandular structures and the cellular layer close to the endometrial lumen. Stromal cells can be observed forming the connective tissue surrounding intact glands. (b, d) Close-up of a region from images (a) and (c).

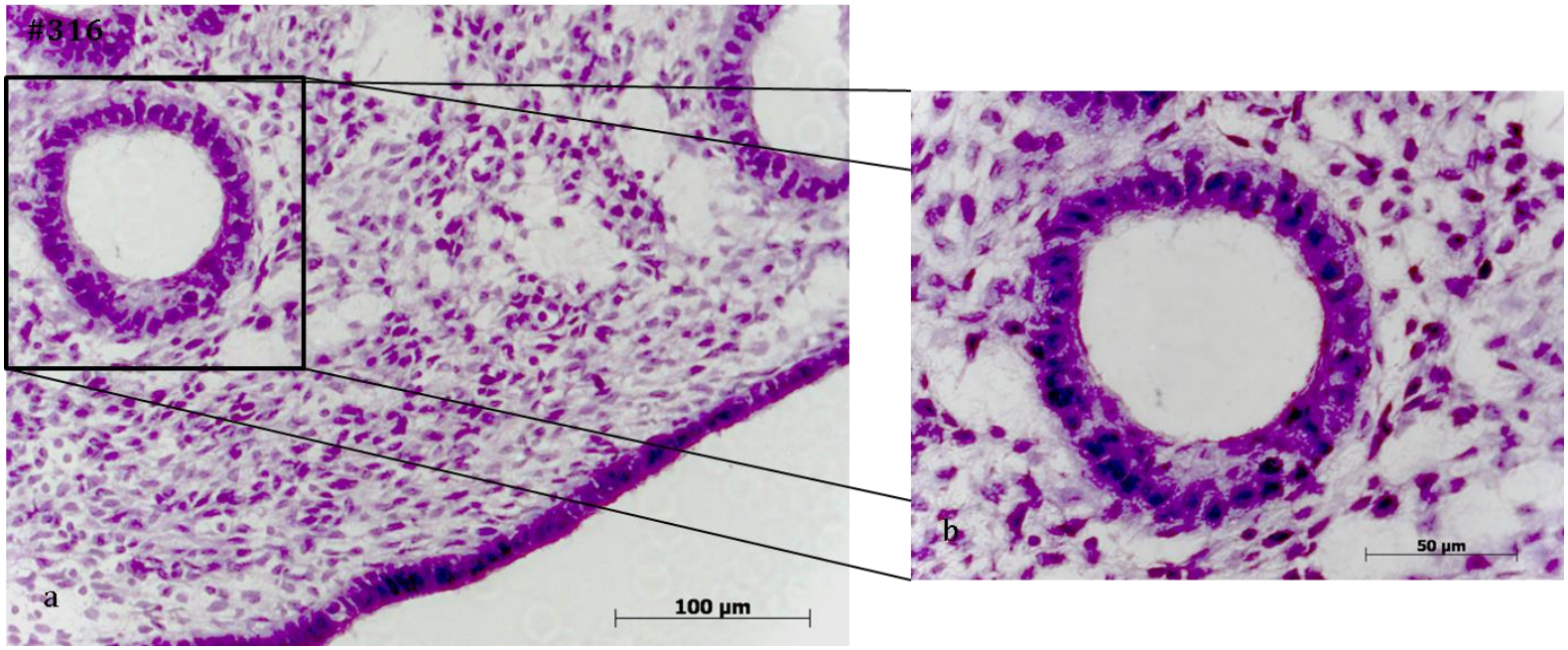


**Figure 6.2. Hematoxylin staining of endometrial tissue.** Functional layer of endometrial tissue stained with Hematoxylin. (a) Endometrial sections from patient number 316 show good tissue integrity. Epithelial cells form intact glandular structures and the cellular layer close to the endometrial lumen. Stromal cells can be observed forming the connective tissue surrounding intact glands. (b) Close-up of a region from image (a).

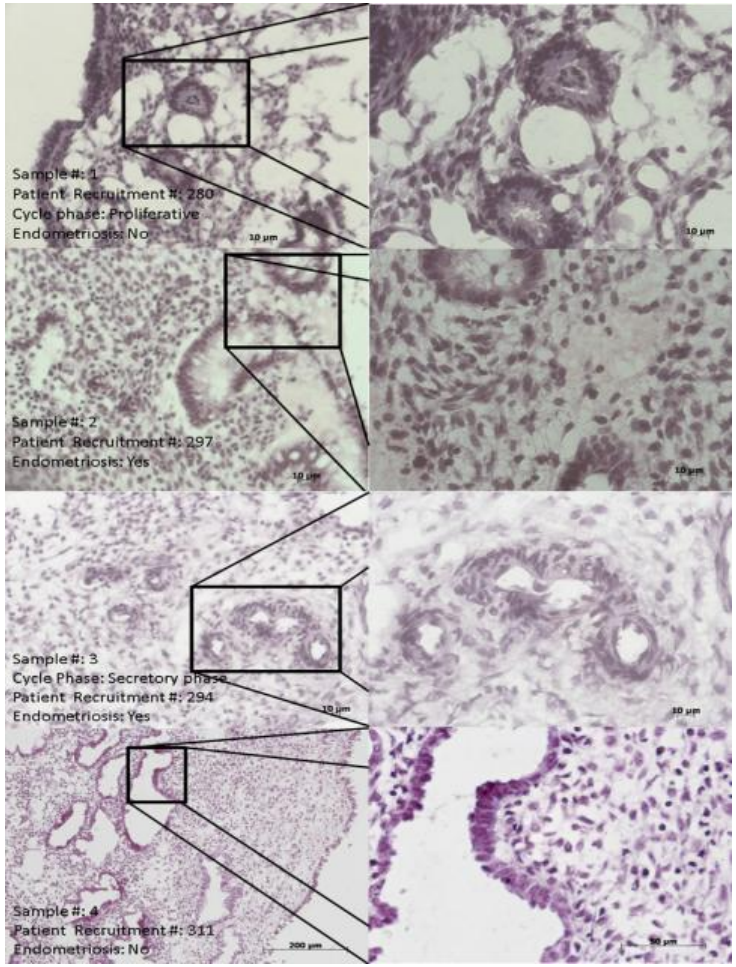


**Figure 6.3. Hematoxylin staining of endometrial tissue.** Hematoxylin staining of functional layer of endometrial tissue from patient numbers 280, 297 and 294 showed poor tissue integrity. Endometrial glands are not intact and holes appeared at the connective tissue which surrounds the glands.

## 6.3 Synthesis of polymersomes: assessment of size distribution

The size of the polymersomes is measured with the method called, dynamic light scattering (DLS). DLS measures the hydrodynamic diameter. The polymersomes were freshly prepared by standard techniques (see Chapter 5.1), however their size distribution had to be assessed, using dynamic light scattering (DLS) technique before they were introduced into the experiments. It was important that the NPs were monodispersed, i.e. the whole population of NPs had to be of similar size, firstly in order to show that the experiments are repeatable (standardization) and secondly because cellular uptake of NPs is size-dependant.

The size of the PEG-b-PCL polymersomes which were used in these experiments, the date of their preparation and the tissue that was incubated with them are shown in Table 6.1.

| **Date of synthesis of NPs** | **Patient recruitment number used for endometrial tissue incubation** | **Diameter of the polymersomes (nm)** |
|---|---|---|
| 16.07.12 | 311 | No TAT: 69.48 ± 17.10<br>TAT: 83.03 ± 20.75 |
| 01.10.12 | 321 | TAT: 73.26 ± 16.78 |
| 15.10.12 | 326, 27 | No TAT: 46.34 ± 7.46 |
| 22.10.12 | 325, 324, 330 | No TAT: 45.58 ± 7.40<br>TAT: 62.12 ± 11.76 |

**Table 6.1. Nanoparticle size distribution.** Nanoparticles with and without TAT peptide on their surface were checked after their preparation and tissue incubation for their monodispersity using dynamic light scattering.

Details of the DLS results (Chapter 6.2.4) with regards to the polymersomes displayed on Table 6.1 are presented in figures 6.4 to 6.7.

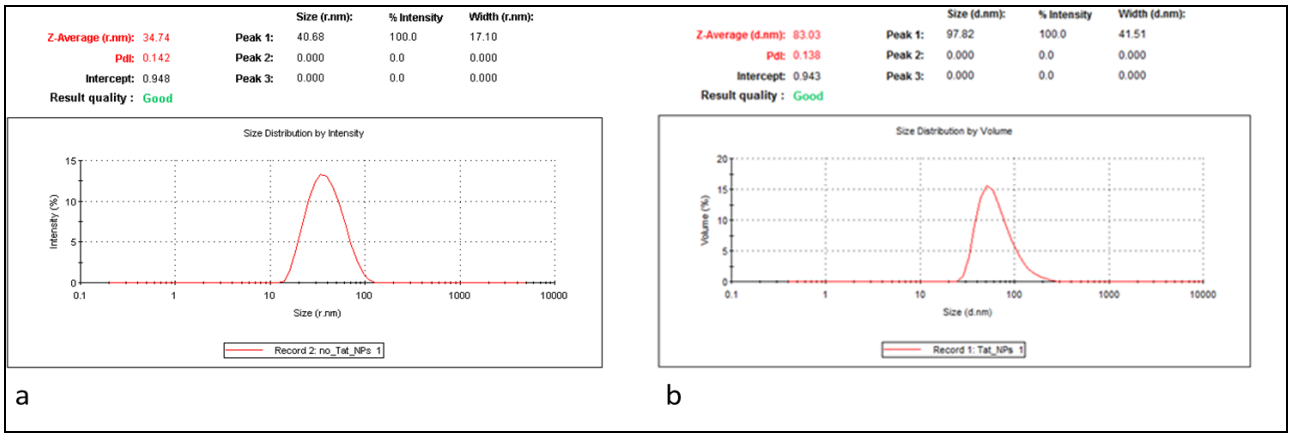


**Figure 6.4. Characterisation with DLS of TAT and No TAT polymersomes made on 16.07.12 used for tissue from patient number 311.** (a) Polymersomes functionalised with TAT peptide on their surface, Z-Average (diameter): 69.48 nm and width 17.10 nm (size: 69.48 ± 17.10 nm). (b) Polymersomes without TAT peptide on their surface, Z-Average: 83.03 nm and width 20.75 nm (size: 83.03 ± 20.75 nm).

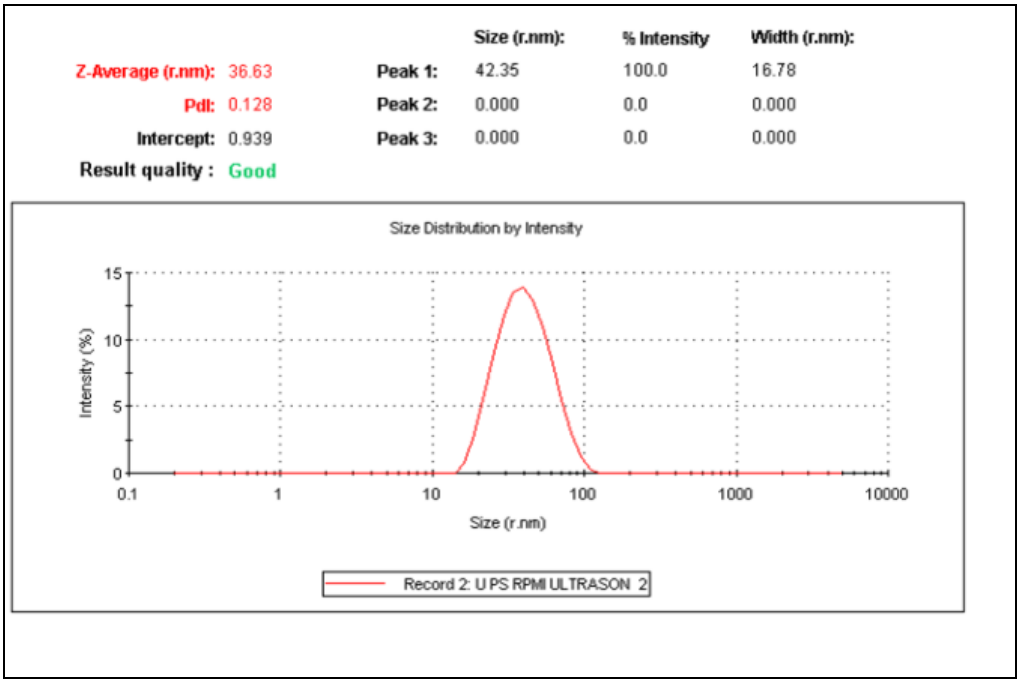


**Figure 6.5. Characterisation with DLS of TAT and No TAT polymersomes made on 01.10.12 used for tissue from patient number 321.** Polymersomes functionalised with TAT peptide on their surface, Z-Average (diameter): 73.26 nm and width 16.78 nm (size 73.26 ± 16.78 nm).

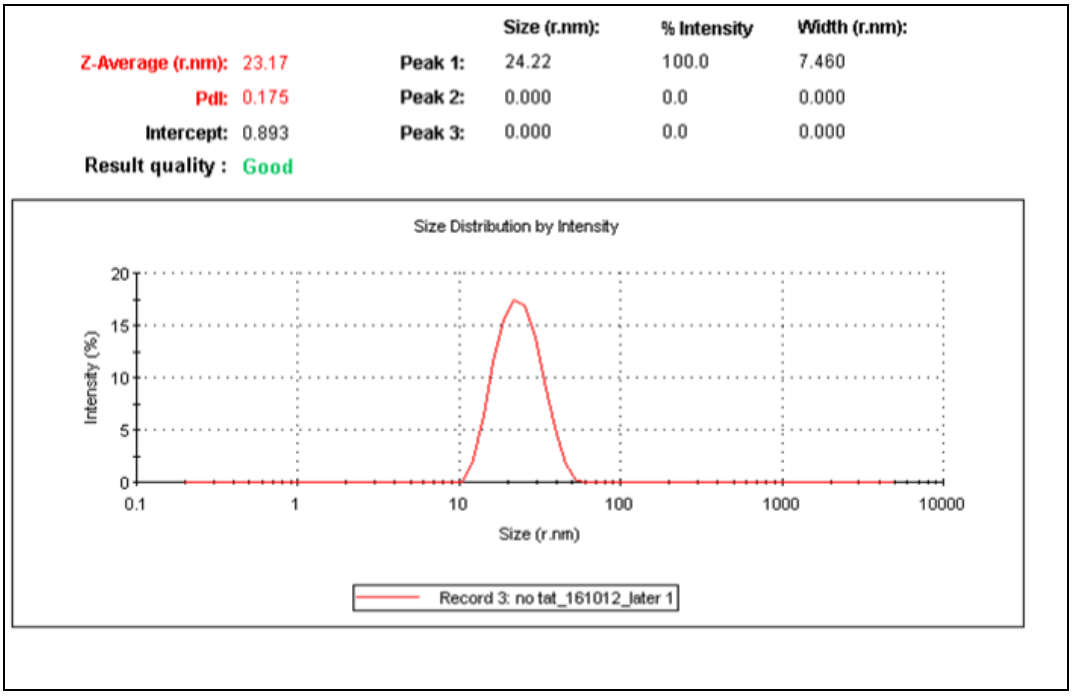


**Figure 6.6. Characterisation with DLS of TAT and No TAT polymersomes made on 15.10.12 used for tissue from patient numbers 326 and 327.** Polymersomes functionalised with TAT peptide on their surface, Z-Average (diameter): 46.34 nm and width 7.46 nm (size 46.34 ± 7.46 nm).

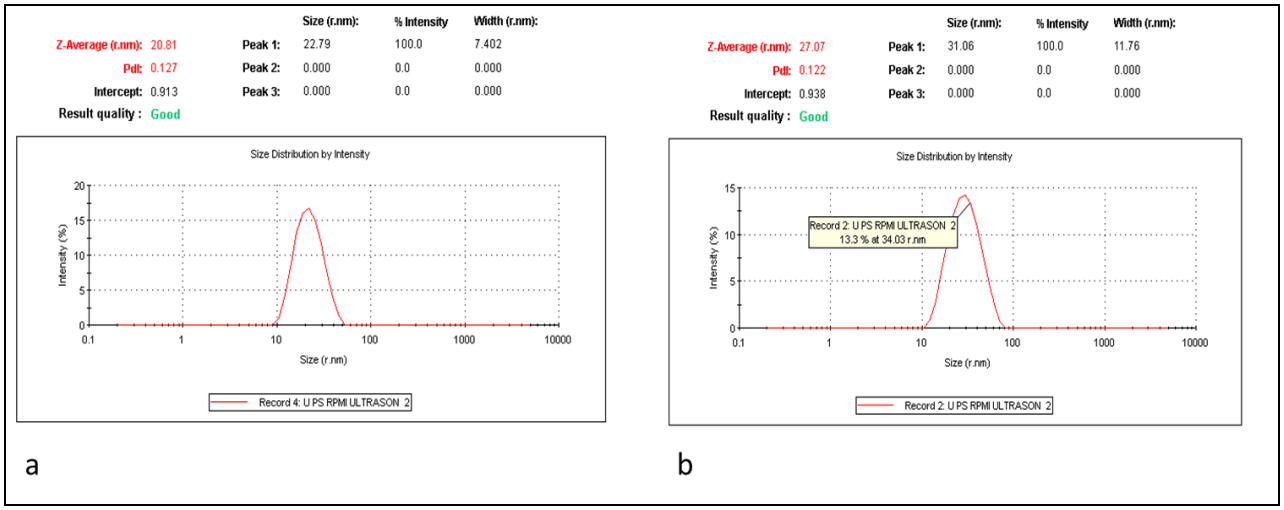


**Figure 6.7. Characterisation with DLS of TAT and No TAT polymersomes made on 22.10.12 used for tissue from patient numbers 325, 324 and 330.** (a) Polymersomes without TAT peptide on their surface, Z-Average (diameter): 45.58 nm and width 7.40 nm (size: 45.58 ± 7.40

nm). (b) Polymersomes functionalised with TAT peptide on their surface, Z-Average (diameter): 62.12 nm and width 11.76 nm (size: 62.12 ± 11.76 nm).

These results show clearly that the process of polymersomes synthesis was repeatable, producing polymersomes of similar size. Thus the only variable parameter in the experiments presented below was the tissues/endometrial cells, which were collected from different patients every time.

## 6.4 Uptake of polymersomes by *ex vivo* human endometrium and release of fluorescent FITC load into the tissue

Immunohistochemistry was performed to investigate the localisation of the NPs in the endometrial tissue. As previously described (see Chapter 5.1.1) polymersomes were loaded with sodium fluorescent (cargo) to allow assay of positive cellular uptake of NPs and the release of this model cargo.

To make sure that the uptake of fluorescence was dependent on the NPs, control experiments were used. In the control experiments, sections of endometrial tissue were treated only with PBS without polymersomes as a control for FITC uptake without NPs (Figure 6.8). In addition Mucin-1 (MUC-1), a glycoprotein which lines the apical surface of epithelial cells, was used as a marker of epithelial cells. MUC-1 was detected on the lumen side of epithelial cells which form glands and the borders of the endometrial tissue. MUC-1 was used as positive control to demonstrate the efficacy of the IHC protocol and the presence of endometrial glands in the sectioned tissue (Figure 6.9). Finally as a third control tissue, sections were incubated only with the secondary antibody in order to check if the secondary antibody binds non-specifically on the tissue. These controls were repeated in every IHC experiment.

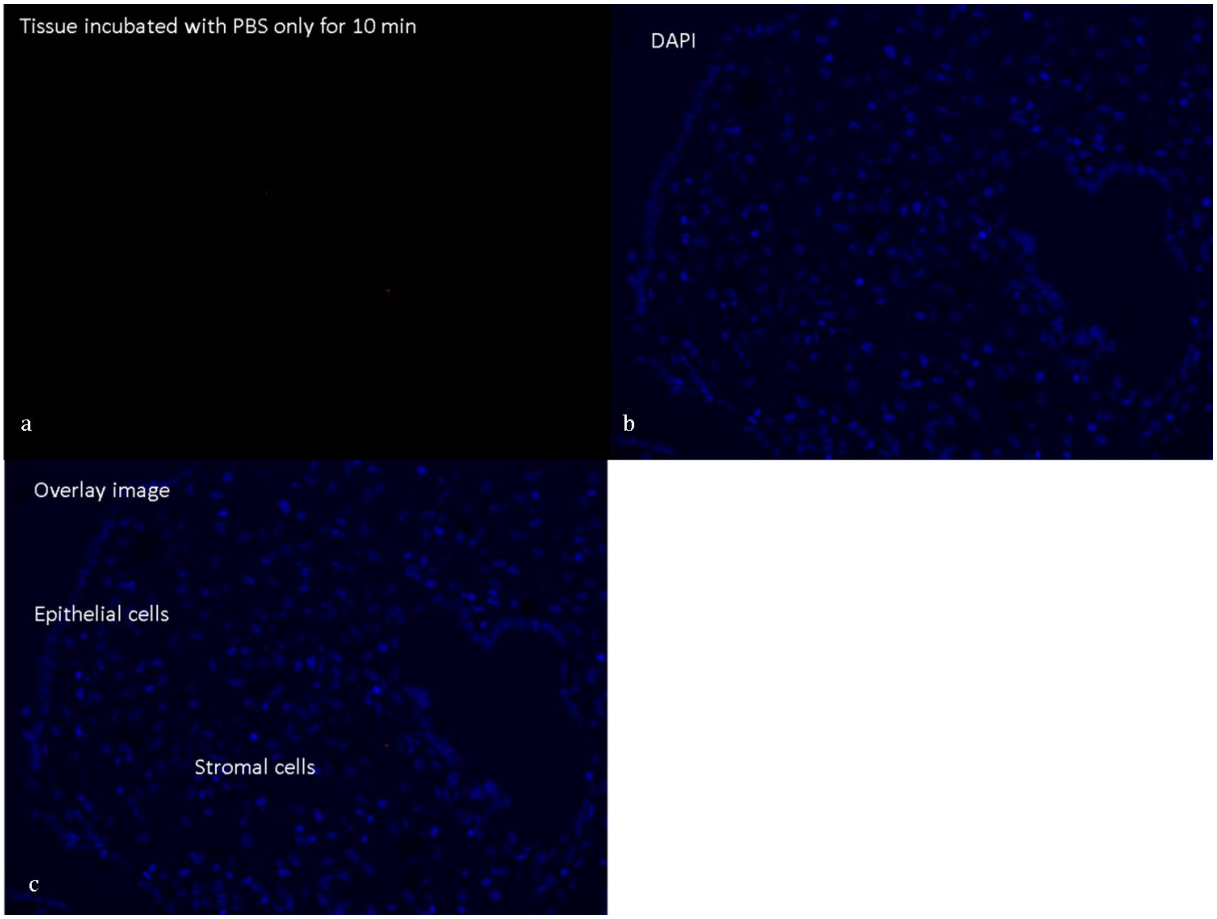


**Figure 6.8. Anti FITC labelling in tissue treated with PBS (No NPs) for 10 min at room temperature.** Tissue sections were incubated with PBS and not polymersomes are processed for IHC. (a) No signal at the wavelength of FITC (518nm) was observed. (b) Stain of cell nucleus with DAPI (blue). (c) Overlay image of images (a) and (b).

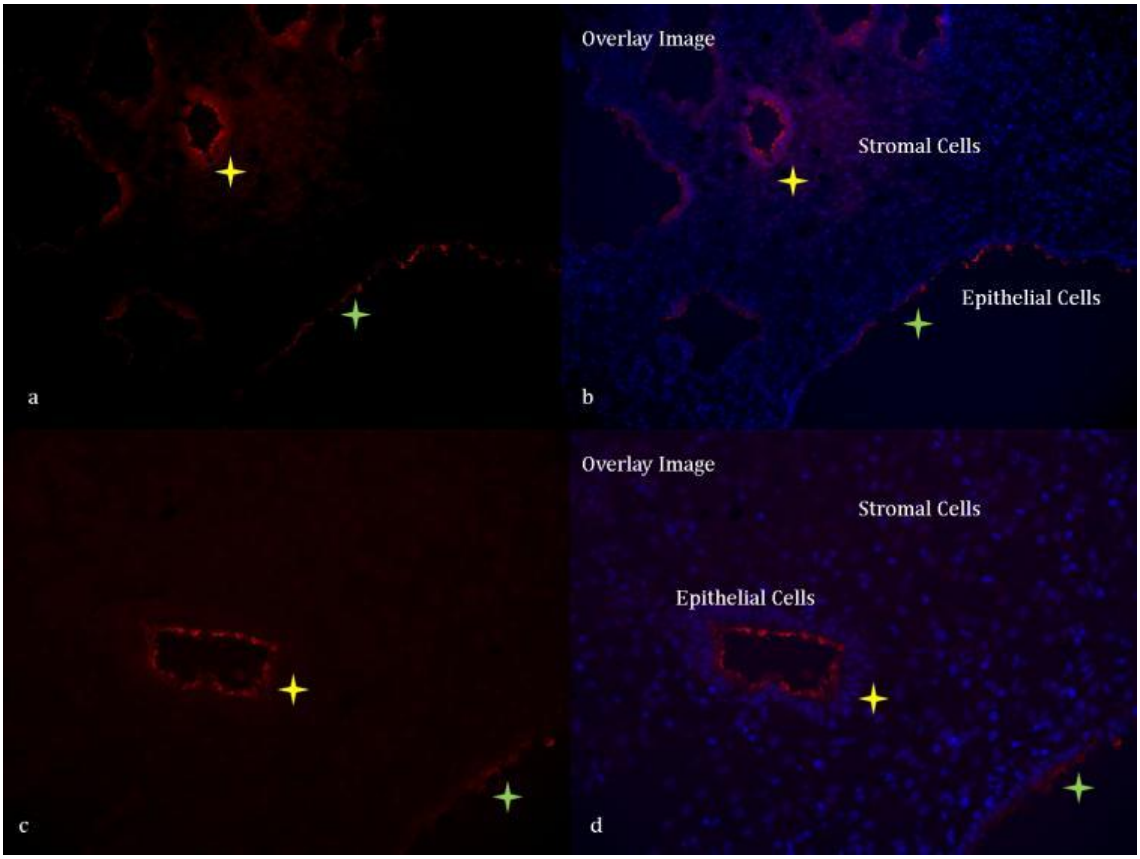


**Figure 6.9. MUC-1 positive control.** Functional layer of endometrial sections stained with MUC-1. MUC-1 can be observed marking the inside of glands demonstrating intact glandular structures (yellow stars) and the luminal surface of the epithelial cells that form the borders of the endometrial tissue (green stars).

FITC is water soluble, highly fluorescent and has an excitation of $\lambda_{ex}$ 496nm and an emission at $\lambda_{em}$ 521nm. However, in aqueous solutions at concentrations above 2.7 mmol it self-quenches and does not fluoresce. When FITC is encapsulated in the aqueous core of polymersomes above the quenching concentration, as what

happened in these experiments, it creates non-fluorescent PEG-b-PCL polymersomes carrying a payload which will fluoresce once released into cells.

Immunohistochemistry of the tissue sections which were incubated with polymersomes (concentration 3 μg/ ml), and functionalised with TAT peptide for 10 minutes at room temperature, shows that polymersomes are taken up by both stromal and epithelial cells (Figures 6.10 to 6.13).

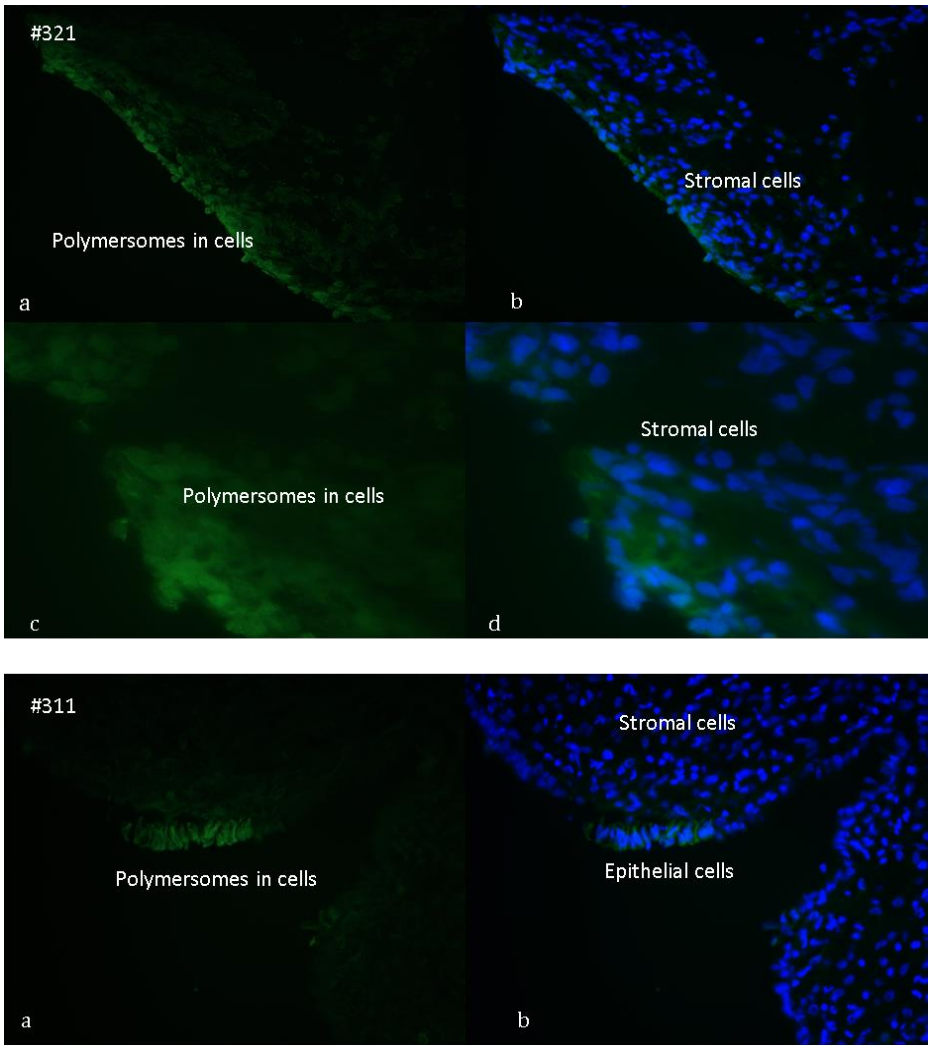


**Figure 6.10. Functional layer of endometrial tissue** from patient numbers 321 and 311 was incubated with polymersomes with TAT peptide on their surface at the concentration of

3ug/ml, sectioned in 7μm thick sections and labelled for NPs. Endometrial tissue from patient number 321 was incubated with polymersomes. (a) 40x magnification image showing that polymersomes are taken up by endometrial stromal cells and release their cargo FITC into them (green). (b) Overlay image of DAPI (blue) which stains the cell nucleus and FITC (green). (c, d) close-up (100x magnification) of a region (a, b) presenting FITC signal in endometrial cells. Endometrial tissue from patient number 311 was incubated with polymersomes. (a) 40x magnification image showing that polymersomes are taken up by endometrial epithelial cells, which form the borders of the endometrial tissue, and release their cargo FITC into them (green). (b) Overlay image of DAPI (blue) which stains the cell nucleus and FITC (green).

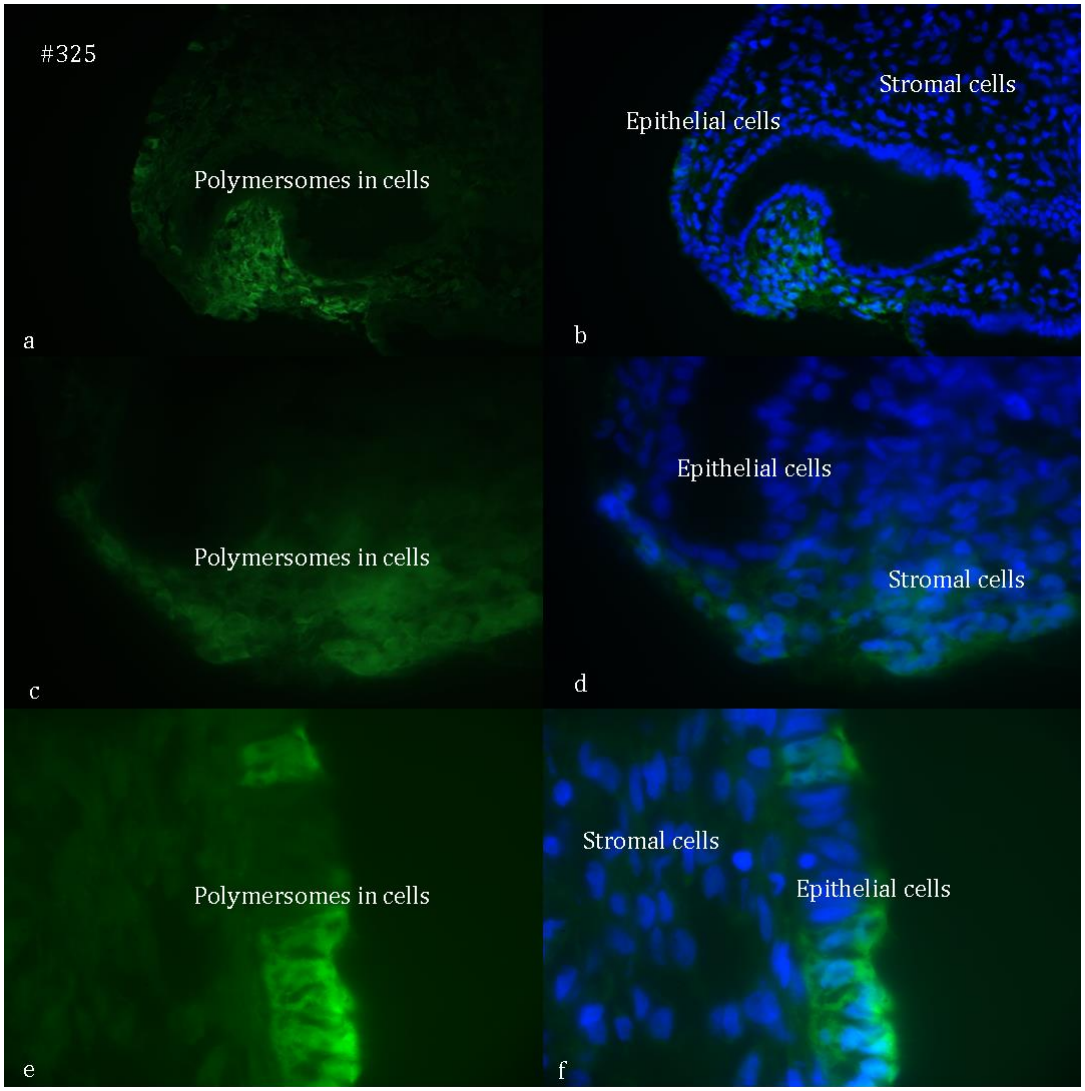


**Figure 6.11. Functional layer of endometrial tissue from patient number 325 was incubated with polymersomes with TAT peptide on their surface at the concentration of 3ug/ml, sectioned in 7μm thick sections and labelled for NPs.** Endometrial tissue from patient number 325 was incubated with polymersomes. (a) 40x magnification image showing that polymersomes are taken up by endometrial stromal and epithelial cells and release their cargo FITC into them (green). (b) Overlay image of DAPI (blue) which stains the cell nucleus and FITC (green). (c, d) close-up (100x magnification) of a region (a, b) presenting FITC signal in endometrial stromal cells. (e, f) close-up (100x magnification) of a

region (a, b) presenting FITC signal in endometrial epithelial cells.

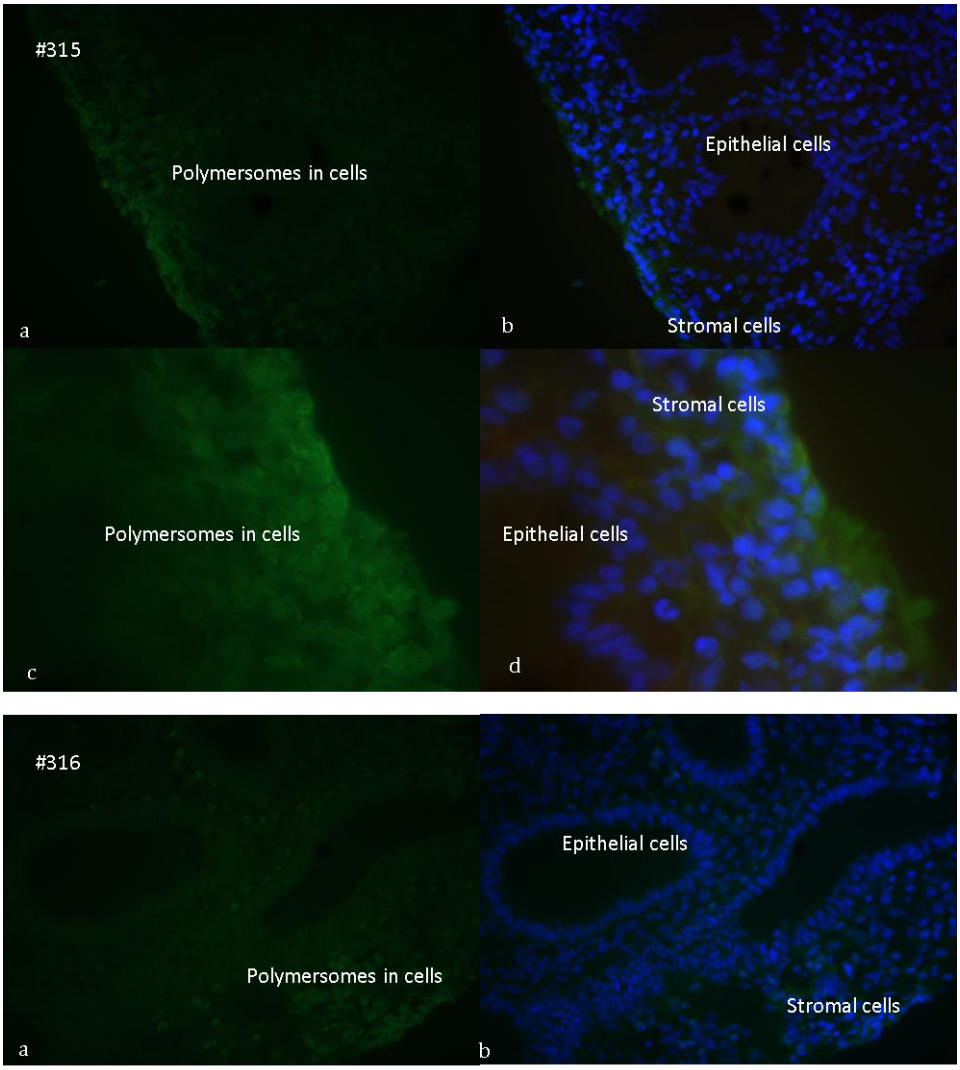


**Figure 6.12. Functional layer of endometrial tissue from patient numbers 315 and 316 was incubated with polymersomes with TAT peptide on their surface at the concentration of 3ug/ml, sectioned in 7µm thick sections and labelled for NPs.** Endometrial tissue from patient number 315 was incubated with polymersomes. (a) 40x magnification image showing that polymersomes are taken up by endometrial stromal cells and release their cargo FITC into them (green). (b) Overlay image of DAPI (blue) which stains the cell nucleus and FITC (green). (c, d) close-up (100x magnification) of a region (a, b) presenting FITC

signal in endometrial stromal cells. Endometrial tissue from patient number 316 was incubated with polymersomes. (a) 40x magnification image showing that polymersomes are taken up by endometrial stromal cells and release their cargo FITC into them (green). (b) Overlay image of DAPI (blue) which stains the cell nucleus and FITC (green).

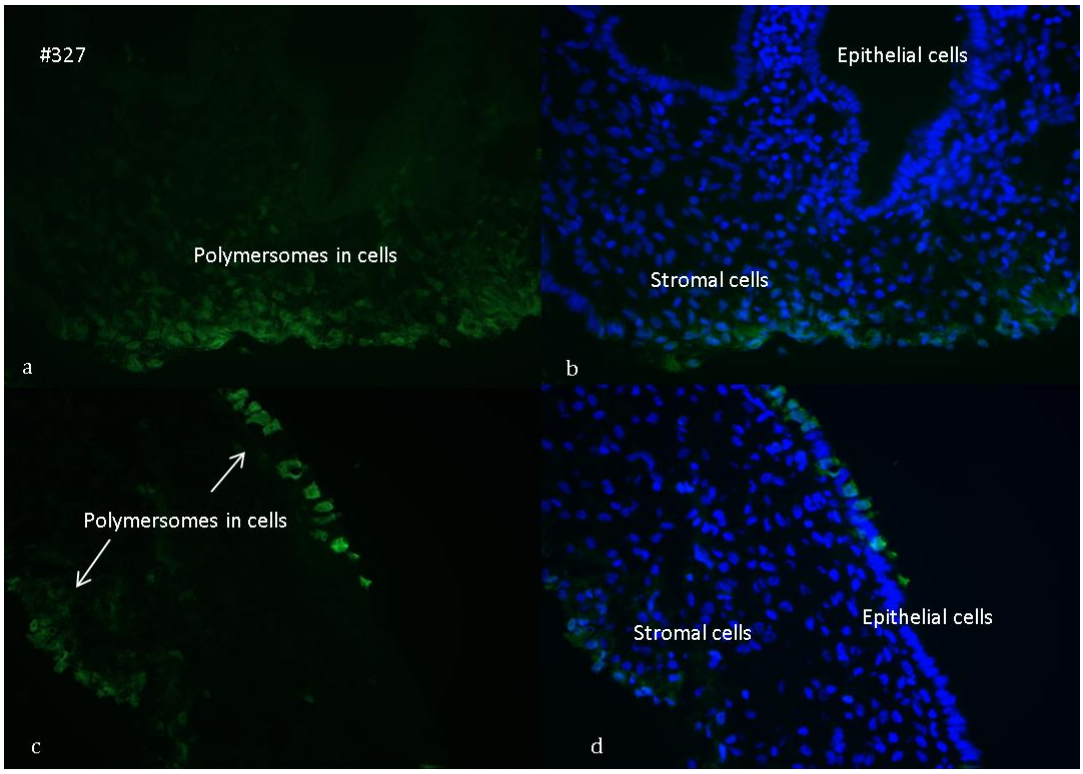


**Figure 6.13. Functional layer of endometrial tissue from patient number 327** was incubated with polymersomes with TAT peptide on their surface at the concentration of 3ug/ml, sectioned in 7μm thick sections and labelled for NPs. Endometrial tissue from patient number 327 was incubated with polymersomes. (a) 40x magnification image showing that polymersomes are taken up by endometrial stromal and release their cargo FITC into them (green). (b) Overlay image of DAPI (blue) which stains the cell nucleus and FITC (green). (c) 40x magnification image showing that polymersomes are taken up by endometrial stromal and epithelial cells and release their cargo FITC into them (green). (d) Overlay image of DAPI (blue) which stains the cell nucleus and FITC (green).

Endometrial tissue was also obtained from women in different phase of the menstrual cycle and labelled for NPs in order to determine whether or not the phase influence NPs' uptake by endometrial cells. Figure 6.13 demonstrates the IHC results from patient numbers 321 and 327 who were in secretory and proliferative phase, respectively, when tissue was collected. The results clearly showed that polymersomes were taken up by endometrial cells at both phases (Figure 6.14). Consequently when endometrial tissue is incubated with polymersomes in high concentrations, such as what was used for this experiment at 3 μg/ml, it can be taken up by endometrial cells independent of cycle phase (Table 6.2).

| **Cycle phase** | **Concentration of polymersomes** | **Uptake of polymersomes by endometrial cells** |
|---|---|---|
| Secretory phase (patient number 321) | 3 μg/ ml | ✓ |
| Proliferative phase (patient number327) | 3 μg/ ml | ✓ |

**Table 6.2.** Summary table present women's cycle phase, polymersomes' concentration during incubation with endometrial tissue and polymersomes' uptake by endometrial cells. When endometrial tissue was incubated with polymersomes in the high concentration of 3ug/ml, NPs were taken up by cells independent of women's cycle phase.

Figure 6.14 illustrates endometrial tissue from patient numbers 321 and 327 in secretory and proliferative phase, respectively, which was incubated with 3ug/ml polymersomes functionalised with TAT on their surface and processed for

immunohistochemistry to label the polymersomes. Polymersomes are taken up by endometrial cells in both cycle phases.

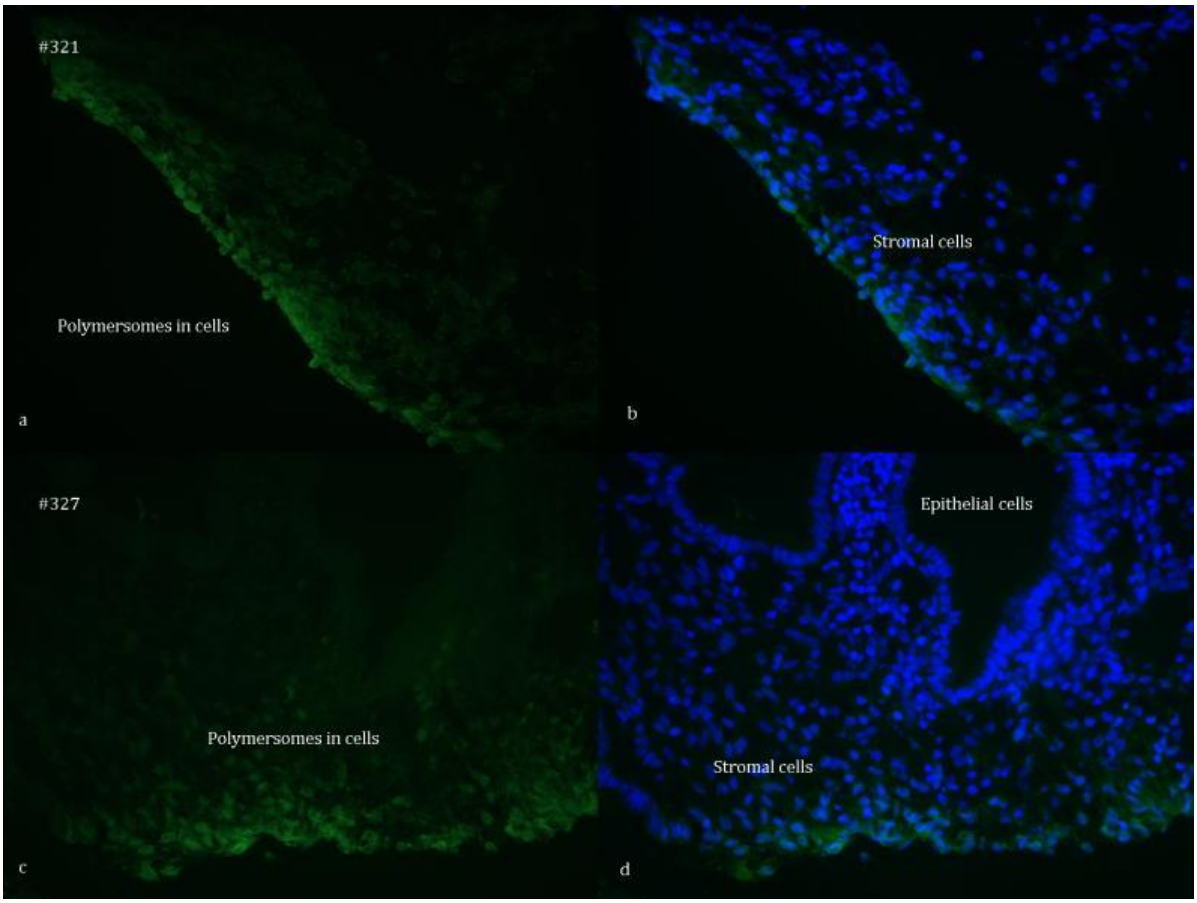


**Figure 6.14. Endometrial tissue from women in different phase of the menstrual cycle.** Endometrial tissue from 2 patients in different phase of the menstrual cycle, patient number 321 in secretory phase (a, b) and patient number 327 in secretory phase (c, d) was labelled for polymersomes. Polymersomes are taken up by endometrial cells from both patients.

Polymersome uptake in endometrial tissue was observed in both TAT and No TAT particles (Figures 6.15 and 6.16). This could be a concentration-dependent effect. Therefore, in order to investigate the ability of the TAT peptide to assist polymersomes uptake into endometrial cells, a reduced concentration of NPs (e.g.

0.06um/ml) might be needed. Preliminary results are demonstrated in Figure 6.16, which shows FITC signal was still detected but at visibly lower levels compared with the tissue incubated with neat polymersomes. Incubation of endometrial tissue with No TAT polymersomes at the reduced concentration was not preformed, but will be addressed in future experiments.

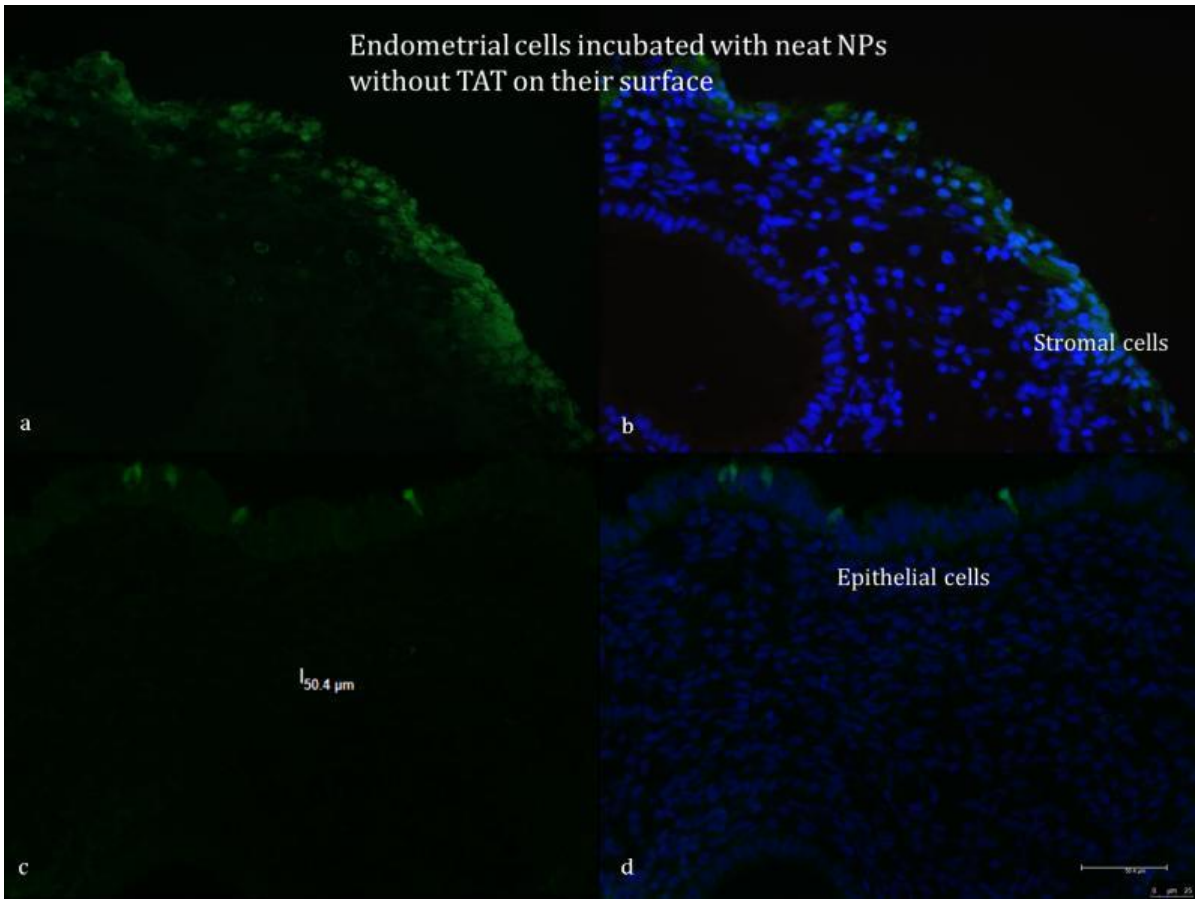


**Figure 6.15. No TAT polymersomes are taken up by endometrial cells.** Polymersomes without TAT peptide on their surface are taken up by both endometrial stromal (a, b) and epithelial cells (c, d).

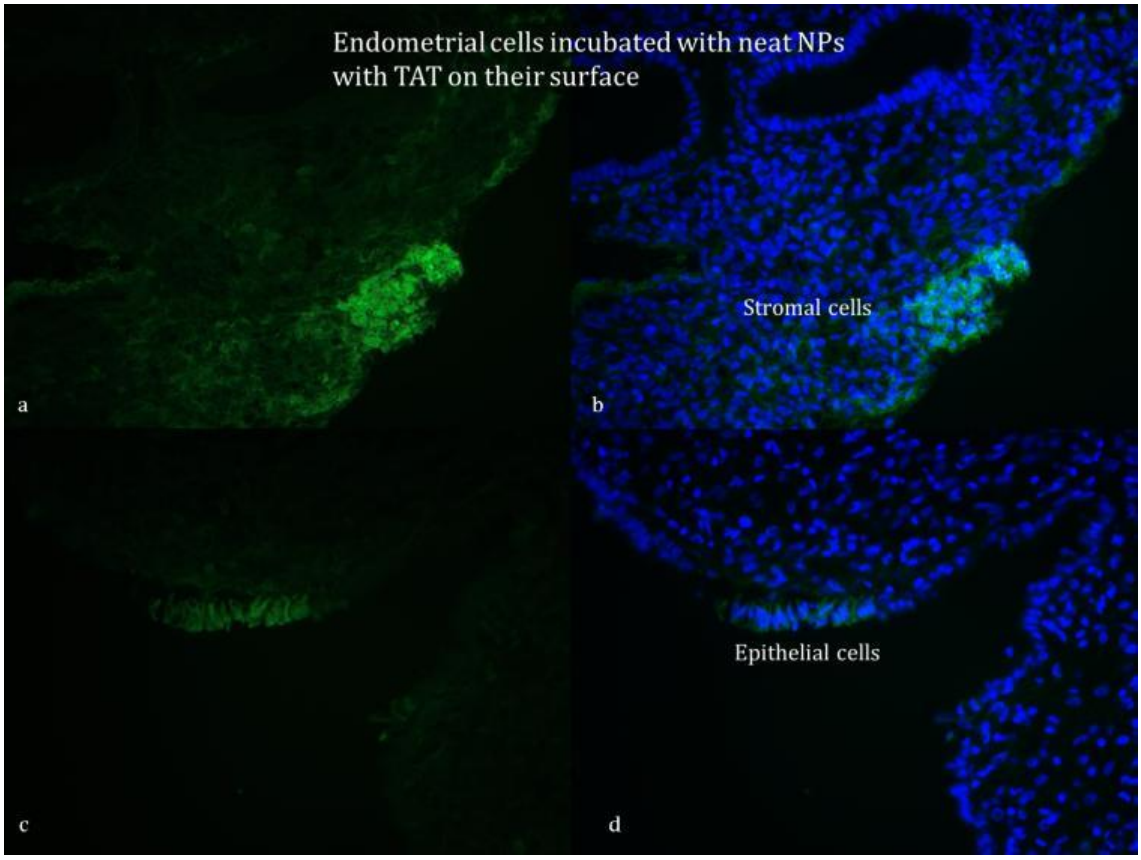


**Figure 6.16. TAT polymersomes are taken up by endometrial cells.** Polymersomes functionalised with TAT peptide on their surface are taken up by both endometrial stromal (a, b) and epithelial cells (c, d).

The figures 6.15 and 6.16 present immunohistochemistry results from endometrial tissues that were previously incubated with 3ug/ml of polymersomes without TAT and with TAT on their surface, respectively.

The immunohistochemistry results from tissue that was previously treated with only 0.06 ug/ml polymersomes functionalised with TAT peptide, are presented in Figure 6.17.

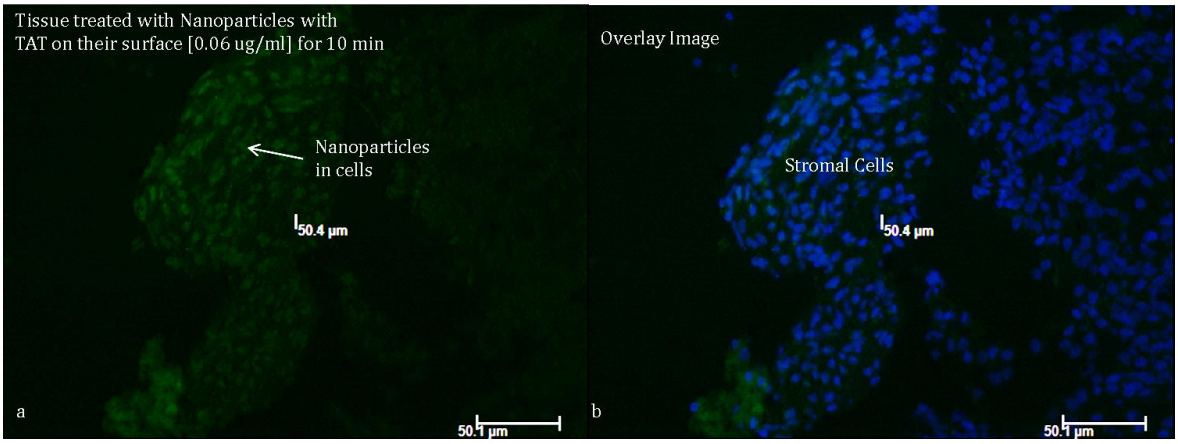


**Figure 6.17. Endometrial tissue incubated with polymersomes functionalised with TAT peptide in 0.06ug/ml concentration.** Endometrial tissue was incubated with NPs functionalised with TAT in the concentration of 0.06ug/ml. (a) NPs are taken up by endometrial stromal cells even in this low concentration. (b) Overlay image of DAPI (blue) which stains the cell nucleus and FITC (green).

To assess which cells the nanoparticles were taken up into Vimentin, a stromal cell marker and Cytokeratin, an epithelial cell marker, were used. Vimentin, which is a major subunit protein of the intermediate mesenchymal cells, can be used as a stromal cell marker and Cytokeratin, which reacts only with normal reactive and neoplastic epithelial tissue, can be used as a marker for epithelial cells. Before the co-localisation assay Vimentin and Cytokeratin antibodies were checked for their cell-specific labelling. This is shown in Figures 6.18 and 6.19.

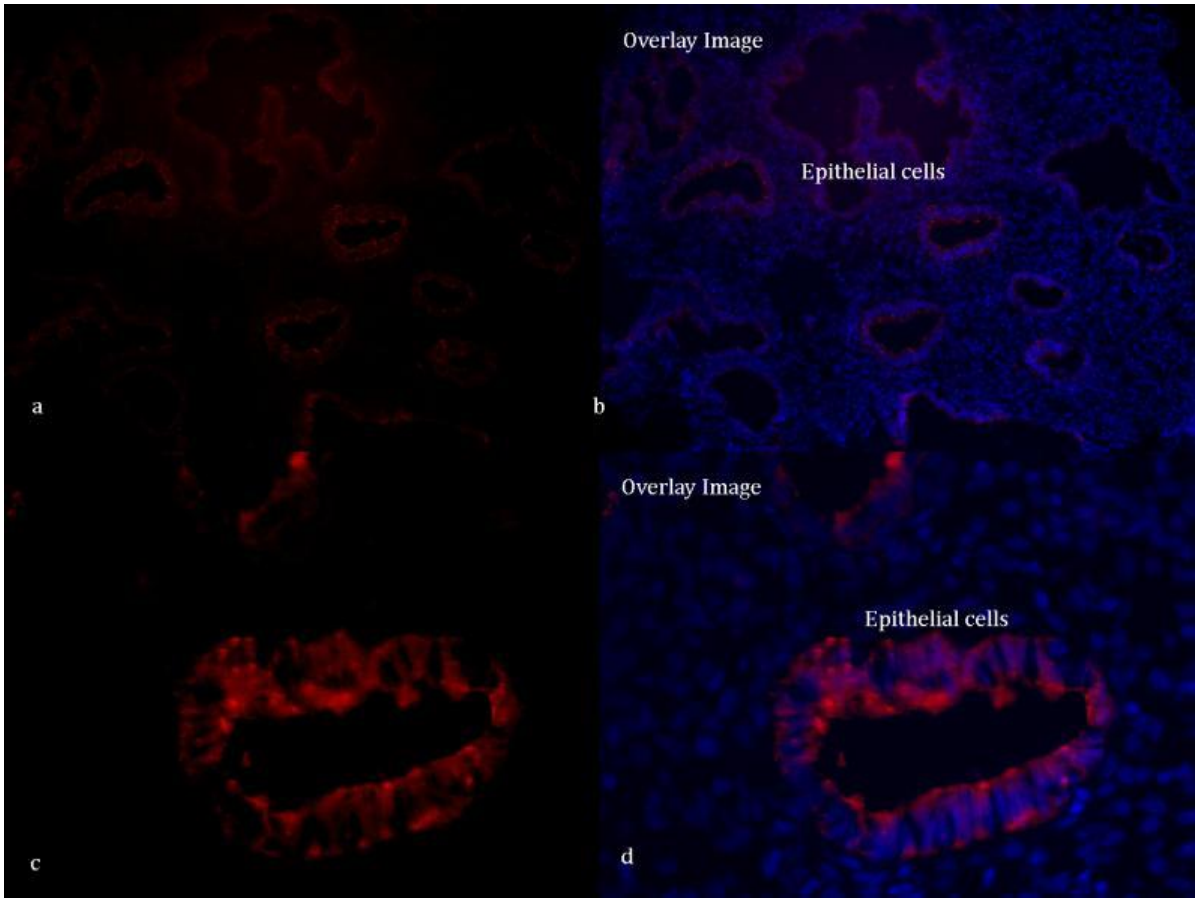


**Figure 6.18. Endometrial tissue is stained for Cytokeratin.** (a, b) Successful labelling of epithelial cells with Cytokeratin in endometrial tissue. (c,d) Close-up of a region from figure (a) clearly shows that Cytokeratin (red signal) reacts only with epithelial cells and not with stromal cells in endometrial tissue.

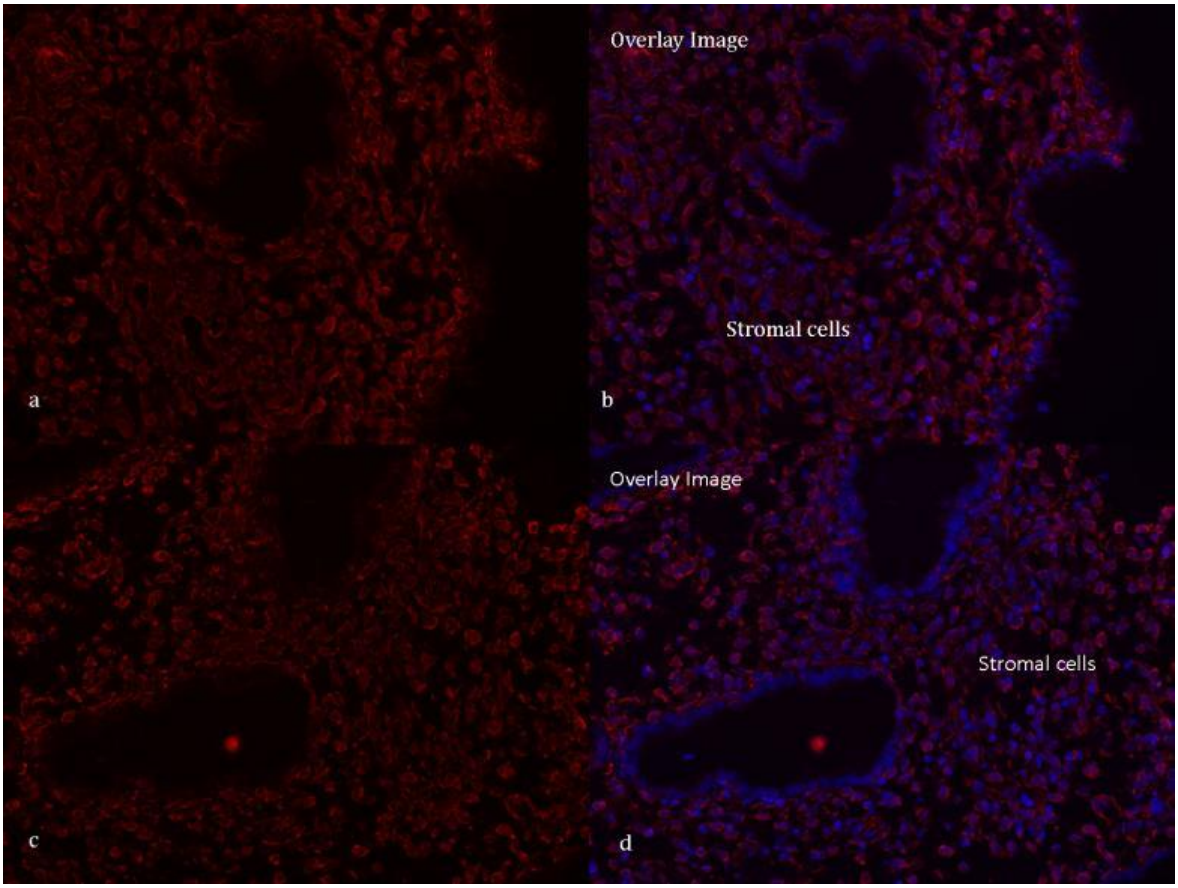


**Figure 6.19. Endometrial tissue is stained for Vimentin.** (a, b) Vimentin is an effective marker for endometrial stromal cells. (c,d) Close-up of a region from figure (a) demonstrate that Vimentin stains effectively only stromal cells in endometrial tissue.

The next step of the experiment was to double-stain endometrial tissue for Vimentin or Cytokeratin and anti-FITC. In these experiments the incubation time of the antibodies was 90 or 60 min (Chapter 5.5). When initial tissue sections were treated with antibodies for 90 min, Vimentin stained not only the endometrial stromal cells but also the epithelial cells as well (Figure 6.20). Therefore the experiment was repeated, decreasing the antibody's incubation time to 60 minutes. However the result was the same, with Vimentin staining not only the endometrial stromal cells

but also the epithelial cells (Figure 6.21). This could be explained as a non-specific cross reaction.

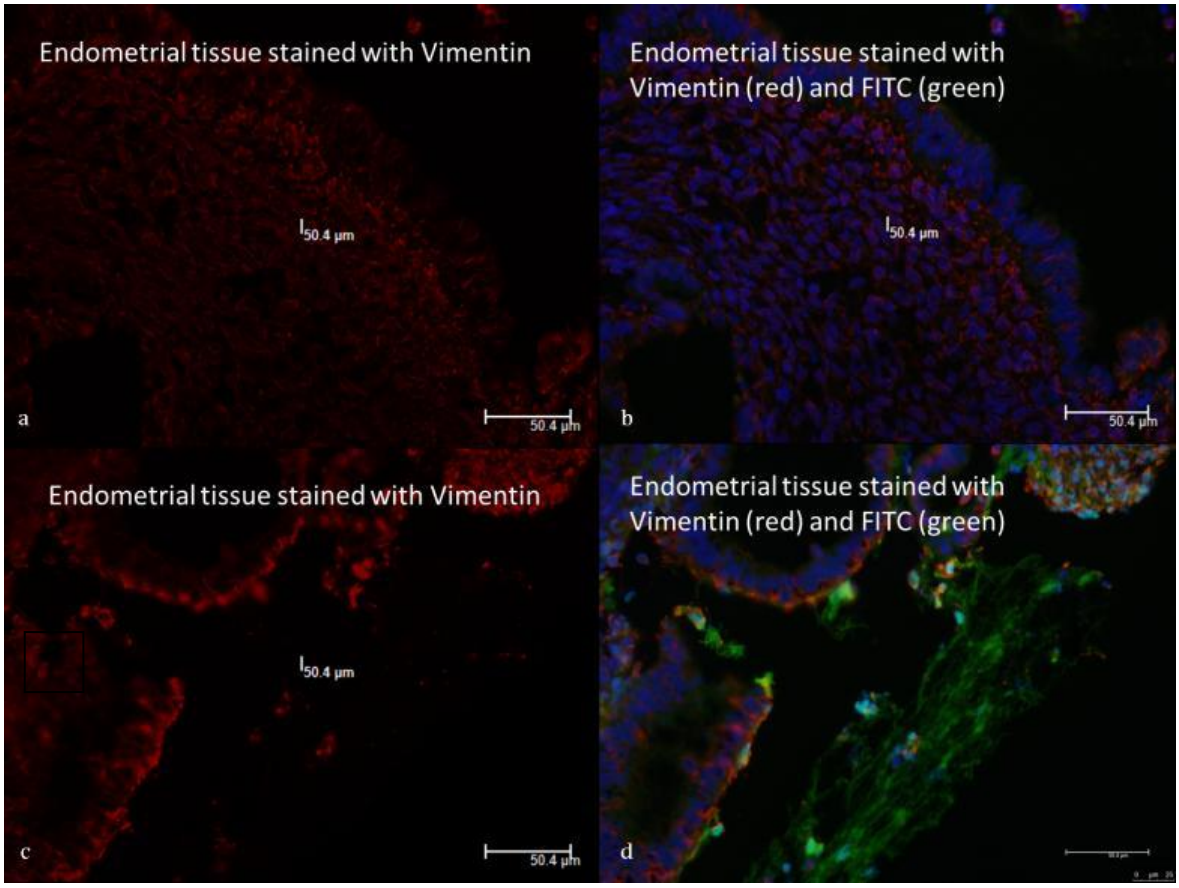


**Figure 6.20. Functional layer of endometrial tissue was stained for Vimentin and FITC (antibodies incubation 90min).** (a, c) Vimentin (red) which is a marker for stromal cells stained also endometrial epithelial cells which form the borders of the endometrial tissue and glands. (b, d) Tissue sections were labelled for Vimentin (red), FITC (green) and DAPI (blue).

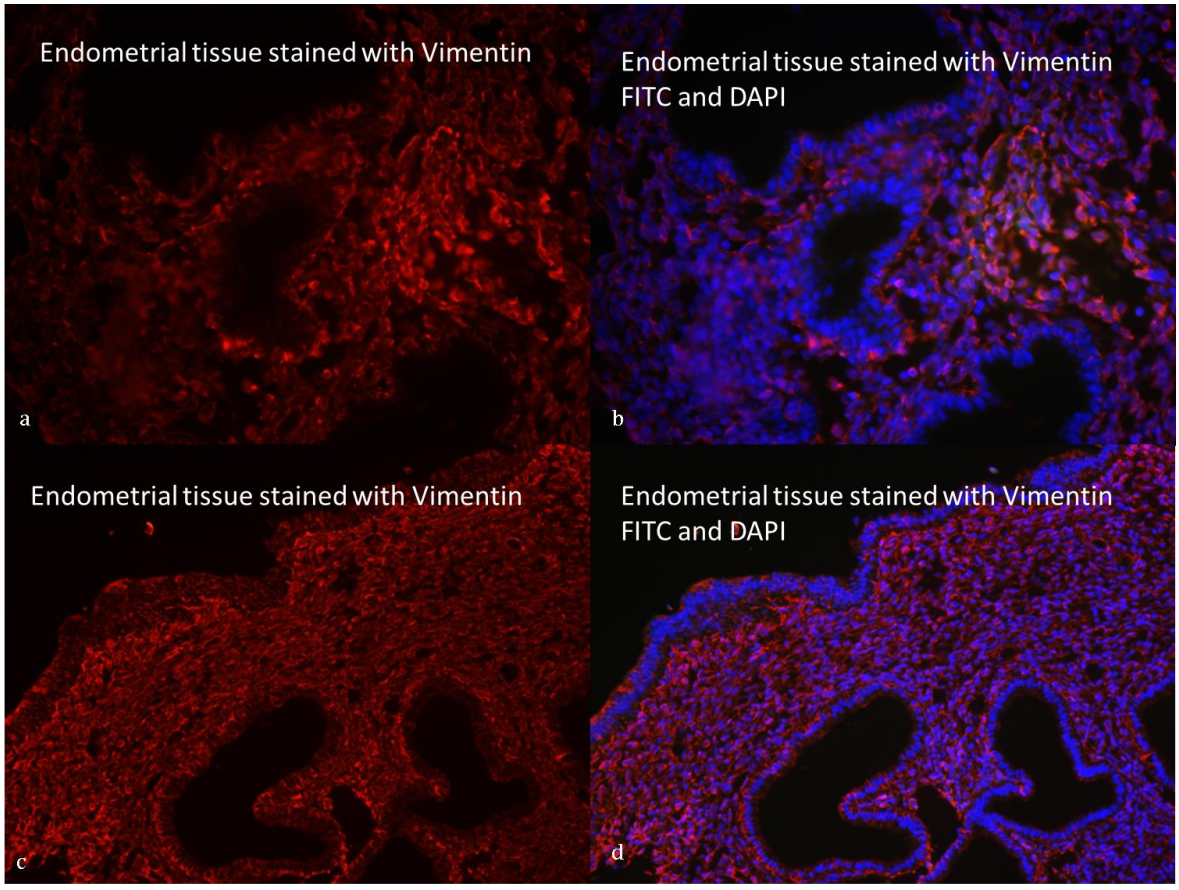


**Figure 6.21. Functional layer of endometrial tissue was stained for Vimentin and FITC (antibodies incubation 60min). (**a, c) Vimentin (red) which is a marker for stromal cells stained also endometrial epithelial cells which form the borders of the endometrial tissue and glads. (b, d) Tissue sections were labelled for Vimentin (red), FITC (green) and DAPI (blue).

## 6.5 Uptake of polymersomes by primary endometrial cells

Polymersomes were taken up by primary endometrial cells within the first minutes of incubation. When cells were fixed after 10 min of incubation with polymersomes and the FITC signal was detected with immunohistochemistry, strong punctate fluorescent signal from FITC was observed within the cell indicating

payload release. When cells were then fixed after 45 and 90 min of incubation, signal was dispersed over the time. Previous live cell imaging experiments in fibroblasts support these results [105]. In these experiments, strong fluorescence is seen within the cell that appears to be within endocytic vesicles which then disappeared after 10 min to be replaced by a homogenous signal across the cell. Thus, indicating that FITC was released from the endocytic vesicles into the cytoplasm. Results from the experiments in fibroblasts suggest that polymersomes are not only getting into cells but also release their payload. Finally, as accumulation of fluorescence wasn't observed elsewhere in the cell, except of the endocytic vesicles first and then into the cytoplasm, it can be assumed that FITC was not trafficked to another compartment such as lysosomes, the endoplasmic reticulum or Golgi apparatus. Therefore macropinocytosis is the most likely route of polymersomes' internalisation as opposed to clathrin or caveolae mediated endocytosis (Chapter 1.3.2). Furthermore, it was observed that TAT polymersomes are able to enter primary endometrial stromal cells and release their cargo. Immunohistochemistry experiments showed green fluorescent signal within cells, indicating that NPs' cargo was released into the cells. Hence, NPs had taken up by endometrial cells. Finally, as mentioned above, primary endometrial cells were incubated with NPs for different length of times. This was done, first of all, to see when the uptake of polymersomes by cells happens; secondly, to draw some conclusion of the route of NPs' uptake by the endometrial cells; and finally, to observe how the FITC signal was changing over time.

Therefore due to unforeseen circumstances, this part of the study was not completed.

# Chapter 7

## Discussion

## 7.1 Discussion

The accurate non-invasive and early diagnosis and treatment of endometrial pathologies, and in particular endometriosis, is limited by the lack of sensitivity and specificity of the current detection techniques. Therefore, there is pressing need for the development of new methods for both diagnosis and treatment of endometrial pathologies.

Over the last decades nanoparticles (NPs) have been introduced to the discipline of medicine for imaging, diagnosis and treatment [8]. Targeted deliveries of therapeutic or diagnostic agents using biocompatible and biodegradable NPs were also introduced for different disorders. These entities can enhance the diagnosis and treatment of reproductive pathologies.

Several studies have been conducted using nanoparticles against ovarian, endometrial and cervical carcinoma (see Table 1.1) but very few studies have reported the role of nanomedicine in gynaecological pathologies such as endometriosis. A recent study however has shown that cerium oxide nanoparticles can eliminate endometrial lesions induced in mice by reducing oxidative stress and angiogenesis [106]. However, several research groups have demonstrated that this type of nanoparticle exhibited toxicity which necessitates further investigation [107]. Furthermore Kumar et al. have used PLGA nanoparticles, organic nanoparticles used against several types of cancer cells, loaded with two drugs for endometriosis treatment in order to check *in vivo* the combinatorial effect of the drugs [108]. Regression of the lesions has been shown after an exposure of mice, induced with the disease, to these NPs [108]. However, none of these studies have tested NPs interaction with human eutopic endometrium.

The present project investigated the feasibility of an innovative diagnostic method, that of the delivery and detection of nanoparticles (NPs) on *ex vivo* endometrial tissue/cells. In particular, that of the use of polymersome nanoparticles, comprising of biodegradable amphiphilic block copolymers (PEG-b-PCL) and engineered for endometrial cell-specific targeting and delivery. In this way, it explored the interaction between endometrial cells and PEG-b-PCL polymersomes targeted ubiquitously to all cell types and loaded with a novel hydrophilic model cargo, i.e. quenched FITC.

The paradigm of using organic nanoparticles (NPs) targeted to endometrial cells was introduced for the first time in this project. The study was carried out in endometrial tissues from women undergoing gynaecological laparoscopic procedures for chronic pelvic pain and/or infertility. It followed the synthesis of organic polymersomes (PEG-b-PCL) and the delivery of NPs, loaded with a hydrophilic model drug, to *ex vivo* endometrial tissue to simulate drug release. Then, primary derived cells were used to study the mechanism of cellular entry of the polymersomes into this tissue.

The present study has demonstrated the uptake of polymersome nanoparticles by human endometrium epithelial and stromal cells, and the subsequent release of fluorescent FITC from within the particles. Polymersomes loaded with drugs or imaging agents can be used to target endometrial cells. The delivery of hydrophilic drugs, directly targeted for endometrial cells, may therefore be achieved by a minimally invasive, non-surgical procedure. The study highlights the potential of targeted NP therapy for future diagnosis and treatment of endometrial pathologies.

However, the study also highlighted several limitations including the following.

### 7.1.1 *Hematoxylin staining of endometrial tissue*

In order to ensure the reproducibility and reliability of the experiments before the immunohistochemistry experiments were conducted, the first step was to stain the tissues with hematoxylin. Hematoxylin staining is widely used and is a successful way to assess the integrity of the tissue before its usage for further experiments such as immunohistochemistry.

From the 21 samples of endometrial tissue collected, 19 were cut and stained with Hematoxylin to check tissue integrity and the morphology of the cells. Six of these sample sections (from patient numbers 316, 321, 315, 327, 311 and 325) showed good tissue integrity with intact glands and stromal cells surrounding them. Tissue from the other patients showed poor integrity when sectioned on the cryostat, probably due to the low temperature in the cryostat. Fluctuations in temperature when cutting tissue can result in ice crystal formation which then leads to tissue disruption and cell lysis.

### 7.1.2 *Dynamic light scattering*

Dynamic light scattering (DLS) was used to measure the hydrodynamic diameter of the polymersomes and to assess their size distribution before they were used in subsequent experiments. This was necessary because it is important that the whole population of NPs should be of similar size, as cellular uptake of NPs is size-dependant. In this way it was ensured that the experiments were repeatable.

The size of polymersomes for the No TAT was expected to be around 40nm, although this can vary between batches of polymer. The DLS results from the polymersomes used for these experiments are summarised in Table 6.1. The size of the polymersomes made on 16.07.2012 and 01.10.2012 was around 70nm. The

different size of the first polymersomes TAT and No TAT (made on 16.07.2012) might be due to the FITC (FITC-PEG-PCL) conjugating only on their surface. The different size of the TAT polymersomes made on 01.10.2012 could be due to the delay (20 days) between the polymersomes preparation and the DLS measurements. As TAT (TAT-PEG-PCL) becomes unstable in the long term after its conjugation on the surface of the polymersomes, this could have affected the DLS results.

### 7.1.3 *Immunohistochemistry*

The polymersomes were taken up by *ex vivo* endometrial cells and successfully delivered their cargo (FITC). The FITC signal was detected in both endometrial stromal and epithelial cells. Co-localisation of DAPI, which stains the nucleus blue, with FITC in some cases, might be due to TAT peptide and tissue fixation (see Chapter 5.1). Thus there is a need for further experiments to examine the use of unfixed endometrial tissue or with different cell penetrating peptides conjugated on the polymersomes' surface, such as Penetratin/pAntp peptide, Transportan and pVEC (Table 7.1).

| Name | Sequence | Reference |
|---|---|---|
| Penetratin/ pAntp peptide | R*QIKIWFQNRRMKWKK amide | [[109] [110] [111] |

| | | |
|---|---|---|
| Transportan | GWTLNSAGYLLGK*INLKALAA LAKKIL amide | [112] |
| pVEC | L*LIILRRRIRKQAHAHSK amide | [113] |

**Table 7.1. Cell penetrating peptides.** Penetratin, Transportan and pVEC are cell penetrating peptides that have been used to deliver in cells a broad variety of cargos.

Polymersomes were shown to be taken up by endometrial cells in both the proliferative and secretory phase. However, further experiments should be done to prove this as the tissue from the woman who was in proliferative phase showed poor integrity when it was checked with Haematoxylin staining. Furthermore both polymersomes with and without TAT on their surface were taken up by endometrial cells. This could be due to the high concentration of polymersomes when endometrial tissue was incubated with them.

The experiments in the present study with primary endometrial stromal cells and PEG-b-PCL polymersomes loaded with FITC and functionalised with TAT, support the *ex vivo* results, which demonstrate that polymersomes are successfully taken up by these cells and release their payload into them. Furthermore, these experiments demonstrate that NPs are rapidly entering the cells and that cargo release occurs within endocytic vesicles followed by its cytoplasmic release.

## 7.2 Investigating polymersomes uptake by primary endometrial cell

In the primary endometrial cells experiments we focused on the uptake of FITC into endometrial cells as endometrial stromal cells play a key role throughout woman's menstrual cycle by undergoing changes which prepare the endometrium for implantation (Chapter 2.2). However, as this technology could also be used for the

treatment of endometrial cancer, it would be useful to extend the experiments by also using endometrial epithelial cells as most of the endometrial cancers are derived from endometrial epithelial cells.

## 7.3 Future studies

The present study has opened the way for further questions and experiments. The next step is to analyse the uterine fluid and blood samples collected from these patients (Table 7.2) with endometrial pathologies by using mass spectrometry and proteomics in order to identify any alterations in the physiological levels of biomolecules during pathological situations. Information from this analysis can establish the basis for quick diagnosis in the early stages, which will offer many advantages compared to the current treatment. Also fluorescently labelled nanoparticles of these tissues may enable identification of pathologies by fluorescence imaging.

The early detection of the pathologies could improve and extend the patient's life and may help to avoid surgical procedures. Furthermore, targeted delivery of PEG-b-PCL polymersomes to the diseased area could be achieved by functionalising the surface of the NPs with biomarkers identified by mass spectrometry and proteomics analysis. In addition to the mass spectrometry and proteomics *in vivo* experiments are needed in order to improve the system and bring it closer to clinical use.

| **Patient number** | **Pathology** | **Endometrial fluid (not blood stained)** | **Serum (blood)** |
|---|---|---|---|

| | | | |
|---|---|---|---|
| 313 | Chronic pelvic pain | - | ✓ |
| 326 | Chronic pelvic pain | ✓ | ✓ |
| 337 | Chronic pelvic pain | - | ✓ |
| 314 | Subfertility | - | ✓ |
| 316 | Subfertility | - | ✓ |
| 321 | Subfertility | - | ✓ |
| 322 | Subfertility | - | ✓ |
| 331 | Subfertility | - | ✓ |
| 332 | Subfertility | - | ✓ |
| 323 | Subfertility | ✓ | ✓ |
| 324 | Subfertility | ✓ | ✓ |
| 330 | Subfertility | ✓ | ✓ |
| 333 | Subfertility | - | ✓ |
| 352 | Subfertility | - | ✓ |
| 353 | Subfertility | ✓ | - |
| 326 | Endometriosis | ✓ | ✓ |
| 325 | Endometriosis | ✓ | ✓ |
| 317 | Endometriosis | ✓ | - |
| 337 | Endometriosis | - | ✓ |
| 329 | Endometriosis | - | ✓ |
| 332 | Endometriosis | - | ✓ |
| 333 | Endometriosis | - | ✓ |
| 325 | Recurrent miscarriages | ✓ | ✓ |

**Table 7.2. Samples of uterine fluid (n=20) and blood (n=12) from 23 women with endometrial pathologies.**

To answer the questions raised by the present study further experiments are needed to investigate the following issues:

A. Whether polymersomes are equally taken up by endometrial cells in both the proliferative and secretory phase by using more samples.
B. Whether TAT or not TAT peptides assist polymersomes uptake by endometrial cells. Further experiments with incubation of endometrial cells at 1:50 dilution of TAT and No TAT polymersomes should be done. This is important as in the future, functionalised polymersomes with the appropriate ligand, instead of TAT, could be delivered to specific cells.
C. Whether Nanoparticles are taken up by endometrial stromal or epithelial cells by experimenting with a stromal and epithelial cell marker like Vimentin and Cytokeratin, respectively.
D. Whether co-localisation of DAPI with FITC might be due to TAT peptide (chapter 1.2.4), since it has been shown by co-workers that there is co-localization of FITC signal with the cell nucleus. To answer this question unfixed endometrial tissue was collected, incubated with TAT and No TAT NPs and sectioned. The last step to be done in these sections is the Immunohistochemistry assay.

# Chapter 8

## References

[1] El-Ansary A, Al-Daihan S. On the Toxicity of Therapeutically Used Nanoparticles: An Overview. *Journal of Toxicology*. **2009**;2009:1-9.

[2] Yoo HS, Lee KH, Oh JE, Park TG. In vitro and in vivo anti-tumor activities of nanoparticles based on doxorubicin-PLGA conjugates. *J Control Release*. **2000**;68:419-431.

[3] Sahni JK, Doggui S, Ali J, Baboota S, Dao L, Ramassamy C. Neurotherapeutic applications of nanoparticles in Alzheimer's disease. *J Control Release*. **2011;**152:208-231.

[4] Chattopadhyay N, Zastre J, Wong HL, Wu XY, Bendayan R. Solid lipid nanoparticles enhance the delivery of the HIV protease inhibitor, atazanavir, by a human brain endothelial cell line. *Pharm Res*. **2008**, 25, 2262-2271.

[5] Lin JJ, Ghoroghchian *P*, Zhang Y, Hammer DA. Adhesion of antibody-functionalized polymersomes. *Langmuir*. ***2006;*** 22:3975-3979.

[6] Werner ME, Karve S, Sukumar R, Cummings ND, Copp JA, Chen RC, Zhang T, Wang AZ. Folate-targeted nanoparticle delivery of chemo- and radiotherapeutics for the treatment of ovarian cancer peritoneal metastasis. *Biomaterials*. **2011**;32:8548-8554.

[7] Brooks H, Lebleu B, Vivès E. Tat peptide-mediated cellular delivery: back to basics. *Adv Drug Deliv Rev*. **2005**;57:559-577.

[8] Zhang L, Gu FX, Chan JM, Wang AZ, Langer RS, Farokhzad OC. Nanoparticles in medicine: therapeutic applications and developments. *Clin Pharmacol Ther*. **2008**; 83:761-769.

[9] Milane L, Duan Z, Amiji M. Development of EGFR-targeted polymer blend nanocarriers for combination paclitaxel/lonidamine delivery to treat multi-drug resistance in human breast and ovarian tumor cells. *Mol Pharm*. **2011**;8:185-203.

[10] Yang C, Ding N, Xu Y, Qu X, Zhang J, Zhao C, Hong L, Lu Y, Xiang G. Folate receptor-targeted quantum dot liposomes as fluorescence probes. *J Drug Target*. **2009**;17: 502-511.

[11] Shen LF, Chen J, Zeng S, Zhou RR, Zhu H, Zhong MZ, Yao RJ, Shen H. The Superparamagnetic Nanoparticles Carrying the *E1A* Gene Enhance the Radiosensitivity of Human Cervical Carcinoma in Nude Mice. *Mol Cancer Ther*. **2010**;9:2123-2130.

[12] Abdulla-Al-Mamun M, Kusumoto Y, Mihata A, Islam MS, Ahmmad B. Plasmon-induced photothermal cell-killing effect of gold colloidal nanoparticles on epithelial carcinoma cells. *Photochem Photobiol Sci*. **2009;**8:1125-1129.

[13] Sirotkina MA, Elagin VV, Shirmanova MV, Bugrova ML, Snopova LB, Kamensky VA, Nadtochenko VA, Denisov NN, Zagaynova EV. OCT-guided laser hyperthermia with passively tumor-targeted gold nanoparticles. *J Biophotonics*. **2010**;3:718-727.

[14] Corsi F, Fiandra L, De Palma C, Colombo M, Mazzucchelli S, Verderio P, Allevi R, Tosoni A, Nebuloni M, Clementi E, Prosperi D. HER2 expression in breast cancer cells is downregulated upon active targeting by antibody-engineered multifunctional nanoparticles in mice. *Acs Nano*. **2011**;5:6383-6393.

[15] Talaei F, Azizi E, Dinarvand R, Atyabi F. Thiolated chitosan nanoparticles as a delivery system for antisense therapy: evaluation against EGFR in T47D breast cancer cells. *Int J Nanomed*. **2011**;6:1963-1975.

[16] Liang C, Yang Y, Ling Y, Huang Y, Li T, Li X. Improved therapeutic effect of folate-decorated PLGA-PEG nanoparticles for endometrial carcinoma. *Bioorg Med Chem*. **2011;**19:4057-4066.

[17] Koziara JM, Lockman PR, Allen DD, Mumper RJ. Paclitaxel nanoparticles for the potential treatment of brain tumors. *J Control Release*. **2004**;99:259-269.

[18] Abhilash M. Potential applications of Nanoparticles. *International Journal of Pharma and Bio Sciences*. V1 (1). **2010**.

[19] Woodle M, Lasic D. Sterically stabilized liposomes. *Biochim Biophys Acta*. **1992**:1113:171-199.

[20] Al-Jamal KT, Al-Jamal WT, Akerman S, Podesta JE, Yilmazer A, Turton JA, Bianco A, Vargesson N, Kanthou C, Florence AT, Tozer GM, Kostarelos K. Systemic antiangiogenic activity of cationic poly-L-lysine dendrimer delays tumor growth. *Proc Natl Acad Sci U S A*. **2010**;107:3966-3971.

[21] van Dongen SF, de Hoog HP, Peters RJ, Nallani M, Nolte RJ, van Hest JC. Biohybrid polymer capsules. *Chem Rev*. **2009**;109:6212-6274.

[22] Tong R, Christian DA, Tang L, Cabral H, Baker JR, Kataoka K, Discher DE, Cheng JJ. Nanopolymeric therapeutics. *Mrs Bull*. **2009;**34:422-431.

[23] Meng F, Zhong Z, Feijen J. Stimuli-responsive polymersomes for programmed drug delivery. *Biomacromolecules*. **2009;**10:197-209.

[24] Moghimi SM. Recent developments in polymeric nanoparticle engineering and their applications in experimental and clinical oncology. *Anticancer Agents Med Chem*. **2006;**6:553-561.

[25] Libutti SK, Paciotti GF, Byrnes AA, Alexander HR Jr, Gannon WE, Walker M, Seidel GD, Yuldasheva N, Tamarkin L. Phase I and pharmacokinetic studies of

CYT-6091, a novel PEGylated colloidal gold-rhTNF nanomedicine. *Clin Cancer Res*. **2010**;16:6139-6149.

[26] Discher DE, Eisenberg A. Polymer vesicles. *Science*. **2002**;297:967-973.

[27] Li S, Byrne B, Welsh J, Palmer AF. Self-Assembled Poly(butadiene)-b-Poly(ethylene oxide) Polymersomes as Paclitaxel Carriers. *Biotechnol Prog*. **2007**;23:278-285.

[28] Qiu LY, Bae YH. Polymer architecture and drug delivery. *Pharm Res*. **2006;**23:1-30.

[29] Cegnar M, Kristl J, Kos J. Nanoscale polymer carriers to deliver chemotherapeutic agents to tumours. *Expert Opin Biol Ther*. **2005**;5:1557-1569.

[30] Christian NA, Milone MC, Ranka SS, Li G, Frail PR, Davis KP, Bates FS, Therien MJ, Ghoroghchian PP, June CH, Hammer DA. Tat-functionalized near-infrared emissive polymersomes for dendritic cell labeling. *Bioconjug Chem*. **2007;**18:31-40.

[31] Kim SY, Lee YM, Baik DJ, Kang JS. Toxic characteristics of methoxy poly(ethylene glycol)/poly(ε-caprolactone) nanospheres; in vitro and in vivo studies in the normal mice. *Biomaterials*. **2003;**24:55-63.

[32] Roy S, Glueckert R, Johnston AH, et al. Strategies for drug delivery to the human inner ear by multifunctional nanoparticles. *Nanomedicine (Lond)*. **2012;7:55-63.**

[33] Park K, Lee S, Kang E, Kim K, Choi K, Kwon IC. New Generation of Multifunctional Nanoparticles for Cancer Imaging and Therapy. *Adv Funct Mater*. **2009**;19:1553-1566.

[34] Sharma US, Balasubramanian SV, Straubinger RM. Pharmaceutical and physical properties of paclitaxel (Taxol®) complexes with cyclodextrins. *J Pharm Sci*. **1995;**84:1223-1230.

[35] Kim DW, Kim SY, Kim HK, Kim SW, Shin SW, Kim JS, Park K, Lee MY, Heo DS. Multicenter Phase II Trial of Genexol-PM, a Novel Cremophor-Free, Polymeric Micelle Formulation of Paclitaxel, with Cisplatin in Patients with Advanced Non-small-Cell Lung Cancer. *Ann Oncol*. **2007**;18:2009-2014.

[36] Kim TY, Kim DW, Chung JY, Shin SG, Kim SC, Heo DS, Kim NK, Bang YJ. Phase I and pharmacokinetic study of Genexol-PM, a cremophor-free, polymeric micelle-formulated paclitaxel, in patients with advanced malignancies. *Clin Cancer Res*. **2004**;10:3708-3716.

[37] Lee KS, Chung HC, Im SA, Park YH, Kim CS, Kim SB, et al. Multicenter phase II trial of Genexol-PM, a Cremophor-free, polymeric micelle formulation of paclitaxel, in patients with metastatic breast cancer. *Breast Cancer Res Treat*. **2008;**108:241-250.

[38] Ahmed F, Pakunlu RI, Brannan A, Bates F, Minko T, Discher DE. Biodegradable polymersomes loaded with both paclitaxel and doxorubicin permeate and shrink tumors, inducing apoptosis in proportion to accumulated drug. *J Control Release*. **2006;**116:150-158.

[39] Ghoroghchian PP, Frail PR, Susumu K, Blessington D, Brannan AK, Bates FS, Chance B, Hammer DA. Therien M. J. Near-infrared-emissive polymersomes: Self-assembled soft matter for *in vivo* optical imaging. *Proc Natl Acad Sci U S A*. **2005**;102:2922-2927.

[40] Tsourkas A, Shinde-Patil VR, Kelly KA, Patel P, Wolley A, Allport JR, Weissleder R. In vivo imaging of activated endothelium using an anti-VCAM-1 magnetooptical probe. *Bioconjug Chem*. **2005**;16:576-581.

[41] Zhang Y, Zhang W, Johnston AH, Newman TA, Pyykko I, Zou J. Targeted delivery of Tet1 peptide functionalized polymersomes to the rat cochlear nerve. *Hear Res*. **2010;**269:1-11.

[42] Roy S, Johnston AH, Newman TA, et al. Cell-specific targeting in the mouse inner ear using nanoparticles conjugated with a neurotrophin-derived peptide ligand: potential tool for drug delivery. *Int J Pharm*. **2010**;390:214-224.

[43] Zhang Y, Zhang W, Johnston AH, Newman TA, Pyykkö I, Zou J. Improving the visualization of fluorescently tagged nanoparticles and fluorophore-labeled molecular probes by treatment with CuSO(4) to quench autofluorescence in the rat inner ear. *Int J Nanomedicine*. **2012**;7:1015-1022.

[44] Surovtseva EV, Johnston AH, Zhang W, Zhang Y, Kim A, Murakoshi M, Wada H, Newman TA, Zou J, Pyykkö I. Prestin binding peptides as ligands for targeted polymersome mediated drug delivery to outer hair cells in the inner ear. *Int J Pharm*. **2012**;424:121-127.

[45] Soumen R, Johnston AH, Moin ST, Dudas J, Newman TA, Hausott B, Schrott-Fischer A, Glueckert R. Activation of TrkB receptors by NGFβ mimetic peptide conjugated polymersome nanoparticles. *Nanomedicine*. **2012**;8:271-274.

[46] Davis ME, Zuckerman JE, Choi CH, Seligson D, Tolcher A, Alabi CA, Yen Y, Heidel JD, Ribas A. Evidence of RNAi in humans from systemically administered siRNA via targeted nanoparticles. *Nature*. **2010**;464:1067-1070.

[47] Pangburn TO, Georgiou K, Bates FS, Kokkoli E. Targeted polymersome delivery of siRNA induces cell death of breast cancer cells dependent upon Orai3 protein expression. *Langmuir*. **2012**;28:12816-12830.

[48] Vives, E., P. Brodin, and B. Lebleu. A truncated HIV-1 TAT protein basic domain rapidly translocates through the plasma membrane and accumulates in the cell nucleus. *J Biol Chem*. **1997**;272:16010-16017.

[49] Sandgren S, Cheng F, Belting M. Nuclear targeting of macromolecular polyanions by an HIV-Tat derived peptide. Role for cell-surface proteoglycans. *J Biol Chem*. **2002**;277:38877-38883.

[50] Ferrari A, Pellegrini V, Arcangeli C, Fittipaldi A, Giacca M, Beltram F. Caveolae-mediated internalization of extracellular HIV-1 tat fusion proteins visualized in real time. *Mol Ther*. **2003**;8:284-294.

[51] Ignatovich IA, Dizhe EB, Pavlotskaya AV, Akifiev BN, Burov SV, Orlov SV, Perevozchikov AP. Complexes of Plasmid DNA with Basic Domain 47-57 of the HIV-1 Tat Protein Are Transferred to Mammalian Cells by Endocytosis-mediated Pathways. *J Biol Chem*. **2003**;278:42625-42636.

[52] Potocky TB, Menon AK, Gellman SH. Cytoplasmic and nuclear delivery of a TAT-derived peptide and a β-Peptide after endocytic uptake into HeLa Cells. *J Biol Chem*. **2003;**278:50188-50194.

[53] Zhao MD, Sun YM, Fu GF, Du YZ, Chen FY, Yuan H, Zheng CH, Zhang XM, Hu FQ. Gene therapy of endometriosis introduced by polymeric micelles with glycolipid-like structure. *Biomaterials*. **2012**;33:634-643.

[54] Kocbek P, Obermajer N, Cegnar M, Kos J, Kristl J. Targeting cancer cells using PLGA nanoparticles surface modified with monoclonal antibody. *J Control Release*. **2007;**120:18-26.

[55] Arora S, Rajwade JM, Paknikar KM. Nanotoxicology and in vitro studies: The need of the hour. *Toxicol Appl Pharmacol*. **2009**;236:310-318.

[56] Zhao X, Yu SB, Wu FL, Mao ZB, Yu CL. Transfection of primary chondrocytes using chitosan-pEGFP nanoparticles. *J Control Release*. **2006;**112:223-228.

[57] Hillaireau H, Couvreur P. Nanocarriers' entry into the cell: relevance to drug delivery. *Cellular and Molecular Life Sciences*. **2009**;66:2873-2896.

[58] Conner SD, Schmid SL. Regulated portals of entry into the cell. *Nature*. **2003;**422:37-44.

[59] Swanson JA, Watts C. Macropinocytosis. *Trends Cell Biol*. **1995**;5;424-428.

[60] Shier D, Butler J, Lewis R. Hole's Human Anatomy & Physiology. India: McGraw-Hill Education; **2007.**

[61] Ellis H. Anatomy of the uterus. *Anaesth Intens Care Med*. **2011**;12:99-101.

[62] Al-Jefout M. **2009**.

[63] Jiménez-Ayala M, Jimenez-Ayala Portillo B. Endometrial Adenocarcinoma: Prevention and Early Diagnosis. Basel: Karger Publishers, **2008**.

[64] Viganò P, Parazzini F, Somigliana E, Vercellini P. Endometriosis: epidemiology and aetiological factors**.** *Best Pract Res Clin Obstet Gynaecol*. **2004**;18:177-200.

[65] Shaw RW. An atlas of endometriosis. Carnforth, UK: The Parthenon Publishing Group; **1993**.

[66] Hsu Al, Khachikyan I, Stratton P. Invasive and Noninvasive Methods for the Diagnosis of Endometriosis. *Clin Obstet Gynecol.* **2010**;53(2):413-419.

[67] Cramer DW, Missmer SA. The epidemiology of endometriosis. *Ann NY Acad Sci*. **2002;**955:11-22.

[68] Vinatier D, Orazi G, Cosson M, Dufour P. Theories of endometriosis. *Eur J Obstet Gynecol Reprod Biol*. **2001**;96:21-34.

[69] Nakamura M, Katabuchi H, Tohya T, Fukumatsu Y, Masuura K, Okamura H. Scanning electron microscopic and immunohistochemical studies of pelvic endometriosis. *Human Reproduction*. **1993**;8(12):2218-2226.

[70] Meresman GF, Vighi S, Buquet RA, Contreras-Ortiz O, Tesone M, Rumi LS. Apoptosis and expression of Bcl-2 and Bax in eutopic endometrium from women with endometriosis. *Fertil Steril*. **2000**;74:760-766.

[71] Chung HW, Lee JY, Moon HS, Hur SE, Park MH, Wen Y, Polan ML. Matrix metalloproteinase-2, membranous type 1 matrix metalloproteinase, and tissue inhibitor of metalloproteinase-2 expression in ectopic and eutopic endometrium. *Fertil Steril*. **2002**;78:787-795.

[72] Healy DL, Rogers PA, Hii L, Wingfield M. Angiogenesis: a new theory for endometriosis. *Hum Reprod Update*. **1998**;4:736-740.

[73] Bourlev V, Volkov N, Pavlovitch S, Lets N, Larsson A, Olovsson M. The relationship between microvessel density, proliferative activity and expression of vascular endothelial growth factor-A and its receptors in eutopic endometrium and endometriotic lesions. *Reproduction*. **2006**;132:501-509.

[74] Tiberi F, Tropea A, Romani F, Apa R, Marana R, Lanzone A. Prokineticin 1, homeobox A10, and progesterone receptor messenger ribonucleic acid expression in primary cultures of endometrial stromal cells isolated from endometrium of healthy women and from eutopic endometrium of women with endometriosis. *Fertil Steril*. **2010;**94:2558-2563.

[75] Evans J, Catalano R D, Morgan K, Critchley H O, Millar R P, Jabbour H N. Prokineticin 1 signaling and gene regulation in early human pregnancy. *Endocrinology*. **2008**;149:2877-2887.

[76] Burney RO, Talbi S, Hamilton AE, Vo KC, Nyegaard M, Nezhat CR, Lessey BA, Giudice LC. Gene expression analysis of endometrium reveals progesterone resistance and candidate susceptibility genes in women with endometriosis. *Endocrinology*. **2007**;148:3814-3826.

[77] Attia GR, Zeitoun K, Edwards D, Johns A, Carr BR, Bulun SE: Progesterone receptor isoform A but not B is expressed in endometriosis. *J Clin Endocr Metab*. **2000;**85:2897-2902.

[78] Sundqvist J, Andersson K, Scarselli G, Gemzell-Danielsson K, Lalitkumar P: Expression of adhesion, attachment and invasion markers in eutopic and ectopic endometrium: a link to the aetiology of endometriosis. *Hum Reprod*. **2012**;27:2737-2746.

[79] Ametzazurra A, Matorras R, García-Velasco JA, Prieto B, Simón L, Martínez A, Nagore D. Endometrial fluid is a specific and non-invasive biological sample for protein biomarker identification in endometriosis. *Human Reproduction*. **2009**;24:954-965.

[80] Chung HW, Wen Y, Chun SH, Nezhat C, Woo BH, Lake Polan M. Matrix metalloproteinase-9 and tissue inhibitor of metalloproteinase-3 mRNA expression in ectopic and eutopic endometrium in women with endometriosis: a rationale for endometriotic invasiveness. *Fertil Steril*. **2001**;75:152-159.

[81] Laschke MW, Elitzsch A, Vollmar B, Vajkoczy P, Menger MD. Combined inhibition of vascular endothelial growth factor (VEGF), fibroblast growth factor

and platelet-derived growth factor, but not inhibition of VEGF alone, effectively suppresses angiogenesis and vessel maturation in endometriotic lesions. *Hum Reprod*. **2006**;21:262-268.

[82] McLaren J. Vascular endothelial growth factor and endometriotic angiogenesis. *Hum Reprod Update*. **2000**;6:45-55.

[83] Royal College of Obstetricians and Gynaecologists. Guideline on the management of women with endometriosis. 18 September **2013**.

[84] Kyama CM, T'Jampens D, Mihalyi A, Simsa P, Debrock S, Waelkens E, Landuyt B, Meuleman C, Fulop V, Mwenda JM, *et al*.:ProteinChip technology is a useful method in the pathogenesis and diagnosis of endometriosis: a preliminary study. *Fertil Steril*. **2006;**86:203-209.

[85] American Society for Reproductive Medicine Revised American Society for Reproductive Medicine classification of endometriosis: 1996. *Fertil Steril*. **1997**;67:817-821.

[86] Royal College of Obstetricians and Gynaecologists. Guideline for the diagnosis and treatment of endometriosis. **2005**.

[87] Kennedy S, Bergqvist A, Chapron C, D'Hooghe T, Dunselman G, Greb R, Hummelshoj L, Prentice A, Saridogan E. ESHRE Special Interest Group for Endometriosis and Endometrium Guideline Development Group. ESHRE guideline for the diagnosis and treatment of endometriosis. *Hum Reprod*. **2005**;20:2698-2704.

[88] Jacobson TZ. Potential cures for endometriosis. *Ann N Y Acad Sci*. **2011**;1221:70-74.

[89] Malik E, Berg C, Meyhofer-Malik A, Buchweitz O, Moubayed P, Diedrich K. Fluorescence diagnosis of endometriosis using 5-aminolevulinic acid. *Surg Endosc-Ultras*. **2000**;14:452-455.

[90] Hillemanns, P, Weingandt, H, Stepp, H, Baumgartner, R, Xiang, W & Korell, M (2000). Assessment of 5-aminolevulinic acid-induced porphyrin fluorescence in patients with peritoneal endometriosis. *Am J Obstet Gynecol*. **2000**;183:52-57.

[91] Colombo N, Preti E, Landoni F, Carinelli S, Colombo A, Marini C, Sessa C, ESMO Guidelines Working Group: Endometrial cancer: ESMO Clinical Practice Guidelines for diagnosis, treatment and follow-up. *Ann Oncol*. **2011**;22(Suppl 6):vi35-39.

[92] Underwood JCE, Cross SS. General and systemic pathology. London: Elsevier (Churchill Livingstone);**2009**.

[93] Fleming GF, Filiaci VL, Bentley RC, Herzog T, Sorosky J, Vaccarello L, Gallion H. Phase III randomized trial of doxorubicin + cisplatin versus doxorubicin + 24-h paclitaxel + filgrastim in endometrial carcinoma: a Gynecologic Oncology Group study. *Ann Oncol*. **2004;**15:1173-1178.

[94] Weiderpass E, Adami H-O, Baron JA, Magnusson I, Bergstrom R, Lindgren A, Correia N, Persson I. Risk of Endometrial Cancer Following Estrogen Replacement with and without Progestins. *J Natl Cancer Inst*. **1999**;91:1131-1137.

[95] Lukanova A, Lundin E, Micheli A, Arslan A, Ferrari P, Rinaldi S, Krogh V, Lenner P, Shore RE, Biessy C, Muti P, Riboli E,Koenig KL, Levitz M, Stattin P, Berrino F, Hallmans G, Kaaks R, Toniolo P, Zeleniuch-Jacquotte A. Circulating levels of sex steroid hormones and risk of endometrial cancer in postmenopausal women†. *Int J Cancer*. **2004**;108:425-432.

[96] Persson I, Weiderpass E, Bergkvist L, Bergström R, Schairer C. Risks of breast and endometrial cancer after estrogen and estrogen-progestin replacement. *Cancer Causes Control*. **1999**;10:253-260.

[97] Rose PG. Endometrial carcinoma. *N Engl J Med*. **1996;**335:640-649.

[98] Bansal N, Yendluri V, Wenham RM. The molecular biology of endometrial cancers and the implications of pathogenesis, classification and targeted therapies. *Cancer Control*. **2009**;16:8-13.

[99] Birkeland E, Wik E, Mjøs S, Hoivik EA, Trovik J, Werner HM, Kusonmano K, Petersen K, Raeder MB, Holst F, Øyan AM,Kalland KH, Akslen LA, Simon R, Krakstad C, Salvesen HB. KRAS gene amplification and overexpression but not mutation associates with aggressive and metastatic endometrial cancer. *Br J Cancer*. **2012**;107:1997-2004.

[100] Berchuck A, Boyd J. Molecular basis of endometrial cancer. *Cancer*. **1995**;76:2034-2040.

[101] Sudimack J, Lee RJ. Targeted drug delivery via the folate receptor. *Adv Drug Deliv Rev*. **2000**;41:147-162.

[102] Dainty LA, Risinger JI, Morrison C, Chandramouli GV, Bidus MA, Zahn C, Rose GS, Fowler J, Berchuck A, Maxwell GL. Overexpression of folate binding protein and mesothelin are associated with uterine serous carcinoma. *Gynecol Oncol*. **2007**;105:563-570.

[103] Amant F, Moerman P, Neven P, Timmerman D, Van Limbergen E, Vergote I. Endometrial cancer. *Lancet*. **2005**;366:491-505.

[104] Temkin SM, Fleming G. Current treatment of metastatic endometrial cancer. *Cancer Control*. **2009**;16:38-45.

[105] Johnston H. A, Baker L.J, Bailey L.J, Newman A.T. Investigating intracellular payload release from polymersome nanoparticles. *Unpublished manuscript*.

[106] Chaudhury K., Babu K.N., Singh A.K., Das S., Kumar A., Seal S. Mitigration of endometriosis using regenerative cerium oxide nanoparticles. *Nanomedicine: NBM* **2013**;9:439-448.

[107] Mittal S, Pandey K. A. Cerium oxide nanoparticles induced toxicity in human lung cells: Role of ROS mediated DNA damage and apoptosis. *BioMed Research International*. **2014**.

[108] Kumar S., Chakravarty B.,Caudhury K. Letrozole and curcumin loaded -PLGA nanoparticles: A therapeutic strategy of endometriosis. *Nanomedicine and Biotherapeutic Discov.* **2014**;4:123.

[109] Console S, Marty C, Garcia-Echeverria C, Schwendener RA, Ballmer-Hofer K. Antennapedia and HIV TAT &quote;protein transduction domains&quote; promote endocy-tosis of high Mr cargo upon binding to cell surface glycosaminoglycans. *J Biol Chem*. **2003**;278:35109-35114.

[110] Xia H, Gao X, Gu G, Liu Z, Hu Q, Tu Y, Song Q, Yao L, Pang Z, Jiang X, Chen J, Chen H. Penetratin-functionalized PEG-PLA nanoparticles for brain drug delivery. *Int J Pharm*. **2012**;436:840-850.

[111] Huang RQ, Yang WL, Pei YY, Jiang C. Gene delivery into brain capillary endothelial cells using Antp-modified DNA-loaded nanoparticles. *Chem Pharm Bull*. **2006;**54:1254-1258.

[112] Pooga M, Kut C, Kihlmark M, Hallbrink M, Fernaeus S, Raid R, Land T, Hallberg E, Bartfai T, Langel U. Cellular translocation of proteins by transportan. *FASEB J*. **2001**;15:1451-1453.

[113] Elmquist A, Lindgren M, Bartfai T, Langel U: VE-cadherin-derived cell-penetrating peptide, pVEC, with carrier functions. *Exp Cell Res*. **2001;**269**:**237-244.